AN ABSTRACT OF THE THESIS OF

Sang Hyouk Choi for the degree of Doctor of Philosophy

in Mechanical Engineering presented on October 17, 1980

Title: Heat Transfer in Magnetic Fluids at Low Reynolds Number

Redacted for Privacy

Abstract approved: Lorin R. Davis

This study was concerned with the flow of a magnetic self-propelled ferrohydrodynamic fluid in a horizontal circular tube subjected to axially varying temperature and magnetic field. The first phase of the study involved the analytical solution to the governing equations for the velocity and temperature profiles within the fully developed flow region of the duct when subjected to linearly varying axial temperature and magnetic field. The results showed the problem to be similar to gravity-induced natural convection flows even though the variables are different. The Nusselt number was found to be a function of a magnetic Rayleigh number.

The second part of the study consisted of an experimental investigation at the thermal entry region of flow caused by a change in tube wall heat flux and a numerical solution to the governing equations for the same problem. Because of the low pyromagnetic coefficient of the water-based Lignosite fluid used in the study, only low Reynolds number flows were obtained. It was found that a hot-wire anemometer could be used for velocity measurements if the overheat ratio was maintained at a low value and measurements were made within

a region of constant magnetic field strength. The experimentally and numerically obtained velocity and temperature profiles generally agreed in magnitude and shape but a shift in maximum velocity point location was observed. This shift was attributed to experimental errors and to physical properties of the magnetic fluid that were approximated due to lack of information.

Heat Transfer in Magnetic Fluids at Low Reynolds Number

by

Sang Hyouk Choi

A THESIS

submitted to

Oregon State University

in partial fulfillment of
the requirements for the
degree of

Doctor of Philosophy

Commencement June 1981

APPROVED:

Redacted for Privacy

Professor of Mechanical Engineering
in charge of major

Redacted for Privacy

Head of Department of Mechanical Engineering

Redacted for Privacy

Dean of Graduate School

Date thesis is presented October 17, 1980

Typed by Donna Lee Norvell-Race for Sang Hyouk Choi

ACKNOWLEDGMENT

My utmost gratitude and appreciation is expressed for the graciousness of my wife without whose encouragement and hearty support this work would not have been completed.

The valuable discussion with my major professor, Dr. L. R. Davis, and his longstanding encouragement and concern are appreciated and memorable.

Sincere thanks and appreciation is expressed to Dr. J. R. Welty for the concern and support he provided so that I could finish up my study here.

The support from O.S.U. Computer Center is appreciated.

Finally, the endless love and prayers of my mother, my brother and sisters, my mother-in-law, and uncle and aunt, Mr. & Mrs. Hi Young Kim, are appreciated.

TABLE OF CONTENTS

Chapter

Chapter

LIST OF ILLUSTRATIONS

Figure

NOMENCLATURES

a	radius	m
B	magnetic flux	Wb/m^2
Bei	a kelvin function	
Ber	a kelvin function	
C	Curie constant	$1.14 \times 10^{-4} \cdot (m^3)(K)/kg$
C	heat capacity in constant volume	J/kg K
c	specific heat capacity	J/kg K
D_i	a coefficient of an imaginary part	
D_{ij}	rate of deformation	s^{-1}
D_r	a coefficient of a real part	
E	volume fraction solids in suspension	
e_{ijk}	generalized Kronecker delta or permutation symbol	-1,0,+1
F	force	N
F	Gibbs free energy (ch. V)	J
g	gravity	9.8 m/s
$g_{ij} = \frac{\partial y^k}{\partial x^i} \frac{\partial x^k}{\partial x^i}$	metric tensor	
H	magnetic field intensity	A/m
$h = \frac{\partial H}{\partial z}$	field intensity gradient	A/m^2
I	moment of inertia	N·m
I_0	a modified Bessel function of first kind	
J_0	an ordinary Bessel function of first kind	

K	pyromagnetic coefficient	Gauss/ K
$\overline{K}_\eta$	magnetic anisotropy constant	
K_o	a modified Bessel function of	second kind
k	thermal conductivity	W/m K
k_o	Boltzman constant	1.38×10^{-23} J/K
$L(x) = \coth(x) - 1/x$	Langevin equation	
M	magnetic moment or magnetization	Gauss
M_o	magnetic saturation at T=0 °K	Gauss
M_s	magnetization saturation in a constant field	Gauss
$\overline{M}_s$	domain magnetization of suspended magnetic material	Gauss
m	mass (ch. V)	kg
m_o	superparamagnetic particles average magnetization saturation	Gauss
N	number of superparamagnetic particles per unit volume	
N	maximum iteration number of r-direction (ch. V)	
N_v	Weiss molecular field constant	
n	a constant in Eq. (10), determined from the experimental curve	
n_i	number of particles of diameter d_i in suspension	
p	pressure	Pa
q''_o	heat flux	W/m^2
r	radius	m

S	entropy (ch. V)	
T	absolute temperature	K
T_c	Curie temperature	K
T_o	average temperature	K
t	time	s
t	scaled temperature (ch. IV)	
t_o	scaled average temperature	
U	z-direction velocity (ch. V)	m/s
V	r-direction velocity (ch. V)	m/s
V	volume (ch. V)	m^3
$\overline{V}$	domain volume	m^3
v	velocity	m/s
v_i	volume of a suspended particle of the diameter d_i	m^3
v_i'	magnetic volume of a suspended particle of diameter d_i	m^3
W	rotatory velocity	m/s
Y_o	an ordinary Bessel function of second kind	
Z	elevation	m
γ_o	coefficient showing the degree of "adherence" of the liquid particle considered to its surroundings	
γ_s	shear rate	s^{-1}
δ_{ij}	Kronecker delta	1 or 0
δ_r	stepsize in r-direction	m
δ_z	stepsize in z-direction	m
λ_o	coefficient of viscosity	Pa·s

μ	viscosity	Pa·s
μ_o	magnetic permeability of free space	N/A^2
ρ	density	kg/m^3
η	colloid viscosity	Pa·s
η_o	carrier fluid voscosity	Pa·s

SUBSCRIPTS

av	average
c	center
m	magnetic
r	r-direction
s	saturation
w	wall
z	z-direction
θ	θ-direction

Heat Transfer in Magnetic Fluids at Low Reynolds Number

I. INTRODUCTION

A magnetic fluid is called exotic or novel because of its magnetic property. This type of fluid is known by several names (such as magnetic fluid [1,2], ferrofluid [3,4,5], magnetic colloid [3,6], ferromagnetic suspension [7] and so on) and is usually synthesized in a laboratory.

The magnetic fluid is a two-phase fluid (a colloid) which has very fine particles of solid ferromagnetic material suspended in a carrier fluid. Such a colloidal suspension may occur in all fluids if the particle size is maintained small enough to allow random motion (Brownian motion) due to thermally agitated by collision with molecules of the fluid. If this Brownian motion is not maintained, flocculation of magnetic particles is unavoidable. That is, in order to have a colloidal suspension the thermal energy kT should be bigger than magnetic energy KV.

However, as the particle size becomes smaller and smaller, flocculation may also arise due to Van de Waals attractive force. This attractive energy between particles is proportional to the inverse sixth power of distance according to London's model. Therefore, as particles approach each other at a distance as small as a particle diameter, the Van der Waals force increases rapidly. The

sufficient thermal agitation energy for Brownian motion is maintained by making very fine particles, but at a certain point the flocculation of particles due to Van der Waals forces will occur. In order to prevent magnetic particle flocculation and improve a high-density colloidal suspension of very fine magnetic particles, the materials are coated. These coating materials are steric acid or oleic acid. For high stability of a colloidal suspension the particle diameters can range from 20 Å to 100 Å. These particles are somewhat less than the dimensions of a single magnetic domain V with no settling or separation under gravity or in a strong magnetic field [8,9,10]. These colloidal suspensions behave like true homogeneous fluids when they are flowing. The ferromagnetic properties of fluids can be improved by using a ferromagnetic material with high saturation magnetization and high concentration.

Magnetic fluids are manufactured mechanically or chemically. The mechanical manufacturing method is a ball mill filled with a magnetic material, a carrier fluid, and a particle coating agent (such as oleic acid). The mill runs for several weeks to make the final product. This method is more expensive and limits the amount of magnetic fluid in each run, but it is not restricted to make only a certain kind of magnetic fluid as with the chemical method. The Ferrofluidics Corporation* has manufactured most of their magnetic

---

*Ferrofluidics Corp.: 144 Middlesex Turnpike, Burlingham, Mass. 01803. Products: water, glycerides, esters, hydrocarbons, silicones, fluorocarbons, and others based magnetic fluids.

fluids by this mechanical method. The Georgia Pacific Corp.** makes a magnetic fluid chemically from a by-product of its pulp-mill, which is called Lignosite. This magnetic fluid was used in the experimental and numerical models of this study. As another method, Popplewell et al. [11,12] made a ferromagnetic liquid containing 2% by weight of iron in mercury by electro-deposition of iron onto an agitated mercury cathode and a mercury/tin amalgam cathode.

A variety of magnetic fluids have been studied and applied in industry. So far most of the research has been on the properties and characteristics of magnetic fluids from a microscopic point of view.

The characteristics of a magnetic fluid in a continuum model are thoseof a micropolar fluid [13] which apparently shows a couple stress and body couple phenomena. In most Navier-Stokes equation applications these phenomena have been omitted since their effects are minimal and can be ignored. But all fluids have these two properties in their momentum and energy equations even though their magnitudes are not visible. In non-Newtonian fluids these flow properties have significant effects. Such discussions have been well established by several scientists for the past 30 years [13,14, 15]. In magnetic fluids, however, this phenomena cannot be ignored. Particular interest has been shown in the development of the thermomechanics of magnetic fluids [14-17]. In addition, a great deal of

---

** Georgia Pacific Corp.: Bellingham Division, Bellingham, Wash. 98225. Product: Lignosite FML.

attention has been paid to the investigation of physico-chemical, mainly static [18,19] and rheological properties of magnetic fluids [20-25].

In the application of magnetic fluids many attempts have been successful, and some of them are still being developed. These diverse applications include vacuum [26] and high pressure [27] rotary seals, controlled lubricants [28], damping systems [29], material separators [30], fluid jet printer [31], visualization and display systems [32], bearings [33], sensors, actuators, switches, accelerometer [1, 34], and magnetocaloric heat pipes and engines [35-37] which rely on the variable magnetization of magnetic fluids with temperature gradient in the presence of an external magnetic field.

The principle of a magnetocaloric energy conversion system has been developed by Resler and Rosensweig [35-37]. The application of the principle has yet to be studied. The idea is based on the changes in magnetic moment of a magnetic particle in a carrier fluid as a function of magnetic field intensity and temperature. When the thermal energy kT is greater than the magnetic anisotrophy energy KV, the moment of a magnetic particle in a magnetic field becomes disoriented from its domain. Contrarily, when the magnetic anisotropy energy KV is greater than the thermal energy kT, the magnetic moment of a magnetic particle in a magnetic field becomes frozen in its domain. Accordingly, magnetic particles of a magnetic fluid change their magnetic moment with respect to temperature and field intensity. Hence, if there is any temperature gradient and/or

magnetic field gradient in the control volume of a magnetic fluid, a magnetic force or a pressure will be built up due to the change in magnetic moment of the particles. Due to the motion of magnetic particles in a carrier fluid, the neighboring fluid particles entrained by the magnetic particles start moving along with the magnetic particles. The magnetic moment development of magnetic particles in the magnetic field rapidly reaches its saturation point. The relaxation time for magnetic moment change to its saturation point is of the order of 10^{-5} to 10^{-9} sec. [38].

Until the magnetic moment vector is parallel to the applied magnetic field vector, $\bar{M} \| \bar{H}$, the interaction of the magnetic fluid with an external magnetic field through magnetic body couples and kinetic processes are considerable. Otherwise, there will be no interaction of the magnetic moment with an external magnetic field. Figure (1) shows this relationship between the magnetic moment $\overline{M}$ and the field intensity $\overline{H}$. The field intensity is of primary importance in Ferrohydrodynamics, since it is a spatial distribution of absolute magnitude of field rather than the vector field itself. Therefore, the magnetic field has a direction of flow that is the resultant of the vector quantities. As a result, this property of a magnetic fluid introduced the idea for direct energy conversion system. Figure (2) shows a simple schematic diagram of an energy conversion system using a magnetic fluid. A magnetic fluid in the presence of a magnetic field increases its temperature by taking energy from a heat source. A magnetic fluid, with a fully saturated magnetic moment at a low

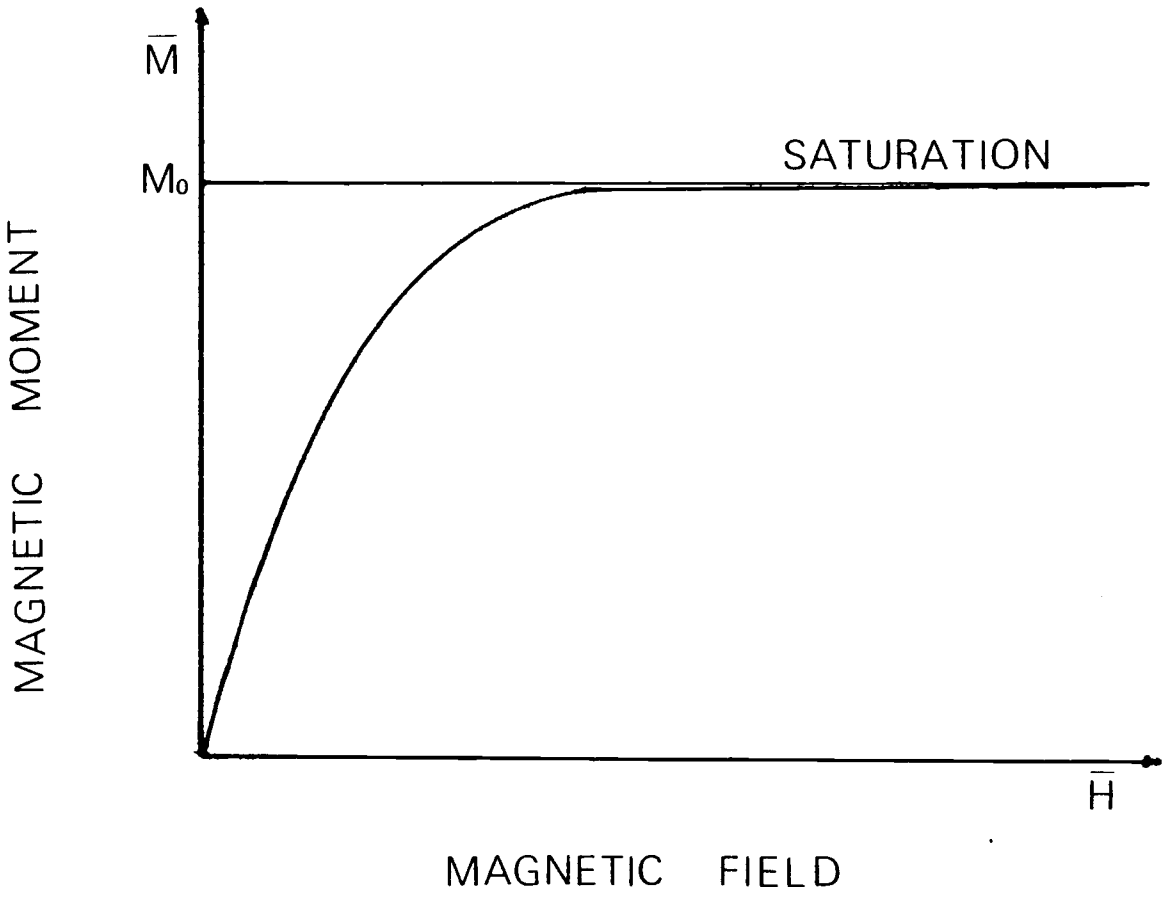

Figure 1. Relation of magnetic moment of a magnetic particle to external magnetic field.

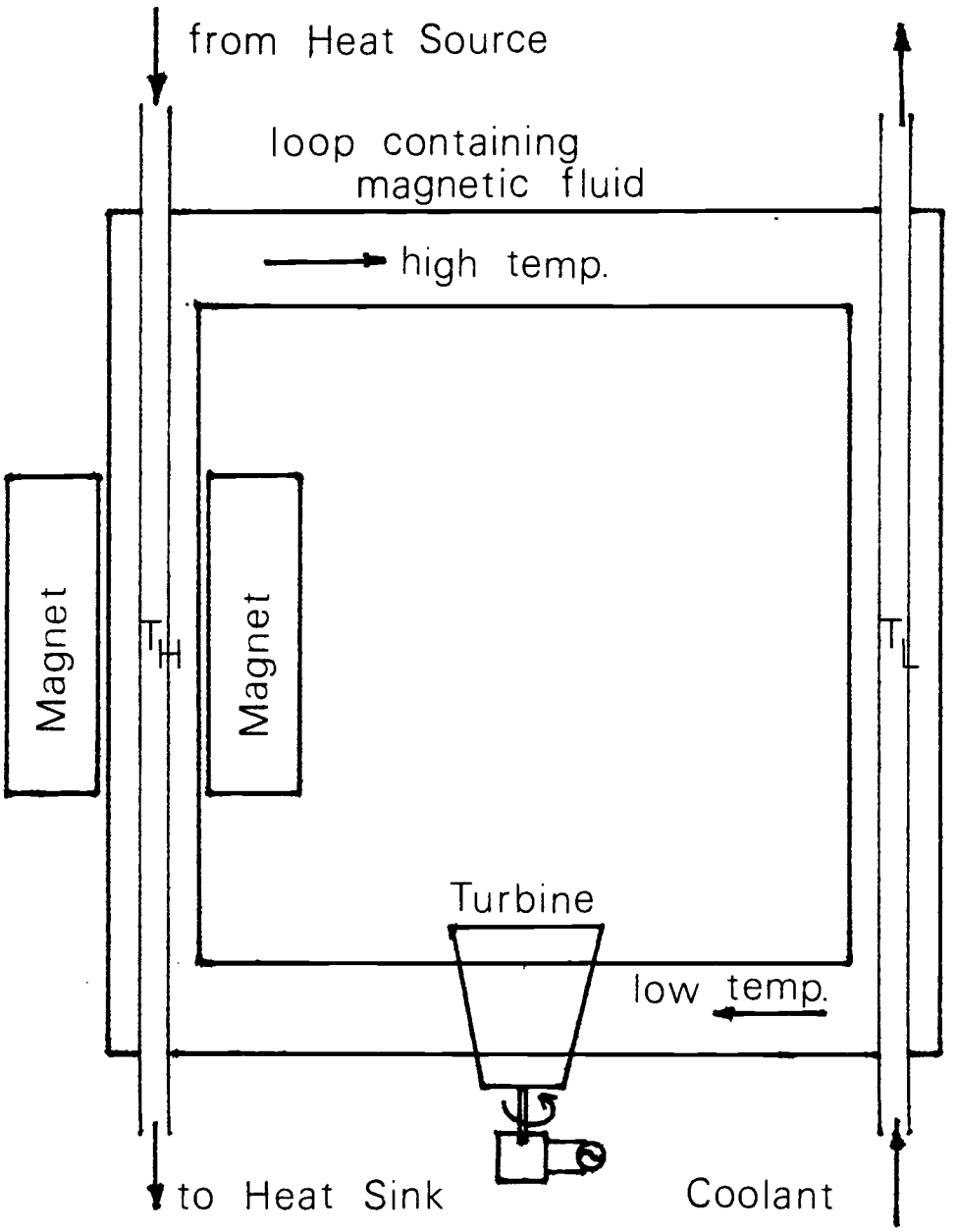

Figure 2. A simple schematic diagram for an energy conversion system.

temperature, drops its magnetic induction (or magnetization or magnetic moment change) due to a thermal energy increase. This happens up to the Curie point temperature, in which magnetic materials completely lose their magnetic moment from their domain. Hence, a pressure difference is formed between the hot fluid portion and the cold fluid portion due to the interaction between high magnetization at low temperature and low magnetization at high temperature. This pressure difference causes the fluid to flow from the cold to the high temperature portion.

The energy conversion device as shown in Figure 2 uses this principle. When a turbine [35] or MHD generator [11] is put between the heat source and sink, heat energy can be transformed into mechanical energy. It should be noted that the efficiency of this cycle with regeneration was found to be close to the Carnot efficiency in principle [35,36,37].

Although there are still many problems to be solved with this idea, it is applicable to many other fields. For example, a solar energy collector can use a magnetic fluid with a natural magnet to speed up the working media through a circulation loop. And if a liquid metal like mercury [11,12] with high concentration of magnetic particle suspension can be obtained, this kind of magnetic fluid can be used in a fast-breeding nuclear reactor or a fusion reactor, combined with an MHD generator, and for a closed cycle MHD generator. There is also another advantage to this device, it does not have any moving mechanical parts.

Under the blessing of such a fascinating working media, there has been much research in magnetic fluids. So far about 800 papers have been published and about 260 patents have been issued in the past 20 years [39]. However, there are still plenty of areas to be studied. The rapid development of basic concepts for magnetic fluid has created its own branch of the hydrodynamics. The area which now studies magnetic fluids and their applications is called Ferrohydrodynamics (FHD) like the ordinary hydrodynamics (OHD), magnetohydrodynamics (MHD), and electrohydrodynamics (EHD).

I-1. Terminology and Basic Concepts

The terminology is explained here so that it might help readers in subsequent chapters.

1. A magnetic fluid has various names:
   a. The magnetic fluid (this name is consistently used in this paper),
   b. Ferro fluid,
   c. Ferromagnetic suspension,
   d. Magnetic colloid,
   e. Magnetic liquid,
   f. Ferro liquid,

2. A typical magnetic fluid as a colloidal mixture is that
   a. it behaves like a true homogeneous fluid,

b. it has extra characteristics of high susceptibility to a magnetic field,

c. it has a magnetic particle concentration in the order of $10^{17}/cm^3$ with their sizes varying from 20 Å - 100 Å in diameter,

d. the magnetic particles in the presence of a uniform magnetic field have torque and then line up with the field, but magnetic fluids respond so rapidly to a magnetic torque ($\sim 10^{-9}$ sec) that one can assume the following condition to hold

$$\overline{M} \times \overline{H} = 0 . \qquad (1)$$

This means that the magnetic moment vector $\overline{M}$ rapidly lines up with the magnetic field vector $\overline{H}$. Hence, the two vectors are parallel to each other ($\overline{M} \parallel \overline{H}$),

e. the magnetic particles in the gradient of a magnetic field experience a force and attempt to slip through its carrier fluid,

f. the magnetic particles with a temperature gradient in the media experience a force due to their magnetic moment change according to temperature change. Figure (3) shows the relation of magnetic moment to temperature for various ferrites,

g. it can be hypothesized as a Newtonian fluid if the carrier fluid is a Newtonian fluid,

h. it is a perfect continuum model,

i. its electric conductivity is very small, so one can assume the electric conductivity of magnetic fluids to be zero,

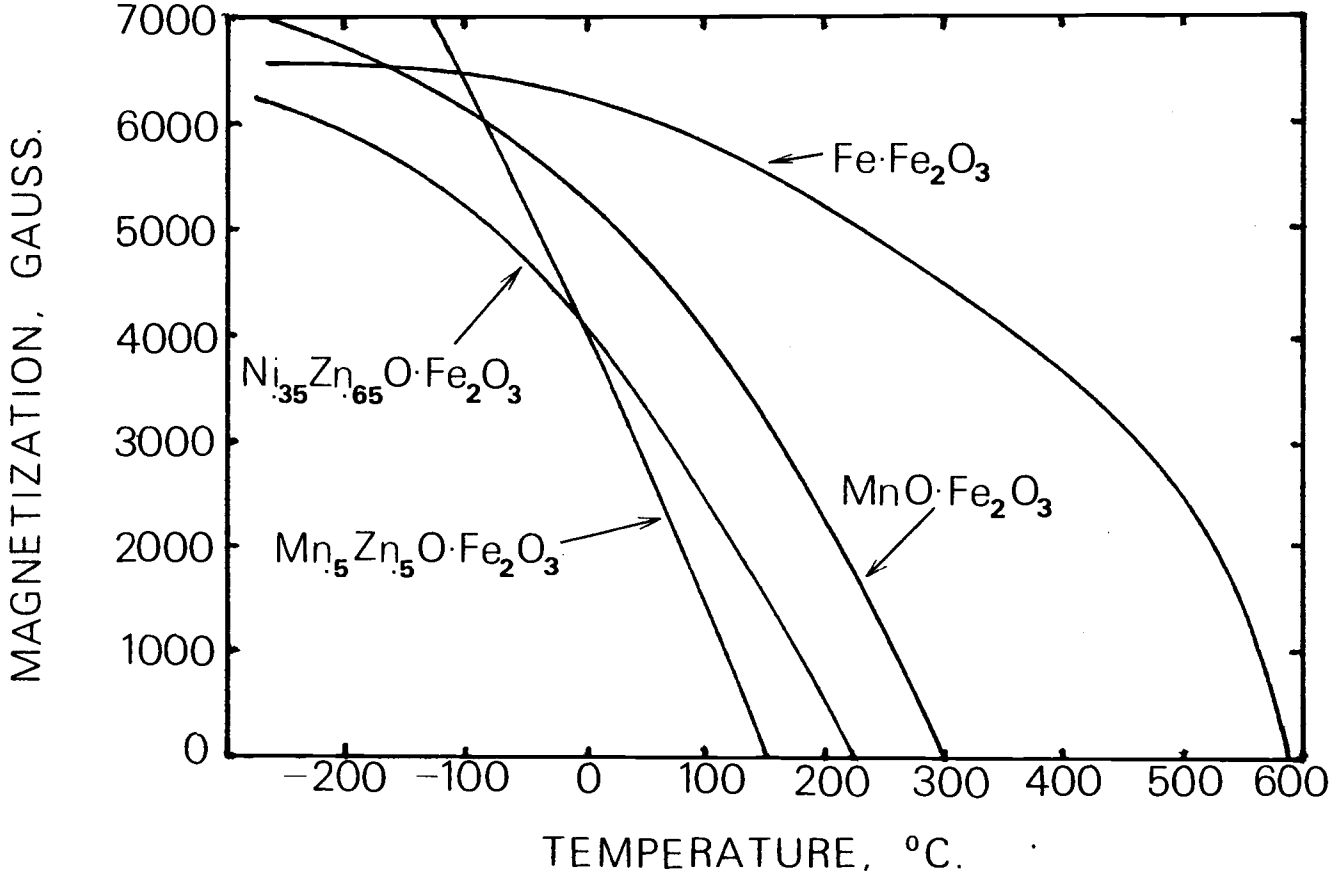

Figure 3. Temperature dependence of magnetic induction for various ferrites (Ref. 40).

$$\overline{J} = 0 ,$$

j. magnetic fluids also satisfy Maxwell's equation. Due to the negligible conductivity of magnetic fluids the Maxwell's equation in most present applications is

$$\nabla \times \overline{H} = 0 \qquad (2)$$

k. it is assumed to be essentially incompressible although its density is temperature dependent.

3. Magnetic properties of magnetic fluids

The magnetization or magnetic induction is closely related to the magnetic moment of magnetic particles in a carrier fluid. From a macroscopic point of view, magnetization M is assumed to be parallel to the applied magnetic field H, that is, $\overline{M} \parallel \overline{H}$, because the interaction happens within the relaxation time. This implies that there is no interaction of the magnetic fluid with the external magnetic field through magnetic body couples and kinetic processes. Figs. (1) and (3) show that for various magnetic materials the magnetic moment is a function of the external magnetic field and temperature. Therefore the equation of magnetic state is described as

$$M = M\,(T,H) . \qquad (4)$$

Magnetization is analytically defined for magnetic materials

whether it is a superpara-magnetic, or paramagnetic, or diamagnetic. Magnetization for a superparamagnetic material is described by the Langevin type formula [36,41].

$$M = m_o N L(\mu_o M_o H/kT) \tag{5}$$

where the Langevin equation is

$$L(x) = \text{Coth } (x) - 1/x. \tag{6}$$

Equation (5) represents the magnetization for superparamagnetic (or ferromagnetic) particles.

Magnetization for magnetic fluids is a function of the composition, size distribution and volume concentration of the particles in suspension. It can be expressed by the following equation [3] modified from Equation (5)

$$\frac{M}{\varepsilon M_s} = \frac{\sum_{i=1}^{\infty} \left[L\left(\frac{v_i \bar{M}_s H}{24kT}\right)\right]^{n_i v_i'}}{\sum_{i=1}^{\infty} n_i v_i} . \tag{7}$$

Another expression is the Weiss formula [42]

$$M = M_o \tanh \frac{T_c(N_v M + H)}{T N_v M_o} . \tag{8}$$

Where Equations (5), (7), (8) predict a temperature dependence of magnetization, above the Curie temperature he temperature dependence becomes [41,43],

$$M = \frac{CH}{T - T_c} \quad . \tag{9}$$

for small values of the ratio H/T.

For magnetization of a magnetic fluid, various factors such as particle size, volumetric concentration, temperature, and applied field intensity should be determined. Rosenweig et al.'s work [36] show the experimentally measured ferric induction curves for fluids with various concentrations of ferrite particles and various particle sizes. It shows that the high volumetric loading of magnetic particles into a fluid gives rise to a strong magnetization for the fluid. It also shows that in approaching magnetization saturation it is a strong function of particle size. That is, large size particles have higher saturation than that of small size particles. The 100 Å size particles are 97 percent saturated in a magnetic field of 10,000 Oersteds at room temperature while 25 Å particles are only about 20 percent saturated under the same condition. In order for ferromagnetic particles to be maintained as a suspended colloid in a fluid, the size and volumetric concentration are limited to certain levels. Otherwise the problems of sedimentation and flocculation of magnetic particles cannot be avoided.

In most cases the magnetization of a magnetic fluid has been approximated from the magnetic equation of state Equation (4), for convenience, even though the magnetization of a magnetic fluid is a function of particle size and volume concentration. That is, the

magnetization of a magnetic fluid in the presence of a constant magnetic field can be regarded as a function of only temperature [35, 37] under the condition that a magnetic fluid is homogeneous. It can be approximated by the linear equation:

$$\mu_o M = \mu_0 K(T_c - T) \tag{10}$$

where the pyromagnetic coefficient, $K = \left[\frac{\partial M}{\partial T}\right]_H$, can be regarded as a slope at a certain point on a curve as shown in Figure (4). The Curie temperature, T_c, has the value of 1043 K for iron. Bashtovoi et al. [45] approximated the dependence of the magnetization for a unit volume of liquid on the temperature by an exponential function

$$\frac{M}{M_o} = \frac{\exp(nT/T_c) - \exp n}{1 - \exp n} \tag{11}$$

where n has the value of 8 for iron.

Another property to be considered is the voscosity of the magnetic fluid. The viscosity of a magnetic fluid is dependent on many variables. A functional relationship can be postulated of the form

$$\eta = f(\eta_o, M_s, D_i, k, T, H, \gamma, n_i) \ . \tag{12}$$

Rosensweig et al. [2], using dimensional analysis, postulated that the viscosity of the fluid in a magnetic field was a function

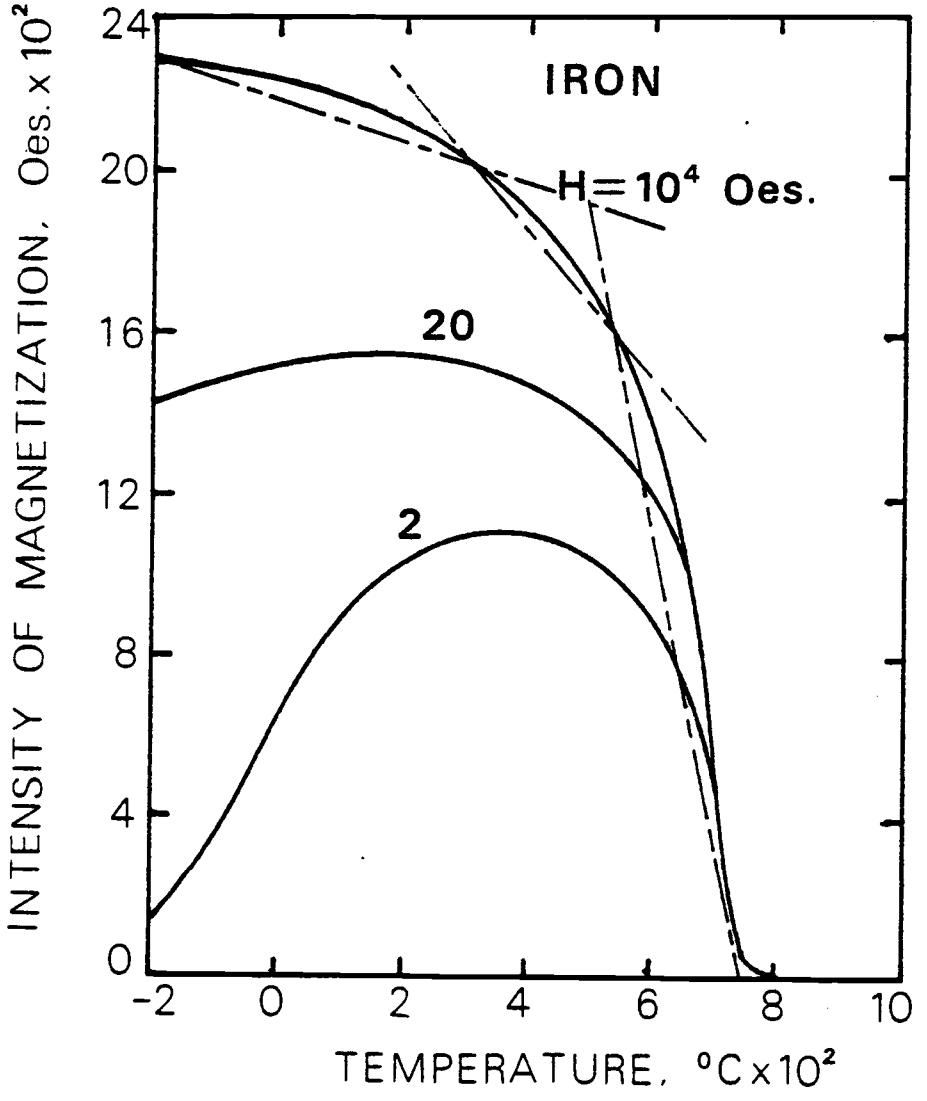

Figure 4. Magnetization for iron as a function of temperature. Broken lines are approximations for magnetization and support (Eq. 10).

of the ratio of hydrodynamic stress to magnetic stress, $\gamma\eta_o/MH$, which implies that there is no change of viscosity in the presence of an applied field. This was verified experimentally for values of $\gamma\eta_o/MH$ greater than 10^{-4}. For values between 10^{-6} and 10^{-4} the viscosity rapidly changes to the maximum value. In this transition region the viscosity is a function of both magnetic field and rate of shear. For values less than 10^{-6} the viscosity does not change and it maintains a uniform maximum value. McTague [6] also carried out an experiment for the magnetoviscosity of magnetic fluids with the condition that the magnetic field dependence of the viscosity is independent of particle size and concentration at low concentration. His results showed a different aspect of viscosity as compared to that of Rosensweig et al. This is because McTague did not regard the effects of particle diameters and concentration and the hydrodynamic stress. The analytical calculation of viscosity by Hall and Busenberg [7] shows some qualitative resemblance to the results of Rosensweig et al.

Consequently, it is found that the field dependence of the viscosity of a magnetic fluid in the presence of an applied field produce significant effects on the flow of such magnetic fluids. Table I [3,8,45,46] is given as a summary of properties of magnetic fluids.

4. Magnetic body force

There are two different types of pondoromotive forces. One is the Kelvin-type force, which can be formulated in terms of

TABLE I

Summary of Physical Properties of Ferrofluids

Carrier Liquid	Initial Susceptibility, x	Saturation Magnetization, Gauss		Density ρ_L (g/cm^3)	Viscosity at 30$_0$C η_s (cP)	Particle Concentration (based on Ferrofluid Density)	Volume-Percent Average Spherical Particle, Volume $\bar{v}$ (cm^3)
		M_0 (at T=0 °K	M_s (at H=10000 Oes				
Kerosene	3.78	735	392	1.54	102	17.5	9.5×10^{-19}
Kerosene	1.10	305	104	1.13	8.6	7.9	3.4×10^{-19}
Paraffin Oil	1.40	405	NA	1.10	122	10.2	3.4×10^{-19}
Paraffin Wax	1.01	285	276	1.12	Solid*	12.2	3.4×10^{-19}
Fluorocarbon	1.18	370	167	2.15	34.4	12.3	2.3×10^{-19}
Silicone Oil	1.60	330	NA	1.45	2500	9.7	3.0×10^{-19}
Water	1.60	256	161	1.24	8.1	3.7	1.0×10^{-18}
Glycerol	0.95	330	NA	1.51	1650	8.0	4.0×10^{-19}
Lignosite	NA		140	1.22	60	10.4	NA
DIO (Diester)	NA		255	1.205	500	10	NA

*Melting point 38°C.

magnetization, and the other Helmholtz-type force which is formulated explicitly using magnetic permeability. With the Helmholtz-type force, it is consistent to use the pressure which would be in the fluid in the absence of an applied field. With the Kelvin-type expression, the total pressure, including the contribution from an applied field, can be considered. Dealing with a magnetic body force of a magnetic fluid in the presence of an applied field, one can guess that the Kelvin-type force is predominant. This difference also can be seen through body forces in MHD and FHD systems.

As a qualitative description of body forces in various hydrodynamic systems, one can see the differences in the following areas:

OHD -- gravitational force = $\rho\bar{g}$,

MHD -- Lorentz force = $\bar{J} \times \bar{B}$/volume,

EHD -- Coulomb force = ne E,
as n number of unipolar ions or particles carries charge e in an electric field E,

FHD -- Kelvin force (in case, including helmholtz force)
$= \mu_o M \nabla H$,
the body force originates from the interaction of a magnetic field H with a ferromagnetic dipole moment (simply saying, magnetic moment) M in a magnetic fluid.

From an expression of Bernoulli's equation,

OHD -- $P + \frac{1}{2}\rho V^2 + \rho gz = \text{const.}$

MHD -- none, because the fluid flow itself generates electricity

EHD -- none, with the same reason as that of MHD

FHD -- [OHD] + magnet body force,

$$P + \frac{1}{2}\rho V^2 + \rho g z - \frac{1}{4\pi}\int_0^H M dH = \text{const.}$$

The direction of the body force is determined by the gradient of the field magnitude regardless of its orientation relative to that of the induced magnetic moment.

I-2. Study Objectives

In the energy conversion system discussed earlier, one can see that the improvement of heat transfer, high thermal conductivity, and high magnetization of a magnetic fluid will give a higher efficiency of energy conversion [35,36,37,48]. Their properties are also desirable for the other applications discussed. Knowledge of temperature and velocity profiles, and heat transfer rates in a magnetic fluid flow, will aid in the development of magnetic fluid systems.

The research reported in this thesis is on the velocity and temperature profiles and heat transfer coefficient of a magnetic fluid flow in a horizontal circular duct initiated by an applied magnetic field and heat transfer rate through the cylindrical wall to the magnetic fluid when exposed to peripheral and axial constant heat flux.

This study was composed of two parts. The first part was to obtain the velocity and temperature profiles analytically from the governing equations of a ferrofluid within the thermally fully

developed region of a cylinder and to determine the heat transfer coefficient, and magnetic Rayleigh number for stability of flow.

The second part was to obtain local velocity and temperature profiles in the radial direction at the thermal entrance region in the presence of an external magnetic field using a hot-wire anemometer and thermocouple. The results were compared to a numerical solution of the equations governing ferrofluidic motion at the thermal entrance region in a cylindrical duct.

A literature review is presented in Chapter II. Experimental work and reduction are presented in Chapter VI. A data table and related figures are given. The discussion and conclusion are given in Chapters VII and VIII.

II. LITERATURE SURVEY

Problems of a similar nature have been scarcely studied till now. However, these problems are frequently suggested by the conceptual idea [1], theoretical work [35,37, and 57], and the experimental work [36] of the energy conversion system using magnetic fluid as a working substance.

Past work concerning velocity profile and heat transfer rate of a magnetic fluid in a circular cylinder have not been directly conducted, but Berkovsky et al. [58 and 59] studied heat transfer across a vertical plane of a ferrofluid layer; and on a vertical circular magnetic fluid layer of an energized cable. Although these studies are not similar to the present study, the results give some examples of the effect of a gradient magnetic field on heat transfer and temperature profiles.

Also Neuringer et al. [57] showed that the temperature and pressure distribution for the steady two-dimensional source flow of a ferrofluid inside the annular region with heat addition are influenced by the azimuthal magnetic field produced by a current-carrying cylindrical conductor; and by the asymptotic solution. This was obtained through their analytical work concerning the temperature and pressure distribution (or expressed as the heat transfer and flow characteristics of ferrofluid) and are well related to the pyromagnetic coefficient of a ferrofluid itself.

There was a lot of research conducted on magnetic fluids when

they first came out. Only a few, however, are related to the hydrodynamic and thermal boundary-layer [60 and 61]. Buckmaster [60] deduced equations from the Neuringer-Rosensweig model [57] for the boundary layer flow of a ferrofluid and solved them numerically for a variety of circumstances. His study is a good example for flow patterns in ferrofluid motion. Luikov et al. [61] studied the convection in ferromagnetic fluid due to magnetocaloric effect. They show through analytical calculations that the temperature and velocity profiles for given conditions of the pyromagnetic coefficient in a duct are a function of the rate of change in an external magnetic field for the isothermal boundary conditions. If we apply a constant heat flux instead of constant temperature to the boundary, it will be obvious that the change of magnetic moment of the substance due to fluid temperature change under a constant applied magnetic field forces the fluid to flow, but the temperature and velocity profiles are different from what Luikov et al. [61] obtained. Gak [6] studied the case where an appreciable volume of vlowing liquid, containing particles with a non-vanishing magnetic moment, was subjected to the effect of local inhomogeneous fields (boundary effects) and passed through a uniform magnetic field of low intensity as an order of 10 - 10^3 Gauss which was perpendicular to the flowing direction of a liquid. The object of his study was to explain the nature of the effects associated with the magnetic treatment of water.

In reviewing the references cited above, it is obvious that

more analytical and experimental work is necessary on the flow structure [47] and heat transfer for magnetic fluid motion under the external magnetic field of variable range of intensity.

III. THEORETICAL ANALYSIS

III-1. Model

A. Model assumption

1. Isotropic,
2. Monophase,
3. Non-conducting,
4. Asymmetrical continuum model.

B. A set of independent variables

1. Scalars:
   a) liquid density,
   b) pressure,
   c) temperature,
   d) thermodynamic coefficients of a magnetic fluid.
2. Vectors:
   a) velocity,
   b) magnetic field intensity,
   c) magnetic field induction of magnetization,
   d) temperature gradient.

C. Governing equations

1. Conservation of mass,
2. Conservation of change in momentum:

   Navier-Stokes equation with the addition of the Maxwellian stress tensor in the fluid for a magnetic field.

3. Conservation of change in intrinsic angular momentum :
4. Conservation of energy
5. Maxwell equation
6. An appropriate equation of magnetization
7. Additional equations.

III-2. Continuum Model Approach

A magnetic fluid is regarded as a perfect continuum model since it behaves every aspect of the continuum properties [49]. Historically, Eringen [49] pioneered and developed a continuum theory with intrinsic rotation. This is often called asymmetrical hydrodynamics because of the asymmetry of the stress tensors which stems from an averaging over the centers of mass of microcontinuum units having rotatory degrees of freedom.

Before describing further details about the field equation, some definitions should be presented for a better understanding of the continuum model of a magnetic fluid.

A. Definitions

1. Body force:

   A rate of arrival of linear momentum.

2. Body couple:

   The moment of body forces like an electromagnetic force about an arbitrary line within or without the domain of the body. It is stated that a body couple is a rate of arrival of internal angular momentum from a magnetic field.

3. Stress:

   The stress is the applied load (or external forces) per unit area acting on the common interface of domains and is directly associated with the flux of linear momentum imparted from one part to its neighbor and from one neighbor to the next through their interfaces.

4. Couple Stress:

   The moment of a body force per unit area about an axis which may cause a rotational effect on the surface through which it is transmitted. Thus, this response of the body consists of the moment of the stress which is clearly associated with the flux of moment of momentum which is transmitted from one body to another through their common interface or from one part of the body to another inside the body through a common bounding surface. This moment stress which acts on such common bounding surfaces and which exerts a rotational effect on such surfaces is also measured per unit area of the surface. In short, it is the rate of arrival of the internal angular momentum from neighboring material surrounding through diffusion.

B. Tensor notations

1. Body couple per unit mass -- G_i (pseudovector)
2. Surface couple per unit area -- $S_i = n_j S_{ij}$ (pseudovector)
3. Couple stress tensor -- S_{ij}
4. Vector surface traction -- $\sigma_i = n_j \sigma_{ij}$

5. Stress tensor -- σ_{ij}

6. Translatory velocity -- V_i

7. Rotatory velocity -- W_i

8. Rate of deformation --

$$\frac{\partial V_i}{\partial x_j} = \frac{1}{2}\left(\frac{\partial V_i}{\partial x_j} + \frac{\partial V_j}{\partial x_i}\right) + \frac{1}{2}\left(\frac{\partial V_i}{\partial x_j} - \frac{\partial V_j}{\partial x_i}\right)$$

$$= D_{ij} + W_{ij}$$

$$= D_{ij} + e_{ijk} W_k$$

= (rate of deformation) + (vorticity or spin tensor)

$$D_{ij} = \frac{\partial V_i}{\partial x_j} - W_{ij} = V_{i,j} - e_{ijk} W_k$$

9. Vector body force --

$$F_i = \mu_o M_j H_{i,j}$$

10. Pseudovector body couple/unit mass --

$$G_i = \mu_o M_j H_k e_{ijk}$$

11. Total energy/unit mass --

= (kinetic energy) + (average energy of intrinsic rotations)

+ (magnetic field energy) + (internal energy)

+ (chemical potential)

$$E = \frac{1}{2}V^2 + \frac{1}{2}IW^2 + \left[\frac{1}{2}\mu_o M^2 - \mu_o H_i (H_i + M_i)\right] + C_v T + \Phi$$

III-3. Comparison to Conventional Continuum Theory

1. The rotatory degrees of freedom of magnetic fluids

   a) The difference can be shown by the introduction of an internal spin field, W, which is essentially different from the bulk angular velocity, defined as half a vorticity vector.

   b) It can be shown by the recognition of the existence of a pseudovector magnetic body couple and couple stress tensor.

   In these cases the stress tensor is asymmetrical and the conservation of the total moment of angular momentum cannot be automatically fulfilled whenever that of the linear momentum can be assured.

III-4. Governing Equations of a Magnetic Fluid in an Asymmetrical Monophase Approximation

1. Conservation of mass:

$$\frac{\partial \rho}{\partial t} + (\rho V_i)_{,i} = 0 \tag{13}$$

2. Conservation of momentum:

   Navier-Stokes equation

$$\rho \frac{dV_i}{dt} = \sigma_{ij,j} + \rho \mu_o M_j H_{i,j} \tag{14}$$

where the stress tensor

$$\sigma_{ij,j} = \frac{\partial}{\partial x_j} [-p\delta_{ij} + \sigma'_{ij}] - \gamma e_{ijk} [e_{jki} V_{k,i} - 2W_j]_{,k}$$

and the viscous stress tensor

$$\sigma'_{ij} = \mu_o \left[\frac{\partial V_i}{\partial x_j} + \frac{\partial V_j}{\partial x_i} - \frac{2}{3}\delta_{ij} \frac{\partial V_k}{\partial x_k} \right] + \lambda_o \delta_{ij} \frac{\partial V_k}{\partial x_k} \quad .$$

Substituting the viscous stress tensor into the stress tensor and writing in a simple form, we have

$$\sigma_{ij,j} = (-p\delta_{ij})_j + \mu g_{ij} V_{i,j} + (\lambda_o + \frac{\mu}{3})(V_{i,j})_j$$

$$- \gamma_o e_{ijk} \left[e_{jki} V_{k,i} - 2W_j \right]_{,k} .$$

Thus the Navier-Stokes equation has the form

$$\rho \frac{dV_i}{dt} = (-p\delta_{ij})_j + \mu g_{ij} V_{i,j} + (\lambda_o + \frac{\mu}{3})(V_{i,j})_j$$

$$-\gamma_o e_{ijk} \left[e_{jki} V_{k,i} - 2W_j \right]_{,k} + \rho \mu_o M_j H_{i,j} \qquad (15)$$

where the fourth and fifth terms of the right-hand side represent the effects due to couple stress and body couple.

3. Conservation of energy --

$$\rho \frac{\partial T}{\partial t} = \lambda \nabla^2 T + \sigma_{ij} V_{i,j} + S_{ij} W_{i,j} + \mu_o \delta T \left(\frac{\partial M}{\partial T} \right)_H \frac{dH_i}{dt} \quad . \qquad (16)$$

4. Conservation of intrinsic regular momentum

$$I \frac{dW_i}{dt} = S_{ij,j} - \sigma_{jk} e_{ijk} + \rho \mu_o M_j H_k e_{ijk} \qquad (17)$$

5. Pressure

$$P = P(\rho, T, H) \qquad (18)$$

6. Additional equations

a) Balance of momentum of inertia of unit mass

$$\frac{\partial I}{\partial t} + (IV_i)_{,i} = 0 \qquad (19)$$

b) Dynamics of magnetization

If the deviation from equilibrium magnetization is not too large, then the following equation is acceptable for rotating with the subcontinuum unit.

$$\frac{\partial M_i}{\partial t} = \frac{1}{\tau}\left(\frac{|M|}{|H|} H_i - M_i\right) \quad , \tag{20}$$

where the relaxation parameter τ has an order of 10^{-5} sec. This is mainly defined by the scale of rotary Brownian motion, $v\eta/kT$.

7. Maxwellian equation

Since the displacement currents and electric conductivity of the magnetic fluid are disregarded.

$$\nabla \times H = 0 \quad , \tag{1}$$
$$\nabla(H + M) = 0 \quad .$$

The equations shown above consist of constitutive equations for a magnetic fluid. In the actual approaches to the problem, a few assumptions are made in order to simplify or linearize equations governing a magnetic fluid flow and heat transfer. The equations, when simplified with the assumptions, must still hold the major effect due to magnetic properties of a magnetic fluid in addition to the conventional setting of equation, and also the changes in the total feature due to the assumptions must be minimal enough as compared to the overall approach. If the assumptions satisfy the above conditions, then the solutions to the governing equation can give

rise to the answers to the physical phenomena.

III-5. Flow Stability Condition

From Equations (13), (15), and (16) the stability condition will be sought for an incompressible fluid and for a fluid which is totally balanced with an external magnetic field by introducing dimensionless variables.

Let

$$v = \bar{v}\,(k/\rho c\ell),$$

$$t = \bar{t}\,(\rho\ell^2/\mu),$$

$$T = \bar{T}\left[\ell\left(A + \frac{\mu_o T_o K h}{\rho c}\right)\right],$$

$$p = \bar{p}\,(\mu k/\rho c\ell^2),$$

where ℓ is the characteristic length,

$$A = -\frac{\partial T}{\partial z},$$

$$h = \frac{\partial H}{\partial z}.$$

Here Equations (13), (15), and (16) will be written in vectorial form for convenience. Thus, we have

$$\nabla\cdot v = 0 \tag{21}$$

$$\rho\frac{dv}{dt} = -\nabla p + \mu\nabla^2 v + \mu_o M\nabla H, \tag{22}$$

$$\rho c\frac{dT}{dt} = k\nabla^2 T + \mu_o T_o\left(\frac{\partial M}{\partial T}\right)_H \frac{dH}{dt}. \tag{23}$$

The magnetic field is constant with respect to time. Rewriting Equations (22) and (23) we have

$$\rho\frac{\partial v}{\partial t} = - \nabla p + \mu\nabla^2 v + \mu_o M\nabla H , \tag{24}$$

$$\rho c\frac{\partial T}{\partial t} + \rho c v\cdot\nabla T = k\nabla^2 T + \mu_o T_o \left(\frac{\partial M}{\partial T}\right)_H \mathbf{v}\cdot\nabla H . \tag{25}$$

By an approximation for the temperature dependence of magnetization (Fig. 4)

$$\left(\frac{\partial M}{\partial T}\right)_H = K ,$$

and $$\mu_o M = KT,$$

where T implies $T_c - T$, which T_c is the Curie temperature. The magnetization decreases with heating, so that a fluid is cooled when it is adiabatically displaced downstream ($dz > 0$) from a position of equilibrium into a region of lower pressure, and is heated if the magnetic field strength increases with distance. The temperature change due to the magnetocaloric effect is

$$\Delta T = \frac{\mu_o T_o K h}{\rho c}\Delta z \tag{26}$$

where the temperature T_o is taken to be average over the distance. Rearranging Equation (25), we have

$$\rho c\frac{\partial T}{\partial t} = k\ \nabla^2 T + [\rho c A + T_o \mu_o K h]\ v . \tag{27}$$

Then substituting dimensionless variables into Equations (24) and (27) gives

$$\frac{\partial \bar{v}}{\partial \bar{t}} = - \nabla \bar{p} + \nabla^2 \bar{v} + \frac{\mu_o \rho c K h \ell^4}{\mu k}\left(A + \frac{\mu_o T_o K h}{\rho c}\right)\bar{T} \tag{28}$$

and

$$\frac{\mu c}{k}\ \frac{\partial \bar{T}}{\partial \bar{t}} = \nabla^2 \bar{T} + \bar{v} \tag{29}$$

In Equation (28) the coefficient of the last term is dimensionless combination of the parameters. Comparing the ordinary convective problems [50,51], the dimensionless combination plays the same role as the Rayleigh number. Thus we can have so-called magnetic Rayleigh number

$$Ra_M = \frac{\mu_o \rho c K h \ell^4}{\mu k} \left(A + \frac{\mu_o T_o K h}{\rho c} \right) . \qquad (30)$$

This number (30) is somewhat similar with that of Shliomis [52], Berkovsky et al. [53], and Lalas et al. [54], Luikov et al. [55] presented.

This magnetic Rayleigh number actually indicates whether the thermomechanical equilibrium of a magnetic fluid can be maintained. Thus, on the basis of known results of the theory of convection it is stated that thermomechanical equilibrium of a magnetic fluid is stable only as long as the magnetic Rayleigh number, Ra_M^*, remains less than the critical value of Ram. For Ram > Ra_M^* the motionless fluid shifts to a steady convective motion. The critical magnetic Rayleigh number is determined by the geometry and the boundary conditions of a model. Berkovsky [53] mentioned that the critical number for a cylindrical layer of magnetic fluid is equal to 1707. Therefore, any value over this critical value of the magnetic Rayleigh number produces a flow field that is regarded as steady motion.

The next chapter presents the assumptions made to the governing equations, and also gives the solutions to the simplified governing equations.

IV. ANALYTICAL SOLUTIONS FOR FULLY DEVELOPED FLOW

IV-1. Physical Model

As mentioned in Chapter I, fluid flow in the circular tube with constant heat flux was chosen. Figure(5)shows a schematic diagram of the model. This has the same dimensions as the experimental test section.

IV-2. Assumptions

In Chapter III, the equations governing a flow field have been established for a magnetic fluid regarded as an asymmetric continuum.

Now by making a few appropriate assumptions which do not change the basic principles of the constitutive equations, one can simplify or linearize the governing equations. This will make it possible to obtain solutions to the governing equation. The following assumptions were made in this study.

1. Steady state

Steady state is assumed. If the magnetic Rayleigh number is larger than a critical number, the flow field will be stable and steady since heat flux and external magnetic field are constant. Therefore, the steady state assumption is reasonable.

2. Axisymmetric, fully developed flow

It is assumed that fluid flows inside a tube far downstream of any entrance or any elbow. Hence,

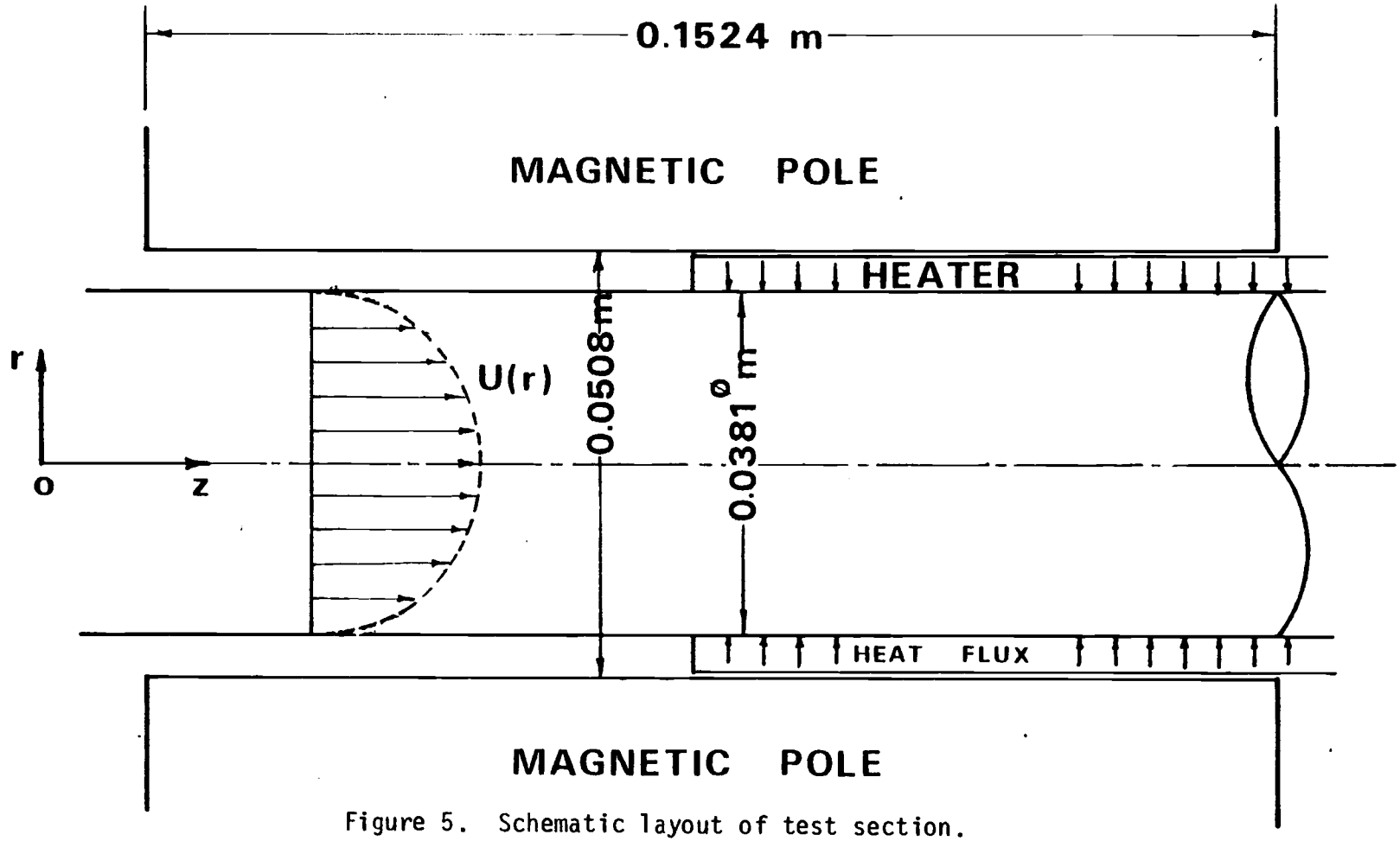

Figure 5. Schematic layout of test section.

$$v_z >> v_r,\ v_\theta\ ,$$

$$\frac{\partial v_z}{\partial r} >> \frac{\partial v_r}{\partial z}\ ,\ \frac{\partial v_r}{\partial r}\ ,\ \frac{\partial v_z}{\partial z}\ .$$

3. Incompressible.

Since the fluid is a liquid, it is assumed to be incompressible.

4. The external magnetic field is constant.

Even though there is any change in an applied field, the relaxation time is so small that the spin energy becomes frozen soon to its domain.

$$H = \left(H_r,\ H_\theta,\ H_z\right) = \text{constant},$$

$$h = \frac{\partial H_z}{\partial z} >> \frac{\partial H_\theta}{\partial r},\ \frac{\partial H_z}{\partial \theta}\ .$$

5. The magnetization is approximated by using Equation (10).

IV-3. Simplification and non-dimensionalization of the Equations

1. Simplification of the equations.

With the above assumptions, the constitutive equations are written in a cylindrical coordinate system.

The conservation of mass:

$$\frac{\partial \rho}{\partial t} + \frac{1}{r}\frac{\partial}{\partial r}(r\rho v_r) + \frac{1}{r}\frac{\partial}{\partial \theta}(\rho v_\theta) + \frac{\partial}{\partial z}(\rho v_z) = 0. \qquad (31)$$

Rewriting the above equation with assumptions we have

$$\frac{\partial \rho}{\partial t} + \rho\frac{\partial v_r}{\partial r} + v_r\frac{\partial \rho}{\partial r} + \frac{\rho v_r}{r} + \frac{v_\theta}{r}\frac{\partial \rho}{\partial \theta} + \frac{\rho}{r}\frac{\partial v_\theta}{\partial \theta}$$

$$+ \rho\frac{\partial v_z}{\partial z} + v_z\frac{\partial \rho}{\partial z} = 0.$$

The final form of equation is

$$\frac{\partial v_r}{\partial r} + \frac{v_r}{r} + \frac{\partial v_z}{\partial z} = 0. \qquad (32)$$

The conservation of momentum:

r-direction:

$$\frac{\partial v_r}{\partial t} + v_r\frac{\partial v_r}{\partial r} + \frac{v_\theta}{r}\frac{\partial v_r}{\partial \theta} + v_z\frac{\partial v_r}{\partial z} - \frac{v_\theta^2}{r}$$

$$= -\frac{1}{\rho}\frac{\partial p}{\partial r} + \nu\left[\frac{\partial^2 v_r}{\partial r^2} + \frac{1}{r^2}\frac{\partial^2 v_r}{\partial \theta^2} + \frac{\partial^2 v_r}{\partial z^2} + \frac{1}{r}\frac{\partial v_r}{\partial r}\right.$$

$$\left. - \frac{2}{r^2}\frac{\partial v_\theta}{\partial \theta} - \frac{v_r}{r^2}\right] + \mu M\left(\frac{\partial H_r}{\partial r} + \frac{1}{r}\frac{\partial H_r}{\partial \theta} + \frac{\partial H_r}{\partial z}\right)$$

Note: The arrow and the circled number means cancellation due to the related assumptions in Section IV-2.

θ-direction:

$$\frac{\partial v_\theta}{\partial t} + v_r \frac{\partial v_\theta}{\partial r} + \frac{v_\theta}{r} \frac{\partial v_\theta}{\partial \theta} + v_z \frac{\partial v_\theta}{\partial z} + \frac{v_r v_\theta}{r}$$

$$= - \frac{1}{\rho} \frac{\partial p}{r \partial \theta} + \nu \left[\frac{\partial^2 v_\theta}{\partial r^2} + \frac{1}{r^2} \frac{\partial^2 v_\theta}{\partial \theta^2} + \frac{\partial^2 v_\theta}{\partial z^2} + \frac{1}{r} \frac{\partial v_\theta}{\partial r} \right.$$

$$\left. + \frac{2}{r^2} \frac{\partial v_r}{\partial \theta} - \frac{v_\theta}{r^2} \right] + \mu_o M \left[\frac{\partial H_\theta}{\partial r} + \frac{\partial H_\theta}{r \partial \theta} + \frac{\partial H_\theta}{\partial z} \right] .$$

Z-direction:

$$\frac{\partial v_z}{\partial t} + v_r \frac{\partial v_z}{\partial r} + \frac{v_\theta}{r} \frac{\partial v_z}{\partial \theta} + v_z \frac{\partial v_z}{\partial z}$$

$$= - \frac{1}{\rho} \frac{\partial p}{\partial z} + \nu \left[\frac{\partial^2 v_z}{\partial r^2} + \frac{1}{r^2} \frac{\partial^2 v_z}{\partial \theta^2} + \frac{\partial^2 v_z}{\partial z^2} + \frac{1}{r} \frac{\partial v_z}{\partial r} \right]$$

$$+ \mu_o M \left[\frac{\partial H_z}{\partial r} + \frac{1}{r} \frac{\partial H_z}{\partial \theta} + \frac{\partial H_z}{\partial z} \right] .$$

Hence, we have

$$\frac{\partial p}{\partial r} = 0, \tag{33}$$

$$\frac{\partial p}{r \partial_\theta} + 0, \tag{34}$$

$$v_r \frac{\partial v_z}{\partial r} + v_z \frac{\partial v_z}{\partial z} = - \frac{1}{\rho} \frac{\partial p}{\partial z} + \nu \left[\frac{\partial^2 v_z}{\partial r^2} + \frac{1}{r} \frac{\partial v_z}{\partial r} \right] + \mu_o M \frac{\partial H_z}{\partial z} . \tag{35}$$

The conservation of energy:

$$\rho c \left[\frac{\partial T}{\partial t} + v_r \frac{\partial T}{\partial r} + v_\theta \frac{\partial T}{\partial \theta} + v_z \frac{\partial T}{\partial z} \right]$$

$$- \mu_o T_o K \left[\frac{\partial H}{\partial t} + v_r \frac{\partial H}{\partial r} + \frac{v_\theta}{r} \frac{\partial H}{\partial \theta} + v_z \frac{\partial H}{\partial z} \right]$$

$$= \frac{1}{r} \frac{\partial}{\partial r} \left[rk \frac{\partial T}{\partial r} \right] + \frac{1}{r^2} \frac{\partial}{\partial \theta} \left[k \frac{\partial T}{\partial \theta} \right] + \frac{\partial}{\partial z} \left[k \frac{\partial T}{\partial z} \right]$$

$$+ \mu \left[2 \left\{ \left(\frac{\partial v_z}{\partial r} \right)^2 + \left(\frac{1}{r} \frac{\partial v_\theta}{\partial \theta} + \frac{v_r}{r} \right)^2 + \left(\frac{\partial v_z}{\partial z} \right)^2 \right\} \right.$$

$$+ \left(\frac{\partial v_z}{\partial \theta} + \frac{\partial v_\theta}{\partial z} \right)^2 + \left(\frac{\partial v_r}{\partial z} + \frac{\partial v_z}{\partial r} \right)^2 + \left(\frac{1}{r} \frac{\partial v_r}{\partial \theta} + \frac{\partial v_\theta}{\partial r} \right)^2$$

$$\left. - \frac{v_\theta}{r} \right)^2 \Bigg] + \lambda \left(\frac{\partial v_r}{\partial r} + \frac{1}{r} \frac{\partial v_\theta}{\partial \theta} + \frac{v_r}{r} + \frac{\partial v_z}{\partial z} \right) .$$

Hence, we have

$$\rho c \left[v_r \frac{\partial T}{\partial r} + v_z \frac{\partial T}{\partial z} \right] - \mu_o T_o K v_z \frac{\partial H}{\partial z}$$

$$= \frac{1}{r} \frac{\partial}{\partial r} \left(kr \frac{\partial T}{\partial r} \right) + k \frac{\partial^2 T}{\partial r^2} + \mu \left(\frac{\partial v_z}{\partial r} \right)^2 . \qquad (36)$$

2. Non-dimensionalization of the equations.

The following dimensionless variables are introduced:

$$U_z = \frac{V_z}{V_{z\,av}} ,$$

$$U_r = \frac{V_r}{V_{z\,av}} ,$$

$$p' = \frac{p}{\rho V_{z\,av}^2} ,$$

$$r' = \frac{r}{a} ,$$

$$z' = \frac{z}{a} ,$$

$$t = (T - T_w)/(T_c - T_w)$$

$$= (T - T_w)/\Delta T ,$$

$$Re = \frac{2a\rho V_{z\,av}}{\mu} ,$$

$$Pr = \frac{\mu c}{k} ,$$

$$H' = \frac{H}{H_o} ,$$

$$M' = \frac{M}{M_s} .$$

Then Equation (32) becomes

$$\frac{\partial U_r}{\partial r'} + \frac{U_r}{r'} + \frac{\partial U_z}{\partial z'} = 0. \qquad (37)$$

Equation (35) is written to a form

$$U_r \frac{\partial U_z}{\partial r'} + U_z \frac{\partial U_z}{\partial z'} = -\frac{\partial p'}{\partial z'} + \frac{2}{Re} \frac{1}{r'} \frac{\partial}{\partial r'} \left(r' \frac{\partial U_z}{\partial r'} \right) + \frac{\mu_0 M_0 H_0}{\rho V_{z\,av}^2} M' \frac{\partial H'}{\partial z'} \qquad (38)$$

where M' is defined by using Equation (10).

$$\mu_o M_o M' = M_o K(t_c - t). \tag{10}$$

Also for a constant field intensity gradient let

$$h = \frac{\partial H'}{\partial z'} \quad ,$$

then (35) becomes

$$U_r \frac{\partial U_z}{\partial r'} + U_z \frac{\partial U_z}{\partial z'} = -\frac{\partial p'}{\partial z'} + \frac{2}{Re} \frac{1}{r'} \frac{\partial}{\partial r'} \left(r \frac{\partial U_z}{\partial r'} \right) + \frac{M_o H_o K h}{\rho V_{z\,av}^2} (t_c - t). \tag{39}$$

The energy Equation (36) is given by

$$\Delta T U_r \frac{\partial t}{\partial r'} + U_z A - \frac{a Q_m}{\rho c V_{zav}^2} = \frac{2}{RePr} \frac{\Delta T}{r'} \frac{\partial}{\partial r'} \left(r' \frac{\partial t}{\partial r'} \right) + \frac{2\Delta T}{RePr} \frac{\partial^2 t}{\partial z'^2} + \frac{\mu V_{zav}}{\rho c a} \left(\frac{\partial U_z}{\partial r'} \right)^2 \tag{40}$$

where $A = \pm \frac{\partial T}{\partial z'}$, and Q_m represents the magnetocaloric energy. The magnetocaloric effect is assumed to be constant since the magnetic fluid flow is under steady motion with constant external magnetic field and heat flux.

Equations (37), (38), and (40) are used for the thermally fully developed flow problem in the next section.

IV-4. Hydrodynamically, Thermally Fully Developed Flow

With a few more assumptions Equations (37), (38), and (40) can be linearized. First, let

$$\frac{\partial T}{\partial z'} = \pm A = \text{constant},$$

where the positive or negative signs are chosen for cooling or heating respectively. Hence

$$\frac{\partial^2 T}{\partial z'^2} = 0.$$

The pressure gradient is assumed to be constant in fully developed flow, and there is no dissipation energy due to the viscosity effect because of the low velocity. Therefore,

$$\frac{\partial \bar{p}}{\partial z} = \text{constant}$$

$$\mu\left(\frac{\partial U_z}{\partial r'}\right)^2 = 0.$$

For fully developed flow,

$$U_r = 0.$$

Hence, from the continuity equation

$$\frac{\partial U_z}{\partial z'} = 0,$$

$$\frac{\partial^2 U_z}{\partial z'^2} = 0.$$

Thus Equations (38) and (40) are reduced to

$$0 = -\frac{\partial p'}{\partial z} + \frac{2}{Re}\frac{1}{r'}\frac{\partial}{\partial r'}\left(r'\frac{\partial u_z}{\partial r'}\right) + \frac{M_o H_o K h}{\rho V_{zav}^2}(t_c - t), \qquad (41)$$

and

$$U_z A = \frac{aQ_m}{\rho c V_{zav}^2} + \frac{2\Delta T}{RePr}\frac{1}{r'}\frac{\partial}{\partial r'}\left(r'\frac{\partial t}{\partial r'}\right). \qquad (42)$$

2. Heating case

For brevity, let us omit any prime notations and subscripts in Equations (41) and (42),

Let $S = \frac{M_o H_o K h}{\rho V_{av}^2}$, $F = \frac{aQ_m}{\rho c V_{av}^2}$,

$St = (St_c - \frac{\partial p}{\partial z}) + \frac{2}{Re}\frac{1}{r}\frac{\partial}{\partial r}(r\frac{\partial u}{\partial r})$, and $P_y = (St_c - \frac{\partial p}{\partial z}) = \text{const.}$

Then Equation (41) is written as

$$St = P_y + \frac{2}{Re}\frac{1}{r}\frac{\partial}{\partial r}(r\frac{\partial u}{\partial r}). \qquad (43)$$

From the energy Equation (42) becomes,

$$-Au = F + \frac{2\Delta T}{RePr}\frac{1}{r}\frac{\partial}{\partial r}(r\frac{\partial t}{\partial r}) . \qquad (44)$$

Differentiating Equation (43) twice and then substituting into Equation (44), we obtain a fourth order Bessel-equation. That is

$$\frac{\partial^4 u}{\partial r^4} + \frac{2}{r}\frac{\partial^3 u}{\partial r^3} - \frac{1}{r^2}\frac{\partial^2 u}{\partial r^2} + \frac{1}{r^3}\frac{\partial u}{\partial r} + \frac{ASRe^2 Pr}{4\Delta T}u$$

$$+ \frac{FSRe^2 Pr}{4\Delta T} = 0. \qquad (45)$$

Let $\gamma = \frac{ASRe^2Pr}{4\Delta T}$,

then we can write Equation (45) in the form

$$\nabla^4 u + \gamma u = \gamma \frac{F}{A} \tag{46}$$

where $\nabla^4 = \nabla^2(\nabla^2) = \nabla^2 \left[\frac{\partial^2}{\partial r^2} + \frac{1}{r}\frac{\partial}{\partial r}\right] = \frac{\partial^4}{\partial r^4} + \frac{2}{r}\frac{\partial^3}{\partial r^3} - \frac{1}{r}\frac{\partial^2}{\partial r^2} + \frac{1}{r^3}\frac{\partial}{\partial r}$.

The solution to Equation (46) is

$$u = -\frac{F}{A} + c_1 J_0(\gamma^{\frac{1}{4}}\sqrt{i}\, r) + c_2 Y_0(\gamma^{\frac{1}{4}}\sqrt{i}\, r) + c_3 I_0(\gamma^{\frac{1}{4}}\sqrt{i}\, r) + c_4 K_0(\gamma^{\frac{1}{4}}\sqrt{i}\, r) \ . \tag{47}$$

In order to get rid of the coefficients of Equation (47) the equation needs four boundary conditions. One boundary condition is presumed that the velocity at centerline is finite. That is,

$$u = \text{finite at } r = 0. \tag{48}$$

Since Y_0 and K_0 are undefined at $r = 0$, the coefficient c_2 and c_4 have to be zero.

Then Equation (47) has to take complex coefficients due to the argument.

$$u = -\frac{F}{A} + (C_{1r} + iC_{1i})\, J_0(\gamma^{\frac{1}{4}}\sqrt{i}\ r) + (C_{3r} + iC_{3i})\, I_0(\gamma^{\frac{1}{4}}\sqrt{i}\, r) \tag{49}$$

By the definitions of Kelvin Functions [56]

$\mathrm{Ber}(\gamma^{\frac{1}{4}} r)$ = real part of $I_0(\gamma^{\frac{1}{4}}\sqrt{i}\, r)$,

$\mathrm{Bei}(\gamma^{\frac{1}{4}} r)$ = imaginary part of $I_0(\gamma^{\frac{1}{4}}\sqrt{i}\, r)$,

and by the properties that the function $J_0(\gamma^{\frac{1}{4}}\sqrt{i}\, r)$ is the complex conjugate of $I_0(\gamma^{\frac{1}{4}}\sqrt{i}\, r)$,

$\mathrm{Ber}(\gamma^{\frac{1}{4}} r)$ = real part of $J_0(\gamma^{\frac{1}{4}}\sqrt{i}\, r)$,

$\mathrm{Bei}(\gamma^{\frac{1}{4}} r)$ = - imaginary part of $J_0(\gamma^{\frac{1}{4}}\sqrt{i}\, r)$.

Equation (49) can be written in the form

$$u = -\frac{F}{A} + [C_{1_r}+C_{3_r}]\ \mathrm{Ber}(\gamma^{\frac{1}{4}}r) + [C_{3_i}-C_{1_i}]\ \mathrm{Bei}(\gamma^{\frac{1}{4}}r).$$

Let $$(C_{1_r} + C_{3_r}) = D_r$$

$$(C_{3_i} - C_{1_i}) = D_i$$

then
$$u = -\frac{F}{A} + D_r\mathrm{Ber}(\gamma^{\frac{1}{4}}r) + D_i\mathrm{Bei}(\gamma^{\frac{1}{4}}r). \qquad (50)$$

The other boundary condition is that the velocity is zero at the wall

$$u = 0 \quad \text{at} \quad r = 1. \qquad (51)$$

Hence
$$D_i = \frac{\frac{F}{A} - D_r\mathrm{Ber}(\gamma^{\frac{1}{4}})}{\mathrm{Bei}(\gamma^{\frac{1}{4}})}.$$

The average velocity is defined by

$$u_{av} = \frac{1}{A}\int u dA$$

where A is the cross-sectional area.

Therefore, for a scaled geometry the average velocity is

$$\frac{1}{2} = \int_0^1 urdr. \tag{52}$$

Applying Equation (50) to (52), then performing the integration, we obtain

$$D_r = \frac{\gamma^{\frac{1}{4}}\left[\frac{1}{2} + \frac{F}{2A} + \frac{F}{A}\frac{1}{\gamma^{\frac{1}{4}}}\frac{Bér(\gamma^{\frac{1}{4}})}{Bei(\gamma^{\frac{1}{4}})}\right]}{\left[Béi(\gamma^{\frac{1}{4}}) + \frac{Ber(\gamma^{\frac{1}{4}})}{Bei(\gamma^{\frac{1}{4}})}\, Bér(\gamma^{\frac{1}{4}})\right]}$$

By defining the coefficients as such, Equation (50) presents the velocity profile along the radial direction.

In order to obtain the temperature profile, substituting Equation (50) into Equation (44) yields,

$$\frac{\Delta T}{r}\frac{\partial}{\partial r}\left(r\frac{\partial t}{\partial r}\right) = G_1 Bei(\gamma^{\frac{1}{4}}r) + G_2 Ber(\gamma^{\frac{1}{4}}r) \tag{53}$$

where $G_1 = -\frac{ARePrD_i}{2}$

$G_2 = -\frac{ARePrD_r}{2}$.

Integrating Equation (53) once

$$\Delta T\, r\frac{\partial t}{\partial r} = -\frac{G_1}{\gamma^{\frac{1}{4}}}[rBér(\gamma^{\frac{1}{4}}r)] + \frac{G_2}{\gamma^{\frac{1}{4}}}[rBéi(\gamma^{\frac{1}{4}}r)] + c_5 .$$

The boundary condition is

$$\frac{\partial t}{\partial r} = 0 \qquad \text{at} \quad r = 0,$$

hence

$$c_5 = 0.$$

Then integrating again

$$\Delta T \cdot t = -\frac{G_1}{\gamma^{\frac{1}{2}}} \mathrm{Ber}(\gamma^{\frac{1}{4}} r) + \frac{G_2}{\gamma^{\frac{1}{2}}} \mathrm{Bei}(\gamma^{\frac{1}{4}} r) + c_6$$

and the boundary condition is

$$t = tw = 0 \qquad \text{at} \qquad r = 1.$$

Then

$$c_6 = \frac{G_1}{\gamma^{\frac{1}{2}}} \mathrm{Ber}(\gamma^{\frac{1}{4}}) - \frac{G_2}{\gamma^{\frac{1}{2}}} \mathrm{Bei}(\gamma^{\frac{1}{4}}).$$

Therefore, we have a temperature profile equation

$$\Delta T \cdot t = \frac{G_1}{\gamma^{\frac{1}{2}}} [\mathrm{Ber}(\gamma^{\frac{1}{4}}) - \mathrm{Ber}(\gamma^{\frac{1}{4}} r)] + \frac{G_2}{\gamma^{\frac{1}{2}}} [\mathrm{Bei}(\gamma^{\frac{1}{4}} r) - \mathrm{Bei}(\gamma^{\frac{1}{4}})] \quad . \tag{54}$$

When $r = 0$, $t = 1$ and $\mathrm{Bei}\,(0) = 0$

$\mathrm{Ber}\,(0) = 1.$

Applying this condition to Equation (54) we have

$$\Delta T = T_c - T_w = \frac{G_1}{\gamma^{\frac{1}{2}}} \left[\mathrm{Ber}(\gamma^{\frac{1}{4}}) - 1\right] - \frac{G_2}{\gamma^{\frac{1}{2}}} \mathrm{Bei}(\gamma^{\frac{1}{4}}). \tag{55}$$

From Equation (55), we can also obtain the value of $A = \pm \frac{\partial T}{\partial z}$ by using a root finding procedure because G_1, G_2 and γ have A in them.

Dividing Equation (54) by Equation (55)

$$\boxed{t = K_1 [\mathrm{Ber}(\gamma^{\frac{1}{4}}) - \mathrm{Ber}(\gamma^{\frac{1}{4}} r)] + K_2 [\mathrm{Bei}(\gamma^{\frac{1}{4}} r) - \mathrm{Bei}(\gamma^{\frac{1}{4}})]} \tag{56}$$

where

$$K_1 = \frac{G_1}{G_1[\mathrm{Ber}(\gamma^{\frac{1}{4}}) - 1] - G_2\mathrm{Bei}(\gamma^{\frac{1}{4}})} ,$$

and

$$K_2 = \frac{G_2}{G_1[\mathrm{Ber}(\gamma^{\frac{1}{4}}) - 1] - G_2\mathrm{Bei}(\gamma^{\frac{1}{4}})} .$$

Thus, the velocity and temperature profile equations have been derived.

The medium temperature is obtained by using the following equation

$$T_m = \frac{1}{AV_{av}} \int_A uTdA ,$$

and the above form of equation can be written in a scaled geometry

$$t_m + \frac{T_w}{\Delta T} = 2\int_0^1 ut\, rdr + \frac{2T_w}{\Delta T} \int_0^1 urdr . \tag{57}$$

Substituting Equations (50) and (56) into (57) we have, therefore,

$$\begin{aligned} t_m + \frac{T_w}{\Delta T} &= (2B_1 - \frac{2T_w}{\Delta T}\ \frac{F}{A}) \int_0^1 rdr \\ &+ (2B_2 + \frac{2T_w}{\Delta T} D_r) \int_0^1 r\ \mathrm{Ber}(\gamma^{\frac{1}{4}}r)dr \\ &+ (2B_3 + \frac{2T_w}{\Delta T} D_i) \int_0^1 r\ \mathrm{Bei}(\gamma^{\frac{1}{4}}r)dr \\ &+ 2B_4 \int_0^1 r[\mathrm{Bei}^2(\gamma^{\frac{1}{4}}r) - \mathrm{Ber}^2(\gamma^{\frac{1}{4}}r)]dr \\ &+ 2B_6 \int_0^1 r\mathrm{Bei}(\gamma^{\frac{1}{4}}r)\cdot\mathrm{Ber}(\gamma^{\frac{1}{4}}r)dr, \end{aligned} \tag{58}$$

where $R = K_1 Ber(\gamma^{1/4}) - K_2 Bei(\gamma^{1/4})$,

$$B_1 = -\frac{F}{A} R,$$

$$B_2 = D_r R + \frac{F}{A} K_1,$$

$$B_3 = D_i R - \frac{F}{A} K_2,$$

$$B_4 = D_i K_2,$$

$$B_5 = D_r K_1 = B_4,$$

and $B_6 = D_r K_2 - D_i K_1$.

Integration of the above functions is performed in Appendix A. Thus, we have the medium temperature

$$t_m + \frac{T_W}{\Delta T} = (B_1 - \frac{T_W}{\Delta T}\frac{F}{A}) + \frac{2}{\gamma^{1/4}}(B_2 + \frac{T_W}{\Delta T} D_r)\, Bei'(\gamma^{1/4})$$

$$- \frac{2}{\gamma^{1/4}}(B_3 + \frac{T_W}{\Delta T} D_i)\, Ber'(\gamma^{1/4})$$

$$- B_4 [Ber^2(\gamma^{1/4}) + Ber_1^2(\gamma^{1/4}) - Bei^2(\gamma^{1/4}) - Bei_1^2(\gamma^{1/4})]$$

$$+ B_6 [Ber(\gamma^{1/4}) Bei(\gamma^{1/4}) + Ber_1(\gamma^{1/4}) Bei_1(\gamma^{1/4})]. \quad (59)$$

Next, the Nusselt number is derived by using the result after integrating Equation (53) with the boundary condition. That is, the temperature gradient is written in a form.

$$\Delta T \frac{\partial t}{\partial r} = \frac{1}{\gamma^{1/4}} [- G_1 Ber'(\gamma^{1/4} r) + G_2 Bei'(\gamma^{1/4} r)]. \quad (60)$$

And the heat flux is expressed by the following equation

$$\overset{\circ}{q}_0'' = - k \left.\frac{\partial T}{\partial r}\right|_{r=a} = h[T_w - T_m] \qquad (61)$$

where $\frac{\partial T}{\partial r} \rightarrow \frac{\Delta T}{a} \frac{\partial t}{\partial r}$, $\rightarrow$ as it has been, $\frac{\Delta T}{a} \frac{\partial t}{\partial r}$.

Therefore

$$-k \frac{\Delta T}{a} \left.\frac{\partial t}{\partial r}\right|_{r=1} = - h [T_m - T_w] \quad . \qquad (62)$$

And rearranging Equation (62) to make a combination of parameters for a Nusselt number,

$$Nu = \frac{2ah}{k} = \frac{2\Delta T \left.\frac{\partial t}{\partial r}\right|_{r=1}}{[T_m - T_w]} \quad . \qquad (63)$$

The medium temperature in a scaled version is defined by

$$t_m = \frac{T_m - T_w}{\Delta T} \quad .$$

Hence, the Nusselt number becomes

$$N_u = \frac{2}{\gamma^{1/4} \Delta T t_m} [- G_1 \acute{Ber}(\gamma^{1/4}) + G_2 \acute{Bei}(\gamma^{1/4})] \qquad (64)$$

2. Cooling Case

In a similar manner we can derive the equations for velocity, temperature, medium temperature, and the Nusselt number.

For a cooling case, the A in Equation (42) has the positive sign. Thus Equation (44) has a form

$$Au = F + \frac{2\Delta T}{RePr} \frac{1}{r} \frac{\partial}{\partial r}\left(r \frac{\partial t}{\partial r}\right) \quad . \qquad (65)$$

Differentiating Equation (43) twice and then substituting it into Equation (65), we also have the fourth order Bessel Equation like Equation (46) except a sign different. It is

$$\Delta^4 u - \gamma u = -\gamma \frac{F}{A} \quad . \tag{66}$$

the solution to Equation (66) is

$$u = \frac{F}{A} + d_1 J_0(\gamma^{\frac{1}{4}} r) + d_2 Y_0(\gamma^{\frac{1}{4}} r) + d_3 I_0(\gamma^{\frac{1}{4}}) + d_4 K_0(\gamma^{\frac{1}{4}} r). \tag{67}$$

By using boundary condition (48),

$$d_2 = d_4 = 0,$$

and by boundary condition (51)

$$d_3 = -\frac{\frac{F}{A} + d_1 J_0(\gamma^{\frac{1}{4}})}{I_0(\gamma^{\frac{1}{4}})} \quad .$$

And then using Equation (52) we have

$$d_1 = \frac{\gamma^{\frac{1}{4}}\left[\frac{1}{2} - \frac{F}{2A} + \frac{F}{A}\frac{1}{\gamma^{\frac{1}{4}}}\frac{I_1(\gamma^{\frac{1}{4}})}{I_0(\gamma^{\frac{1}{4}})}\right]}{\left[J_1(\gamma^{\frac{1}{4}}) - \frac{J_0(\gamma^{\frac{1}{4}})}{I_0(\gamma^{\frac{1}{4}})} I_1(\gamma^{\frac{1}{4}})\right]}$$

Therefore, the velocity profile is given by

$$u = \frac{F}{A} + d_1 J_0(\gamma^{\frac{1}{4}} r) + d_3 I_0(\gamma^{\frac{1}{4}} r) \tag{68}$$

Substituting Equation (68) into Equation (65), and then integrating twice with the boundary conditions

$$\frac{\partial t}{\partial r} = 0 \qquad \text{at} \qquad r = 0,$$

and $t = t_w = 0$ at $r = 1$,

we have

$$\Delta T \cdot t = \frac{D_1}{\gamma^{\frac{1}{2}}} [J_0(\gamma^{\frac{1}{4}}) - J_0(\gamma^{\frac{1}{4}}r)] + \frac{D_2}{\gamma^{\frac{1}{2}}} [I_0(\gamma^{\frac{1}{4}}r) - I_0(\gamma^{\frac{1}{4}})] . \qquad (69)$$

When $r = 0$, $t = 1$, then Equation (69) becomes

$$\Delta T = \frac{D_1}{\gamma^{\frac{1}{2}}} [J_0(\gamma^{\frac{1}{4}}) - 1] + \frac{D_2}{\gamma^{\frac{1}{2}}} [1 - I_0(\gamma^{\frac{1}{4}})] \qquad (70)$$

where $D_1 = ARePrd_3/2$,

and $D_2 = ARePrd_2/2$.

As with Equation (55), we can obtain the value of $A = \frac{\partial T}{\partial z}$ from Equation (70) by the same method.

Dividing Equation (69) by Equation (70), the temperature profile equation is obtained in the form

$$t = E_1 [J_0(\gamma^{\frac{1}{4}}) - J_0(\gamma^{\frac{1}{4}}r)] + E_2 [I_0(\gamma^{\frac{1}{4}}r) - I_0(\gamma^{\frac{1}{4}})] \qquad (71)$$

where

$$E_1 = \frac{D_1}{D_1 [J_0(\gamma^{\frac{1}{4}}) - 1] + D_2 [1 - I_0(\gamma^{\frac{1}{4}})]} ,$$

$$E_2 = \frac{D_2}{D_1 [J_0(\gamma^{\frac{1}{4}}) - 1] + D_2 [1 - I_0(\gamma^{\frac{1}{4}})]} .$$

The medium temperature can also be found the same way.

$$t_m + \frac{T_w}{\Delta T} = 2 \int_0^1 utrdr + \frac{2T_w}{\Delta T} \int_0^1 urdr$$

$$= (a_1 + a_5 - a_6 + \frac{T_w}{\Delta T}\frac{F}{A}) + \frac{1}{\gamma^{\frac{1}{4}}}(2a_2 + \frac{2T_w}{\Delta T} d_1) J_1(\gamma^{\frac{1}{4}})$$

$$+ \frac{1}{\gamma^{\frac{1}{4}}}(2a_3 + \frac{2T_w}{\Delta T} d_3) I_1(\gamma^{\frac{1}{4}}) + \frac{a_4}{\gamma^{\frac{1}{4}}} [J_0(\gamma^{\frac{1}{4}}) I_1(\gamma^{\frac{1}{4}}) + J_1(\gamma^{\frac{1}{4}}) I_0(\gamma^{\frac{1}{4}})]$$

$$- a_5 [J_0^2(\gamma^{\frac{1}{4}}) + J_1^2(\gamma^{\frac{1}{4}})] + a_6 [I_0^2(\gamma^{\frac{1}{4}}) - I_1^2(\gamma^{\frac{1}{4}})] \qquad (72)$$

where $G = E_1 J_0(\gamma^{\frac{1}{4}}) - E_2 I_0(\gamma^{\frac{1}{4}})$,

$a_1 = \frac{F}{A} G$,

$a_2 = d_1 G - \frac{F}{A} E_1$

$a_3 = d_3 G + \frac{F}{A} E_2$

$a_4 = d_1 E_2 - d_3 E_1$

$a_5 = d_1 E_1$

and $a_6 = d_3 E_2$.

For a Nusselt number for cooling case, by using Equation (62) and by differentiating Equation (71)

$$\frac{\partial t}{\partial r} = \gamma^{\frac{1}{4}} [E_1 J_1(\gamma^{\frac{1}{4}} r) + E_2 I_1(\gamma^{\frac{1}{4}} r)] ,$$

the Nusselt number is described as

$$Nu = \frac{2\gamma^{\frac{1}{4}}}{t_m} [E_1 J_1(\gamma^{\frac{1}{4}}) + E_2 I_1(\gamma^{\frac{1}{4}})] . \qquad (73)$$

V. THERMAL ENTRY FLOW FIELD

In a previous chapter the fully developed flow problems were analytically solved with some assumptions. In this chapter the thermal entry problem is solved numerically. The results will be compared with the experimental results in Chapter VII.

First, the Equations (32), (35), and (36) are transformed by using finite difference methods. The governing equations can be written as:

Conservation of mass:

$$\frac{\partial(rV_r)}{\partial r} + \frac{\partial(rV_z)}{\partial r} = 0 \tag{32}$$

Conservation of momentum:

$$V_r \frac{\partial V_z}{\partial r} + V_z \frac{\partial V_z}{\partial z} = -\frac{1}{\rho}\frac{\partial P}{\partial z} + \nu\left[\frac{\partial^2 V_z}{\partial r^2} + \frac{1}{r}\frac{\partial V_z}{\partial r}\right] + \frac{\mu_0 \Delta T}{\rho}\left(\frac{\partial M}{\partial T}\right)_H \frac{\partial H}{\partial z} \tag{35}$$

Here, we define a general pressure term including the magnetic force rather than separate terms. This general pressure term is defined later. Let

$$-\frac{1}{\rho}\frac{\partial P}{\partial z} = -\frac{1}{\rho}\frac{\partial p}{\partial z} + \frac{1}{\rho}\mu_0 \Delta T\left(\frac{\partial M}{\partial T}\right)_H \frac{\partial H}{\partial z} \quad .$$

Thus, Equation (35) becomes

$$V_r \frac{\partial V_z}{\partial r} + V_z \frac{\partial V_z}{\partial z} = -\frac{1}{\rho}\frac{\partial P}{\partial z} + \nu\left[\frac{\partial^2 V_z}{\partial r^2} + \frac{1}{r}\frac{\partial V_z}{\partial r}\right] \tag{35a}$$

Conservation of energy:

$$\rho c\left[V_r \frac{\partial T}{\partial r} + V_z \frac{\partial T}{\partial z}\right] - \mu_0 K h V_z T$$

$$= \frac{k}{r}\frac{\partial}{\partial r}\left(r \frac{\partial T}{\partial r}\right) + k \frac{\partial^2 T}{\partial z^2} + \mu\left(\frac{\partial V_z}{\partial r}\right)^2 \qquad (36)$$

V-1. Difference Equations

All differential terms related to Equations (32), (35) and (36) are depicted in difference equations based on the following mesh diagram

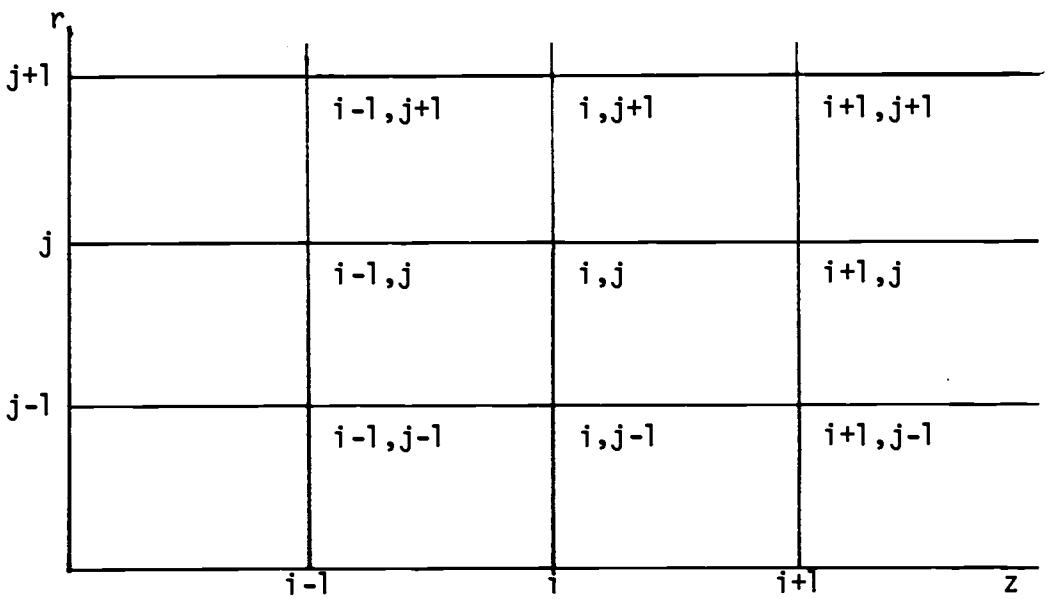

$$\frac{\partial T}{\partial r} = \frac{T_{i+1,j+1} - T_{i+1,j-1}}{2\delta_r}$$

$$\frac{\partial T}{\partial z} = \frac{3T_{i+1,j} - 4T_{i,j} + T_{i-1,j}}{2\delta_z}$$

$$\frac{\partial^2 T}{\partial r^2} = \frac{T_{i+1,j+1} - 2T_{i+1,j} + T_{i+1,j-1}}{\delta_r^2}$$

$$\frac{\partial u}{\partial r} = \frac{u_{i+1,j+1} - u_{i+1,j-1}}{2\delta_r}$$

$$\frac{\partial u}{\partial z} = \frac{3u_{i+1,j} - 4u_{i,j} + u_{i-1,j}}{2\delta_z}$$

$$\frac{\partial^2 u}{\partial r^2} = \frac{u_{i+1,j+1} - 2u_{i\,1,j} + u_{i+1,j-1}}{\delta_r^2}$$

$$u_{i,j} = \frac{u_{i+1,j} + u_{i-1,j}}{2}$$

Using the above difference forms the continuity, momentum, and energy equations are easily transformed in difference equations. The following is the procedure to make these transformations.

V-2. Continuity Equation in a Numerical Form

For continuity equation, it is first integrated with respect to r

$$u_r = -\frac{1}{r}\int_0^r \frac{\partial}{\partial z}(ru_z)dr \quad . \tag{74}$$

From now on, in order to avoid the repeated use of transcripts r and z, we use U and V for z and r-directions, respectively. Therefore, Equation (74) is written, with new variables,

$$V = -\frac{1}{r}\int_0^r \frac{\partial}{\partial z}(rU)dr \tag{74}$$

Then by the Trapezoidal rule Equation (74) has a following form

$$V_{i+1,j} = V_{i+1,j-1} - \frac{\delta r}{2r_j}\left\{\left[\frac{\partial}{\partial z}(rU)\right]_{i+1,j} - \left[\frac{\partial}{\partial z}(rU)\right]_{i+1,j-1}\right\} \quad (75)$$

By expanding the terms in a big bracket, we have a final difference form for Equation (74)

$$V_{i+1,j} = V_{i+1,j-1} - \frac{\delta_r}{2\delta_z}\left[U_{i+1,j} - U_{i,j} + (1 - \frac{1}{j-1})\, U_{i+1,j-1} - (1 - \frac{1}{j-1})\, U_{i,j-1}\right],$$

$i = 1,m$, and
$j = 2,n-1$, (76)

when $j = n$ (at wall)

$$V_{i+1,n} = 0$$

$$U_{i+1,n} = 0$$

and $U_{i,n} = 0$

hence, Equation (76) is reduced as

$$V_{i+1,n-1} = \frac{\delta_r}{2\delta_z}\left[(1 - \frac{1}{n-1})\, U_{i+1,n-1} - (1 - \frac{1}{n-1})\, U_{i,n-1}\right]. \quad (77)$$

When $j = 1$, Equation (76) blows up because of the singularities at $j = 1$ (that is, $r = 0$). This singularity can be avoided by using the boundary condition

$$\frac{\partial U}{\partial r} = 0 \quad \text{at} \quad r = 0.$$

Also we can approximate the singularity term as r is approaching

zero by the following procedure

$$\lim_{r\to o} \frac{1}{r}\frac{\partial U}{\partial r} \Longrightarrow \frac{\partial^2 U}{\partial r^2} \quad . \tag{78}$$

V-3. Momentum Equation

Here for convenience we also replace u_r and u_z from Equation (35a) by V and U, respectively.

$$V\frac{\partial U}{\partial r} + U\frac{\partial U}{\partial z} = -\frac{1}{\rho}\frac{\partial P}{\partial z} + \nu\frac{\partial^2 U}{\partial r^2} + \frac{1}{r}\frac{\partial U}{\partial r} \quad . \tag{35a}$$

Replacing the variables in Equation (35a) by difference forms and arranging terms in order of j we have

$$A_j U_{i+1,j-1} + B_j U_{i+1,j} + C_j U_{i+1,j+1} = D_j$$

$$\text{for} \quad j = 2, n-1 \tag{79}$$

where

$$A_j = -(2V_{i,j} - V_{i-1,j})\frac{\delta_z}{\delta_r} - \frac{2\nu\delta_z}{\delta_r^2} + \frac{\nu\delta_z}{(j-1)\delta_r^2} \quad ,$$

$$B_j = 3(2U_{i,j} - U_{i-1,j}) + \frac{4\nu\delta_z}{\delta_r^2} \quad ,$$

$$C_j = (2V_{i,j} - V_{i-1,j})\frac{\delta_z}{\delta_r} - \frac{2\nu\delta_z}{\delta_r^2} - \frac{\nu\delta_z}{(j-1)\delta_r^2} \quad ,$$

$$D_j = -\frac{2\delta_z}{\rho}\left(\frac{\partial P}{\partial z}\right)_{i+1,j} + (2U_{i,j} - U_{i-1,j})(4U_{i,j} - U_{i-1,j}) \quad .$$

For j = 1, using the boundary condition

$$\frac{\partial U}{\partial r} = 0 \qquad \text{at} \qquad r = 0,$$

and the approximation, Equation (78), we obtain

$$B'_j U_{i+1,j} + (A'_j + C'_j)\, U_{i+1,j+1} = D'_j$$

$$\text{for } j = 1, \tag{80}$$

where

$$A'_j = -(2V_{i,j} - V_{i-1,j}) \frac{\partial z}{\partial_r} - \frac{4\nu\delta_z}{\delta_r^2} ,$$

$$B_j = 3(2U_{i,j} - U_{i-1,j}) + \frac{8\nu\delta_z}{\delta_r^2} ,$$

$$C_j = (2V_{i,j} - V_{i-1,j}) \frac{\partial z}{\partial_r} - \frac{4\nu\delta_z}{\delta_r^2} ,$$

$$D_j = -\frac{2\delta_z}{\rho} \left(\frac{\partial P}{\partial z}\right)_{i+1,j} + (2U_{i,j} - U_{-1,j})(4U_{i,j} - U_{i-1,j}) .$$

For $j = n$, the boundary conditions are

$$U_{i+1,n} = 0 \qquad \text{on wall}$$

$$V_{i+1,n} = 0 \qquad \text{on wall} .$$

Hence, Equation (79) is reduced as a following form

$$A_{j-1} U_{i+1,j-2} + B_{j-1}\, U_{i+1,j-1} = D_{j-1}$$

$$\text{for } j = n, \tag{81}$$

where A_{j-1}, B_{j-1}, and D_{j-1} are defined by replacing j of A_j, B_j, and D_j of Equation (80) by j-1 as $j = n$.

We still have to define the pressure gradient term in Equations

(79), (80), and (81). The pressure is defined in magnetic fluids in the presence of an applied magnetic field by an expression for the free energy F. The differential with constant concentration has the form of the magnetic Gibbs function

$$dF = - SdT - P_0 dV + \mu_0 H \delta M dV \tag{83}$$

where P_0 is the pressure in the absence of an applied field. Taking a derivative with respect to the volume with constant T and M, we have

$$\left(\frac{\partial F}{\partial V}\right)_{T,M} = - p_0 + \mu_0 H \delta M \tag{84}$$

where $$\left(\frac{\partial F}{\partial V}\right)_{T,M} = - P \tag{85}$$

in the presence of a magnetic field. Hence we have

$$\begin{aligned} P &= p_0 - \mu_0 H \delta M \\ &= p_0 - \mu_0 H \left(\frac{\partial M}{\partial T}\right)_H (T_c - T) , \end{aligned} \tag{86}$$

Taking a derivative with respect to Z, then

$$- \frac{1}{\rho} \frac{\partial P}{\partial z} = - \frac{1}{\rho} \frac{\partial P_0}{\partial z} + \frac{\mu_0 K \Delta T}{\rho} \frac{\partial H}{\partial z} - \frac{\mu_0 K H}{\rho} \frac{\partial T}{\partial z} \tag{87}$$

where $\Delta T = T_h - T_\ell$.

Under the assumptions of a fully developed velocity profile, the pressure gradient in the absence of an applied field is expressed in the form

$$- \frac{1}{\rho} \frac{\partial P_0}{\partial z} = \frac{8 \mu U_{av}}{a^2} \tag{88}$$

Therefore, Equation (87)

$$-\frac{1}{\rho}\frac{\partial P}{\partial z} = \left(\frac{8\mu U_{av}}{a^2}\right) + \frac{\mu_0 K\Delta T}{\rho}\frac{\partial H}{\partial z} - \frac{\mu_0 KH}{\rho}\frac{\partial T}{\partial z} \quad . \tag{89}$$

In numerical form of Equation (89), we have

$$\left(-\frac{1}{\rho}\frac{\partial P}{\partial z}\right)_{i+1,j} = \left[\frac{2}{\rho}\left(\frac{8\mu U_{av}}{a^2}\right)_{i,j} - \frac{1}{\rho}\left(\frac{8\mu U_{av}}{a^2}\right)_{i-1,j}\right]$$

$$+ \frac{\mu_0 Kh}{\rho}\left(T_{i,j} - T_{i-1,j}\right) - \frac{\mu_0 KH}{\delta_z \rho}\left[T_{i,j} - T_{i-1,j}\right] \tag{90}$$

V-4. Energy Equation

Equation (36) is transformed into a numerical form in the same manner. As a result of the transformation, we have

$$\alpha_j T_{i+1,j-1} + \beta_j T_{i+1,j} + \gamma_j T_{i+1,j+1} = \delta_j$$

$$\text{for } j = 2,\ n-1 \tag{91}$$

where

$$\alpha_j = -(2V_{i,j} - V_{i-1,j})\frac{\delta_z}{\delta_r} - \frac{2k\delta_z}{\rho c\delta_r} + \frac{k\delta_z}{(j-1)\rho c\delta_r{}^2}$$

$$\beta_j = 3(2U_{i,j} - U_{i-1,j}) + \frac{4k\delta_z}{\rho c\delta_r} - \frac{2k}{\rho c\delta_z} - (2U_{i,j} - U_{i-1,j})\frac{2\delta_z \mu_0 Kh}{\rho c}$$

$$\gamma_j = (2U_{i,j} - U_{i-1,j})\frac{\delta_z}{\delta_v} - \frac{2k\delta_z}{\rho c\delta_r} - \frac{k\delta_z}{\rho c(j-1)\delta_r{}^2}$$

$$\delta_j = (2U_{i,j}-U_{i-1,j})(4T_{i,j}-T_{i-1,j})-(2T_{i,j}-T_{i-1,j})\frac{2k}{\rho c\delta_z}$$

$$+ (U_{i+1,j+1} - U_{i+1,j-1})^2 \frac{\mu\delta_z}{2\rho c\delta_r} \quad .$$

For j=1, the boundary condition is

$$\frac{\partial T}{\partial r} = 0 \qquad \text{at} \qquad r = 0,$$

and

$$\lim_{r\to 0} \frac{1}{r}\frac{\partial T}{\partial r} \longrightarrow \frac{\partial^2 T}{\partial r^2} \quad .$$

Using these conditions, we have

$$\beta_j^1 T_{i+1,j} + (\alpha_j^1 + \gamma_j^1) T_{i+1,j+1} = \delta_j^1 \tag{92}$$

where

$$\alpha_j^1 = -(2V_{i,j} - V_{i-1,j})\frac{\delta z}{\delta_r} - \frac{4k\delta_z}{\rho c\delta_r^2}$$

$$\beta_j^1 = 3(2U_{i,j} - U_{i-1,j}) + \frac{8k\delta_z}{\rho c\delta_r^2} - \frac{2k}{\rho c\delta_z}$$

$$- (2U_{i,j} - U_{i-1,j})\frac{2\delta_z\mu_o Kh}{c}$$

$$\gamma_j^1 = (2V_{i,j} - V_{i-1,j})\frac{\delta z}{\delta_r} - \frac{4k\delta z}{\rho c\delta_r^2}$$

$$\delta_j^1 = (2V_{i,j}-V_{i-1,j})(4T_{i,j}-T_{i-1,j})-(2T_{i,j}-T_{i-1,j})\frac{2k}{\rho c\delta_z}$$

$$+ (U_{i+1,j+1} - U_{i+1,j-1})^2 \frac{\mu\delta_z}{2\rho c\delta_r^2} \quad .$$

For j = n, the boundary condition is assumed to be constant heat flux at the surface. That is,

$$\overset{\circ}{q}''_{o} = k \frac{\partial T}{\partial r} \quad . \tag{93}$$

In a numerical expression of Equation (93), we use the three points scheme as a following equation

$$\overset{\circ}{q}''_{o} = \frac{k}{2\delta_r} [3T_{i+1,j} - 4T_{i+1,j-1} + T_{i+1,j-2}] \quad .$$

Then we have

$$T_{i+1,j-2} - 4T_{i+1,j-1} + 3T_{i+1,j} = \frac{2\delta_r \overset{\circ}{q}''_{o}}{k} \tag{94}$$

where

Substituting Equation (94) into Equation (91), we have

$$\alpha_j = -(2V_{i,j}-V_{i-1,j}) \frac{\delta_z}{\delta_r} - \frac{2k\delta_z}{\rho c \delta_r} + \frac{k\delta_z}{(j-1)\rho c \delta_r^2} - \frac{1}{3}\gamma_j \ ,$$

$$\beta_j = 3(2U_{i,j}-U_{i-1,j}) + \frac{4k\delta_z}{\rho c \delta_r} - \frac{2k}{\rho c \delta_z} + \frac{4}{3}\gamma_j$$

$$-(2U_{i,j} - U_{i-1,j}) \frac{2\delta_z \mu_0 Kh}{\rho c} \quad ,$$

$$\gamma_j = 0 \ ,$$

$$\delta_j = (2U_{i,j}-U_{i-1,j})(4T_{i,j}-T_{i-1,j})-(2T_{i,j}-T_{i-1,j}) \frac{2k}{\rho c \delta_z}$$

$$+ (U_{i+j,j+1} - U_{i+1,j-1})^2 \frac{\mu\delta_z}{2\rho c \delta_r} - \frac{2\delta_r \overset{\circ}{q}''_{o}}{3k}\gamma_j$$

$$\varepsilon_j = 0.$$

For the initial setting, we define the constant values in the following expressions.

For velocity,

$$U_{1,j} = U_{2,j} = U_{av}\left\{1 - \left[\frac{(j-1)\delta_r}{a}\right]^2\right\}, \ U_{1,n} = U_{2,n} = 0. \tag{95}$$

For temperature,

$$U_{1,j} = T_{2,j} = \text{constant.} \tag{96}$$

V-5. Numerical Calculation

From the pervious sections we can see that the Equations (79), (80), and (81) for velocity and (91), (92), and (94) for temperature form tridiagonal matrices respectively.

That is, for velocity

$$\begin{aligned} j = 1, &\quad B'_j U_{i+1,j} + (A'_j + C'_j)\, U_{i+1,j+1} = D'_j \\ j = 2,n-1, &\quad A_j U_{i+1,j-1} + B_j U_{i+1,j} + C_j U_{i+1,j+1} = D_j \\ j = n, &\quad A_{n-1} U_{i+1,j-2} + B_{j-1} U_{i+1,j-1} = D_{j-1}, \end{aligned} \tag{97}$$

and for temperature

$$\begin{aligned} j = 1, &\quad \beta^1_j T_{i+1,j} + (\alpha^1_j + \gamma^1_j) T_{i+1,j+1} = \delta^1_j \\ j = 2,n-1, &\quad \alpha_j T_{i+1,j-1} + \beta_j T_{i+1,j} + \gamma_j T_{i+1,j+1} = \delta_j \\ j = n, &\quad \xi_j T_{i+1,j-2} + \alpha_j T_{i+1,j-1} + \beta_j T_{i+1,j} = \delta_j . \end{aligned} \tag{98}$$

Finally, Equations (97) and (98) can be written as simultaneous equations through n specified nodes. Introducing some arbitrary coefficients instead of those in Equations (97) and (98), we form a matrix with an arbitrary coefficient representing both cases for velocity and temperature together. A matrix in tridiagonal form is $\bar{\bar{a}} \cdot \bar{s} = \bar{b}$, that is

$$\begin{bmatrix} a_{11} & a_{12} & & & & \\ a_{21} & a_{22} & a_{23} & & & \\ & a_{32} & a_{33} & a_{34} & & \\ & & - & - & - & \\ & & & - & - & - \\ & & & a_{n,n-2} & a_{n,n-1} & a_{n,n} \end{bmatrix} \cdot \begin{bmatrix} S_1 \\ S_2 \\ S_3 \\ \cdot \\ \cdot \\ \cdot \\ S_n \end{bmatrix} = \begin{bmatrix} b_1 \\ b_2 \\ b_3 \\ \cdot \\ \cdot \\ \cdot \\ b_n \end{bmatrix} . \qquad (99)$$

Let $\bar{\bar{a}} = \bar{\bar{Q}} . \bar{\bar{R}}$

$$\bar{\bar{Q}} = \begin{bmatrix} 1 & & & & & \\ q_2 & 1 & & & & \\ & q_3 & 1 & & & \\ & & - & - & & \\ & & & - & - & \\ & & & & - & - \\ & & & & e_n & q_n & 1 \end{bmatrix} \quad \text{and} \quad \bar{\bar{R}} = \begin{bmatrix} d_1 & r_1 & & & & \\ & d_2 & r_2 & & & \\ & & d_3 & r_3 & & \\ & & & - & - & \\ & & & - & - & \\ & & & & d_{n-1} & r_{n-1} \\ & & & & & d_n \end{bmatrix} .$$

omparing elements of matrices (99) and (100), we find that

$$d_1 = a_{11},\ d_2 = a_{22},\ q_2 = a_{21},\ r_1 = a_{12},\ r_2 = a_{23}$$

and so on. As a result, we can derive the following relationships

$$q_i = a_{i,i-1}/d_{i-1} ,$$

$$d_i = a_{i,i} - r_{i-1} \cdot q_i ,$$

$$r_i = a_{i,i+1} , \qquad (100)$$

$$e_n = a_{n,n-2}/d_{n-2} , \qquad (101)$$

where $d_1 = a_{1,1}$,

$r_1 = a_{1,2}$,

$i = 2, n-2$,

From the above,

$\bar{\bar{a}} \cdot \bar{s} = \bar{b} = \bar{\bar{Q}} \cdot \bar{\bar{R}} \cdot \bar{S}$.

Let $\bar{\bar{R}} \cdot \bar{S} = \bar{b} = \bar{\bar{Q}} \cdot \bar{\bar{R}} \cdot \bar{S}$.

Then $\bar{\bar{Q}}\ \bar{\bar{z}} = \bar{b}$ is given by

$$\begin{bmatrix} 1 & & & & & & \\ q_2 & 1 & & & & & \\ & q_3 & 1 & & & & \\ & & - & - & & & \\ & & & - & - & & \\ & & & & - & - & \\ & & & & & q_{n-1} & 1 \\ & & & & & e_n & q_n & 1 \end{bmatrix} \cdot \begin{bmatrix} z_1 \\ z_2 \\ z_3 \\ \cdot \\ \cdot \\ \cdot \\ z_{n-1} \\ z_n \end{bmatrix} = \begin{bmatrix} b_1 \\ b_2 \\ b_3 \\ \cdot \\ \cdot \\ \cdot \\ b_{n-1} \\ b_n \end{bmatrix} . \qquad (102)$$

We can also derive the following relationships from the simultaneous Equation (102)

For $i = 1$, $\quad z_i = b_i$

For $i = 2, n - 1$, $\quad z_{i-1} = b_{i-1}$

$$z_i = b_i - q_i \cdot z_{i-1},$$

and for $i = n$, $\quad z_i = b_i - e_i \cdot z_{i-2} - q_i \cdot z_{i-1}$. $\qquad (103)$

And then $\bar{\bar{R}}\ \bar{\bar{S}} = \bar{\bar{Z}}$ is given by

$$\begin{bmatrix} d_1 & r_1 & & & & & \\ & d_2 & r_2 & & & & \\ & & d_3 & r_3 & & & \\ & & & - & - & & \\ & & & & - & - & \\ & & & & & - & - \\ & & & & & & d_{n-1}\ n-1 \\ & & & & & & d_n \end{bmatrix} \cdot \begin{bmatrix} S_1 \\ S_1 \\ S_3 \\ \cdot \\ \cdot \\ \cdot \\ S_{n-1} \\ S_n \end{bmatrix} = \begin{bmatrix} z_1 \\ z_1 \\ z_3 \\ \cdot \\ \cdot \\ \cdot \\ z_{n-1} \\ z_n \end{bmatrix} , \qquad (104)$$

where matrix $\bar{\bar{R}}$ and matrix $\bar{z}$ are already known through Equations (101) and (103). Therefore, we can make an arrangement to have unknown values from $\bar{\bar{R}}\ \bar{s} = \bar{Z}$. The final arrangement is

$$S_n = z_n/d_n$$

and by setting $k = n-j$, $j = 1, n - 1$,

$$S_k = (z_k - r_k \cdot S_{k+1})/d_k \tag{105}$$

where z_n and d_n were defined by Equations (103) and (101). By such a method the velocity and temperature are calculated.

The flowchart in Appendix C describes the program algorithm to solve these equations.

Equations which describe the velocity and temperature profiles, and so on, were programmed. A listing of this program and part of the output data are presented in Appendix C. Calculated results for velocity, temperature, medium temperature, Nusselt number, etc. are discussed in Chapter VII. The input data for PROGRAM FHD were illustrated in Table II.

The input data for PROGRAM MAGNET (Appendix B) are given here. These data were selected to represent magnetic fluid "LIGNOSITE" (Table I). Since some of the data were not available, approximate values have been used.

TABLE II

Data for the Magnetic Fluid "LIGNOSITE"

Kinetic Viscosity*,	$\nu = 7.787 \times 10^{-6}$	m^2/s
Pyromagnetic Coefficient**,	$K = 1.0$	Gauss/ K
Density,	$\rho = 1220$	kg/m^3
Magnetic Permeability at Vacuum,	$\mu_0 = 1.26 \times 10^{-6}$	N/A^2
Thermal Conductivity*,	$k = 0.175$	W/m K
Heat Capacity*,	$c = 5275.4$	J/kg K
Viscosity,	$\mu = 0.00126$	Pa·s
Curie Temperature,	$Tc = 1043$	K
Saturated Magnetization,	$Ms = 57 \sim 150$	Gauss
Field Intensity,	$H = 2500 \sim 8000$	Gauss
Heat Flux	$\overset{\circ}{q}''_{\circ} = 3769.0$	W/m^2

* approximated.

** at a temperature range from 273 K to 373 K.

VI. EXPERIMENTAL WORK

Through the analytical and numerical work in the previous chapters, solution to the velocity and temperature profiles have been obtained. The experimental portion of this study was specially designed to obtain the velocity and temperature profiles in the thermal entrance region of a magnetic fluid in the presence of an external magnetic field. The experimental data obtained were reduced through a regressional analysis and a curve fitting program, and compared to the results of the numerical analysis. The following sections describe the step-by-step procedure of the experimental work done.

VI-1. Basic Idea

Velocity and temperature measurements in the flow of a magnetic fluid, while in the presence of an external magnetic field, are not reported in the literature. A small amount of work has been done on viscosity measurements [2,6], pressure [61] and the hydraulic drag in a turbulent stream [62] for magnetic fluids. But these measurements are not related to the present experimental work of velocity and temperature measurement of magnetic fluids at low Reynolds number initiated by an external magnetic field. The experiments were, therefore, carried out from the probe calibration to the data reduction.

The velocity itself is regarded as a function of temperature, even though the fluid viscosity and density were assumed constant.

This is because the fluid flow is initiated by a temperature dependence of the magnetization of a magnetic fluid in an external magnetic field. Accordingly, the velocity measurement should be accompanied by temperature measurement at the same point. Then, the measured velocities are interpreted by using the velocity calibration fitting equation with respect to the fluid temperatures. In the following section the velocity calibration is described.

VI-2. Velocity Calibration

1. Apparatus

The velocity calibration was done by using the system shown on Figures 6 and 7.* This system includes two major parts.

The first is the standpipe assembly. It maintains the weight bob motion in a pipe filled with water which moves at a constant velodity controlled by valves. There are two valves: one is a large valve which is used to control large velocities, and the other a mini-flow control valve for low velocities. The velocity of the weight bob is controlled by the valve, and is connected to a probe by a steel wire through pulleys. In order to speed up the weight bob motion, the support bar can have weights on its head. The support bar in the weight guide moves linearally.

A fluid container filled with the magnetic fluid (LIGNOSITE)

---

*By courtesy of Dr. J. R. Welty, Liquid Metal Heat Transfer Lab., Department of Mechanical Engineering, Oregon State University, Corvallis, Oregon.

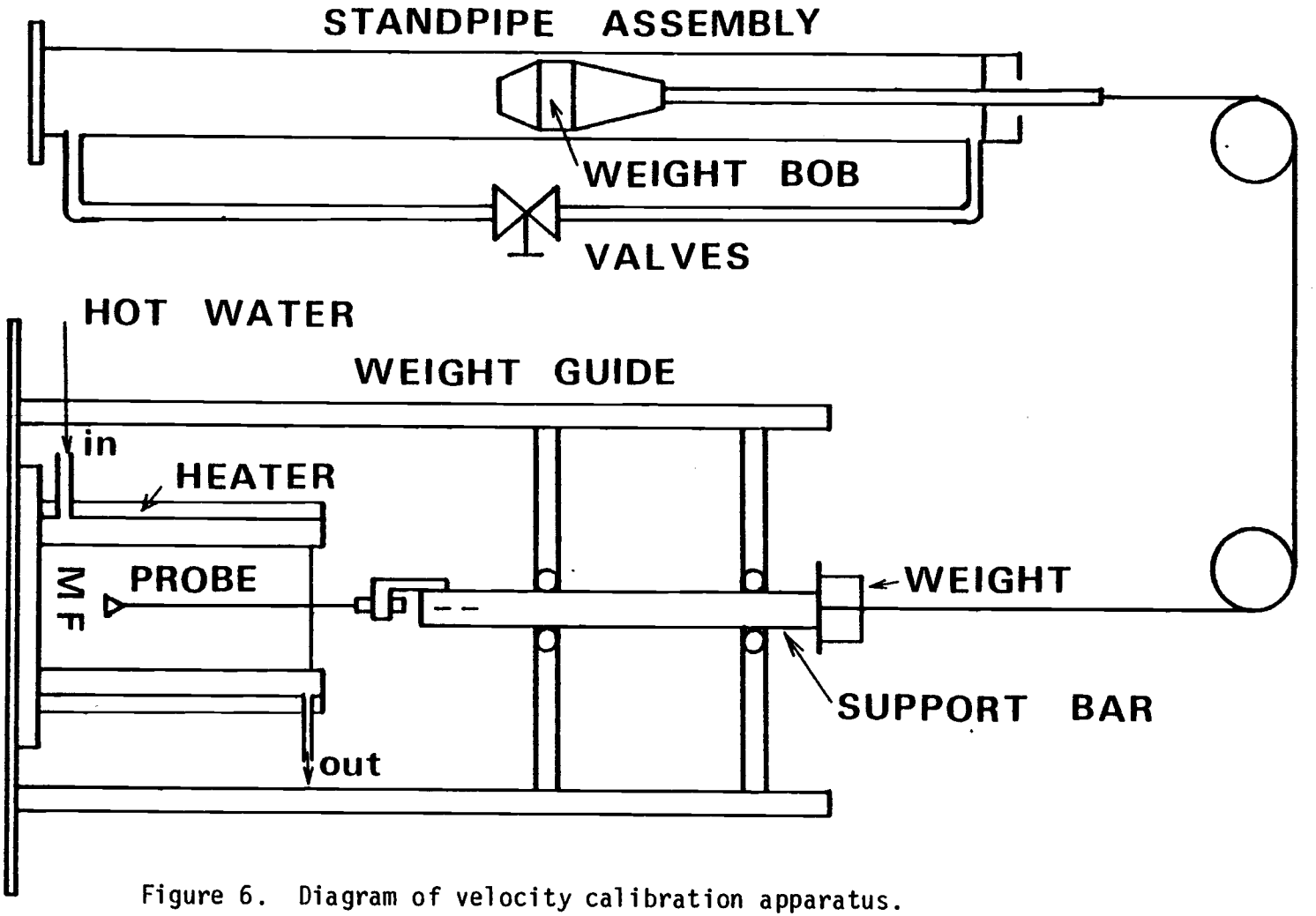

Figure 6. Diagram of velocity calibration apparatus.

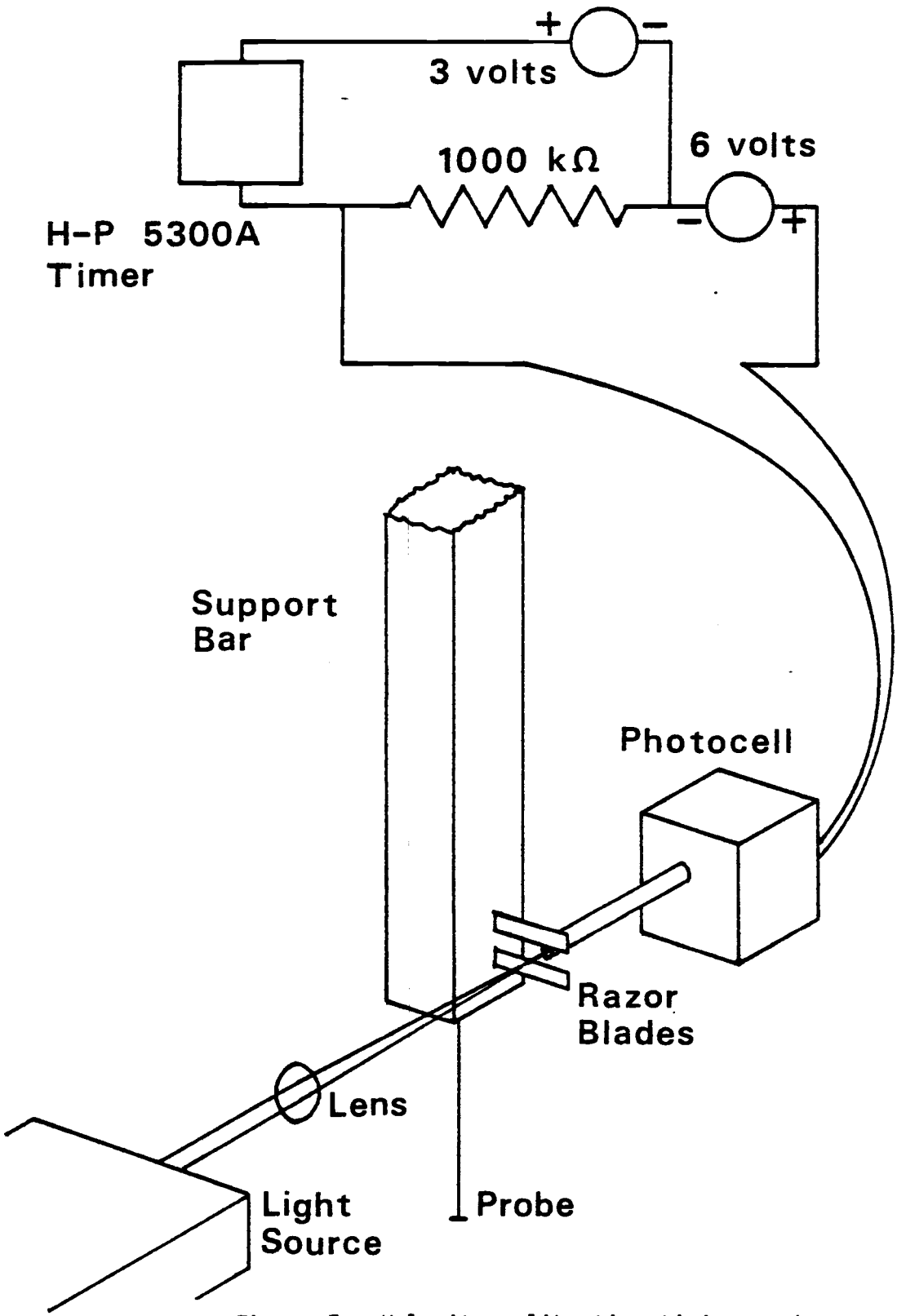

Figure 7. Velocity calibration timing system.

was designed and made to insure constant fluid temperature. Hot water was preheated electrically and circulated through the annular space of the container. The container was also heated by a nickel-chrome wire wound around the container along with insulation. Thus, the fluid temperature was isothermally maintained by a constant water flow rate and two separated electrical heaters.

The probe which was attached to the support bar was kept submerged in the magnetic fluid until the end of calibration to prevent surface contamination.

The other part of the system was the timing system. The timing system and associated wiring diagram are illustrated in Figure 7. It was used to precisely measure the probe motion in the test fluid by measuring the time it took two sharp blades, separated a known distances apart, to cut a thin light beam.

The timing system and anemometer consisted of the following:

a. Two power supplies and two regulators for warming the fluid in the container,
b. A hot-wire anemometer probe TSI 1210-60 W, E479,
c. Hewlett-Packard 5300A Measuring System (timer),
d. Bausch & Lomb Light beam source,
e. Photocell,
f. Lens set,
g. One 6-volt and two 1½-volt batteries,
h. Potentiometer,
i. Anemometer-TSI system,

Monitor and power supply, Model 1051-2

Temperature and Switching Circuit, Model 1040

Constant temperature Anemometer, Model 1053B

Variable Decade,

j. X-Y recorder.

2. Calibration Sequence

The velocity of the probe was controlled by adjusting the flow control valve and adding necessary weights on the top of the probe support bar. The weights were adjusted to define a range between totally opened and closed valve positions for which measurements are desired. The valves were then adjusted to obtain as many points in that range as desired.

Calibration runs were made at four different magnetic fluid temperatures. They were 289, 321, 328, and 345°K. A series of runs was made at each temperature at various probe velocities ranging from 5-100 in/min (0.002117-0.0423 m/s). Sufficient runs were made over this range to give a good statistical average for curve fitting, usually 40-90 runs for each temperature. The probe voltage and knife edge gap traverse time were recorded for each run. A regression analysis was run for each temperature setting using program CURFIT given in Appendix D.

The equations obtained by the CURFIT program are:

For T = 289°K (RCAL1A),

$$U_1 \text{ (m/min)} = 0.0254\ [5.350172 + 22.46685 \times (\Delta V) - 44.35180 \times (\Delta V)^2 + 70.29929 \times (\Delta V)^3]. \quad (106)$$

For T = 321°K (RCAL3A),

$$U_2 = 0.0254\ [39.11619 - 441.1759x\ (\Delta V) + 1873.675x\ (\Delta V)^2 - 2490.655x\ (\Delta V)^3]. \quad (107)$$

For T = 328°K (RCAL4A),

$$U_3 = 0.0254\ [5.103801 + 22.57392x\ (\Delta V) - 52.21068x\ (\Delta V)^2 + 73.08020x\ (\Delta V)^3]. \quad (108)$$

For T = 345°K (RCAL2A),

$$U_4 = 0.0254\ [4.733177 - 3.155512x\ (\Delta V) + 41.58162x\ (\Delta V)^2 - 9.903631x\ (\Delta V)^3]. \quad (109)$$

A plot of these equations and all data points are shown in Figures (8), (9), (10), and (11).

Equations (106), (107), (108), and (109) and Figures (8), (9), (10), and (11) were used to evaluate the velocities experimentally measured in the test section. Detailed discussion is given in Section 4.

VI-3. Velocity and Temperature Measurements

1. Velocity Measurement

Methods for measuring low velocities in an opaque liquid like a magnetic fluid are limited. As a result, a hot-wire Anemometer was used. Initially, all possible methods were studied and tested, but only the anemometer was satisfactory. Other methods were tried but found unsatisfactory.

It was presumed that the use of a hot-wire Anemometer probe in a magnetic fluid in the presence of an external magnetic field

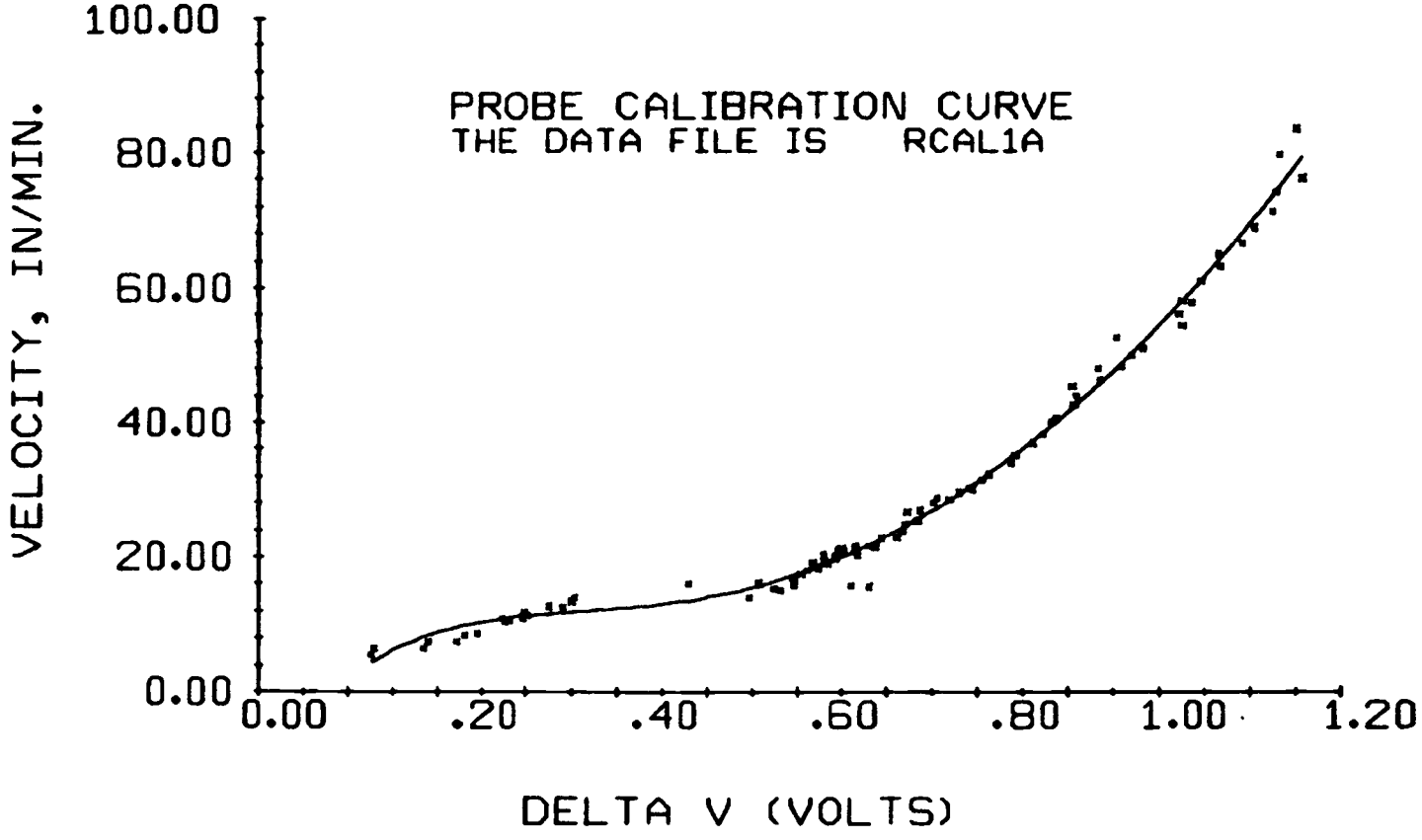

Figure 8. Velocity calibration of a probe in a magnetic fluid "LIGNOSITE" at T = 289 °K (Eq. 106).

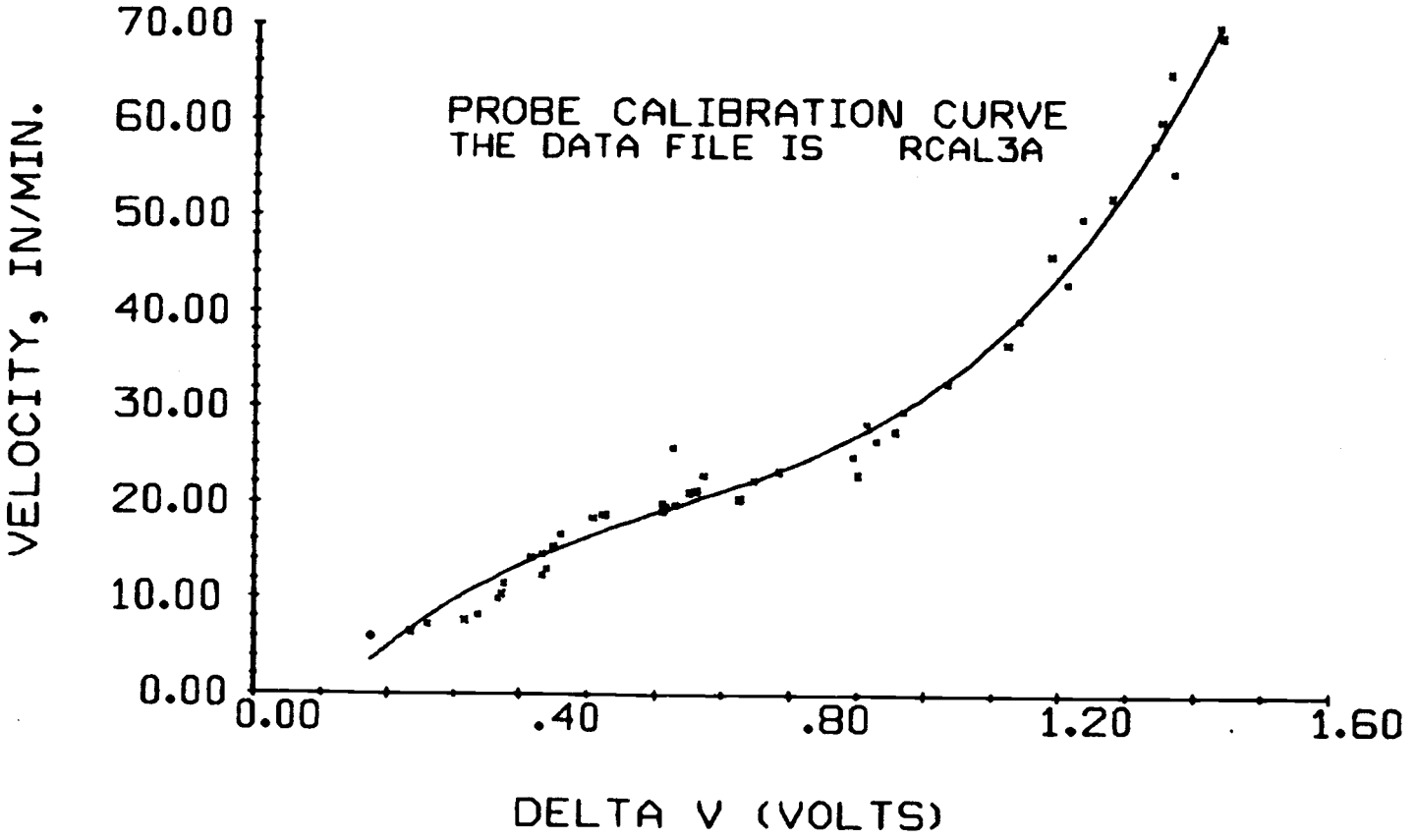

Figure 9. Velocity calibration of a probe in a magnetic fluid "LIGNOSITE" at T = 321 °K (Eq. 107).

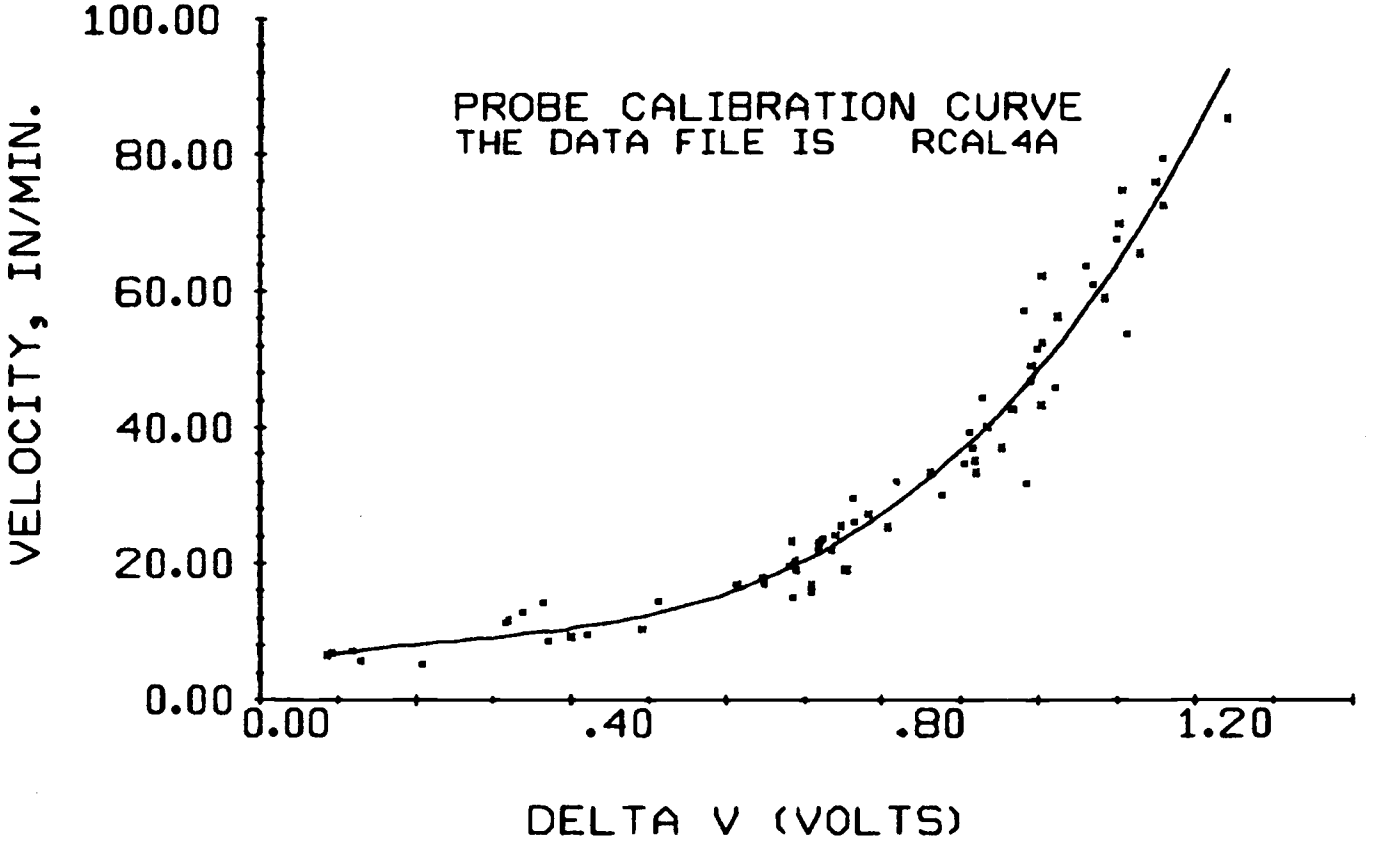

Figure 10. Velocity calibration of a probe in a magnetic fluid "LIGNOSITE" at T = 328 °K (Eq. 108).

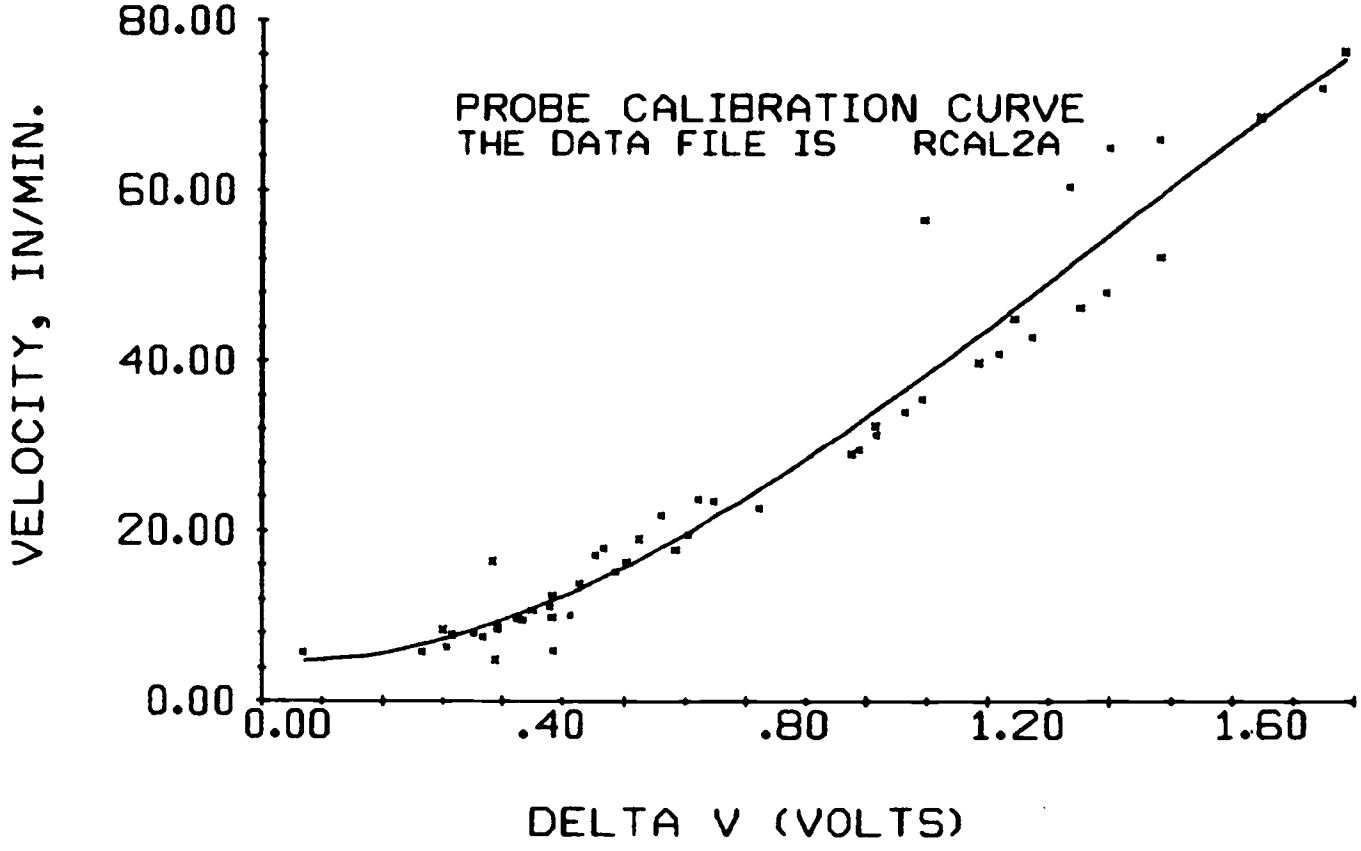

Figure 11. Velocity calibration of a probe in a magnetic fluid "LIGNOSITE" at T = 345 °K (Eq. 109).

should be cautiously interpreted because the probe itself generates a heat energy due to electrical resistance forming a temperature gradient around a probe wire. Accordingly, a change in magnetization due to this temperature gradient is formed. This region is quite small, but when compared to the dimensions of a probe wire, this unexpected flow field might influence the measurement of a hot-wire anemometer. Hence, in order to minimize these effects by the anemometer, the probe was oriented in the magnetic field where there was a small or no magnetic field gradient. This is where the contribution of the magnetic field gradient to a flow field within the region of temperature gradient could be ignored. Accordingly, the measurement of velocity by a hot-wire anemometer where the field gradient is steep is almost impossible.

Secondly, the resistance ratio of the anemometer was set as low as possible. This reduced the heat flux from the heat probe wire. If the resistance ratio was too small, however, the sensitivity of the probe dropped. Therefore, a compromise was made. The resistance ratio was 1.01.

2. Temperature Measurement

Temperatures within the magnetic fluid were measured with copper-constantan thermocouples and an Esterline Anger Data Logger Model PD2064. The Data Logger automatically converted the thermocouple emf into temperature from a pre-programmed calibration curve. It printed out temperature continuously for record thermocouple if desired.

3. Apparatus

The experimental apparatus is illustrated in Figures (12) and (13). The closed loop arrangement comprised of a test section within the magnetic field which was located far downstream from a corner, and two water cooling sections. An alternate test section was on the other side of the electromagnet. The distance upstream of the test section was over 40 times the tube diameter. This was to diminish any effects on the flow due to the entrance or corner. The two cooling jackets were designed to drop fluid temperature from 370°K to 285°K.

The heating section was prepared by winding a Nickel-Chrome wire as a heating element around a thin copper tube. The heating element was covered by insulation and had terminals every 0.025 m interval. Hence, even though there is only one slot for an anemometer probe, by connecting or disconnecting the terminals the distance from the thermal entrance could be varied by 0.025 meter intervals.

The anemometer probe and a thermocouple wire holder were held by the micrometer head, as shown in Figure (13) and could be moved up and down by adjusting the micrometer. The micrometer was also attached to a vernier slide, so about 0.15 m stroke distance could be covered. The probe and a thermocouple holder were sealed by an O-ring and Halo oil. This oil was not soluble in the magnetic fluid. It sealed and lubricated the probe.

The probe wire was moved up and down within the radius of the tube. The probe and support arrangement are shown in Figure (13). The magnetic field was generated by a Varian model V-2200A

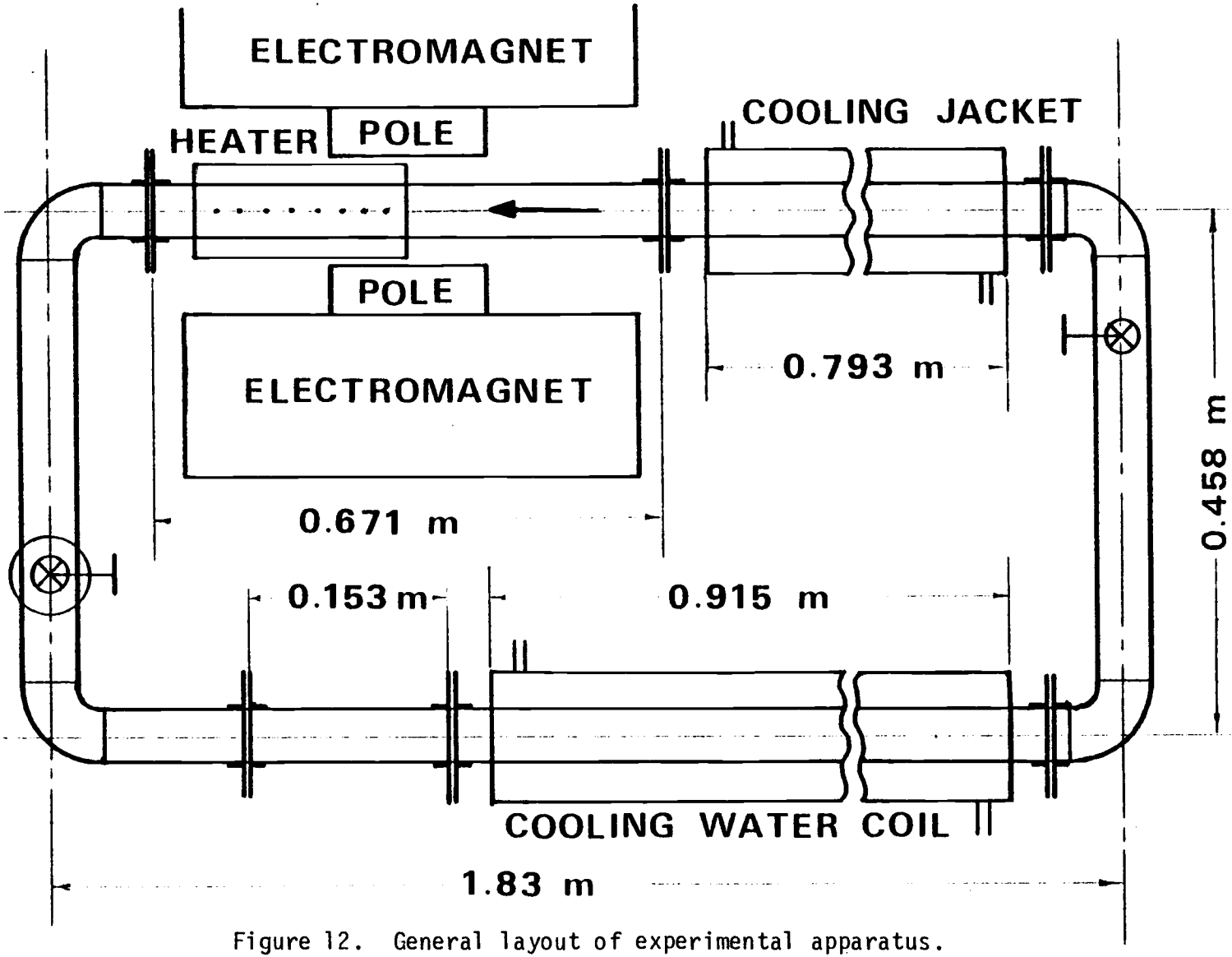

Figure 12. General layout of experimental apparatus.

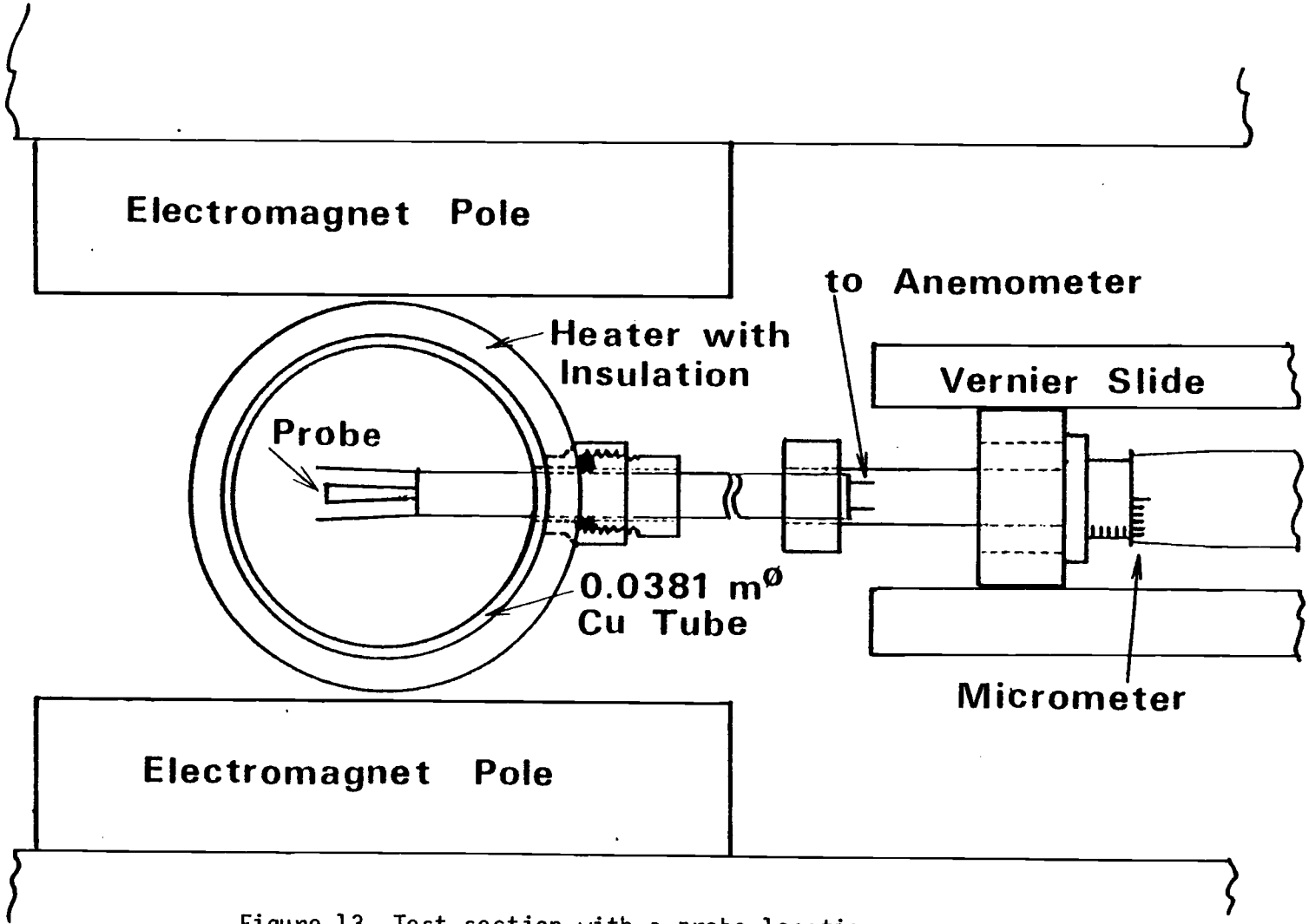

Figure 1.3. Test section with a probe location.

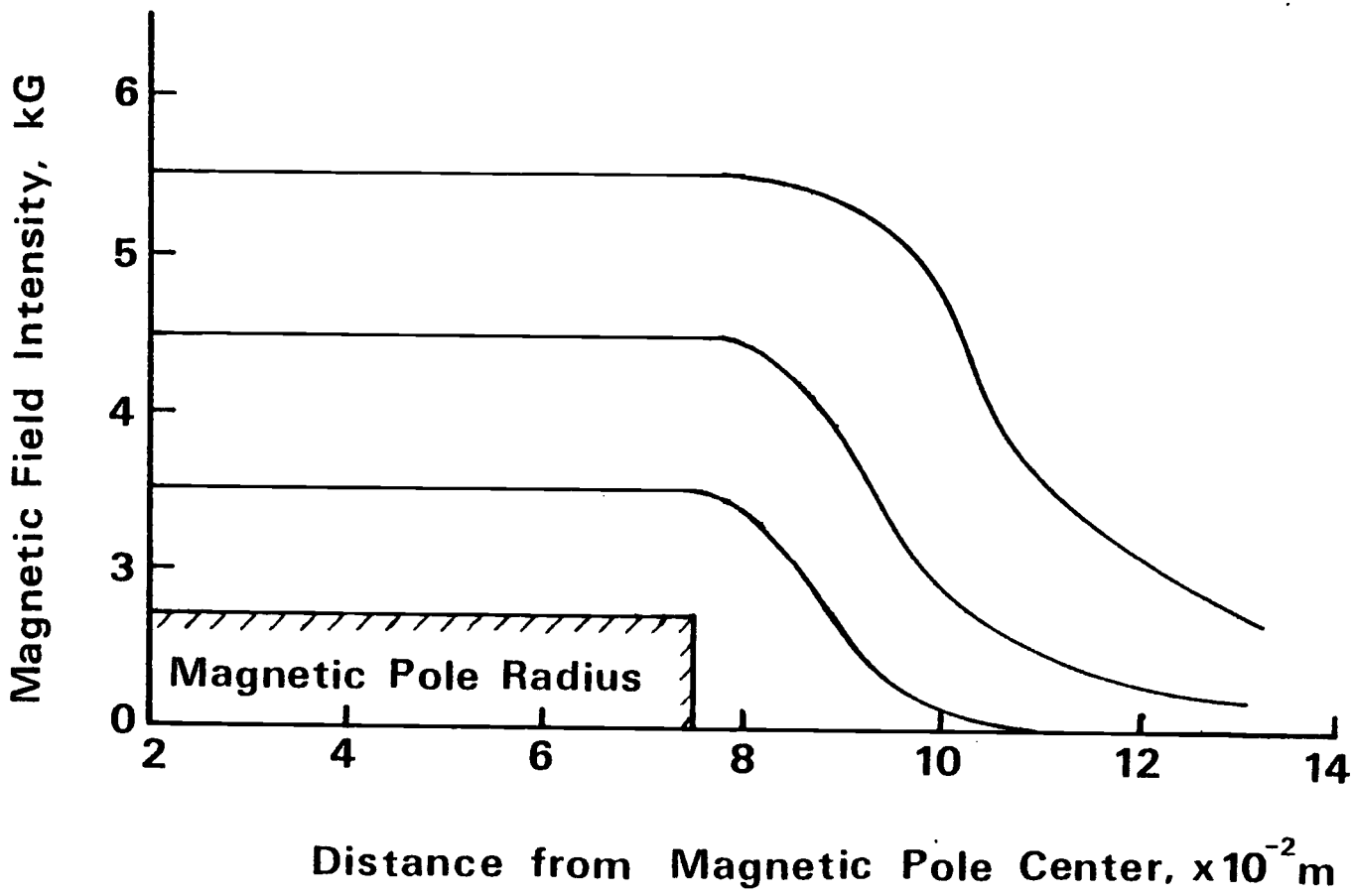

Figure 14. Magnetic field intensities measured along radial direction at the gap between Varian Electromagnet 6 inches poles.

electromagnetic power supply and field regulator. The magnetic field strength could be varied from 0 to 6500 Gauss with a 2 in gap (0.05 m). Figure (14) shows how the magnetic field intensity varied along the radial and axial directions. The data for Figure (14) were taken for various field intensities using a flux meter. The velocity measurements were performed within the region where the field intensity was constant. Thus, the effect due to the field gradient was minimized because of the constant field intensity within the pole radius. As shown in Figure (13), the probe wire was protected by pairs of protection legs from any direct contact with the tube wall.

4. Procedure

The hot-wire anemometer probe and thermocouple holder were first put through a hole in the circuit tube, and then attached to the micrometer. This was done cautiously to insure that the probe wire was parallel to the field intensity vector and perpendicular to the flow direction. The magnetic fluid was then injected into the test loop with a funnel into a valve.

The magnetic field generator was preset for the constant field mode (instead of sweeping mode) for a maximum of 6500 Gauss within a 0.05 meter gap between magnetic poles. If there were any superparamagnetic material between or neighborhood of magnetic poles, the uniform field direction will be deflected through the superparamagnetic material. Therefore, all materials which were used in the magnetic field were selected as non-magnetic materials except for

for the magnetic fluid. All fabrications consisted of copper and brass. After start-up of the electromagnet, the Field Selector Knob was turned to the desired magnetic fields. In this experiment, the field intensity was selected up to 5.5 Kilo Gauss. The first setting of magnetic field was 4 kG.

A check was made to verify that all instruments were properly working and that the probe position was at the starting position. When everything was working, the heating element around the test section and cooling water were turned on and adjusted until a constant surface temperature was obtained. The maximum temperature was 370 °K. The constant heat flux was 3769 W/m^2. After equilibrium was reached, the velocity and temperature measurements were carried out at 10 points along the radial direction for the positions of 0.025 and 0.05 meter from the thermal entrance, and for the field intensity of 4.0 kG and 5.0 kG, respectively.

5. Data Reduction and Analysis

During the measurements of velocity and temperatures, about 200 data points were successful out of about 500 attempts. An unstable flow field was often formed at a certain temperature and magnetic field intermittently. It is still uncertain, but possible interpretations are that the magnetic fluid was on the critical point for stability; that is, the critical magnetic Rayleigh number = 1707. Another interpretation is that the liquid velocity and temperature rose with time and with accelerating motion of the fluid up to their maximum values until, at a certain moment in time, the

fluid temperature suddenly increased and the velocity was slowed down. This phenomenon was well explained by Bashtovoi et al. [44] by their thermoconvective explosion theory due to an accelerated heating up of the magnetic fluid. It is suggested that this be observed further on the scale of temperature and velocity of this study.

The data obtained for velocity and temperature were reduced through the program CURFIT in Appendix D and plotted through the program FHDPLT in Appendix E. The computer programs CURFIT and FHDPLT were developed using regression analysis. The complete program listings are given in Appendices D and E.

The reduced data are illustrated in the following 12 figures. Figures (15), (16), (17), and (18) show the regressed velocity profile along the radial direction with data points. The velocity profile in Figure (15) was drawn with a heat flux of 3769 W/m^2 and the field intensity of 4000 Gauss at 0.025 m downstream from the thermal entrance, Figure (16) with 5000 Gauss at 0.025 m, Figure (17) with 4000 Gauss at 0.05 m, and Figure (18) with 5000 at 0.05 m downstream from the thermal entrance. The effect of magnetic acceleration in this thermal boundary layer is obvious when comparing the profiles at 0.025 and 0.05 m.

The velocity was also measured at the tube centerline as a function of the external magnetic fields. These results are shown in Figure (19) for field strength from zero to 5.5 kG. The velocity is shown to be generally increasing with field strength. Figure (21)

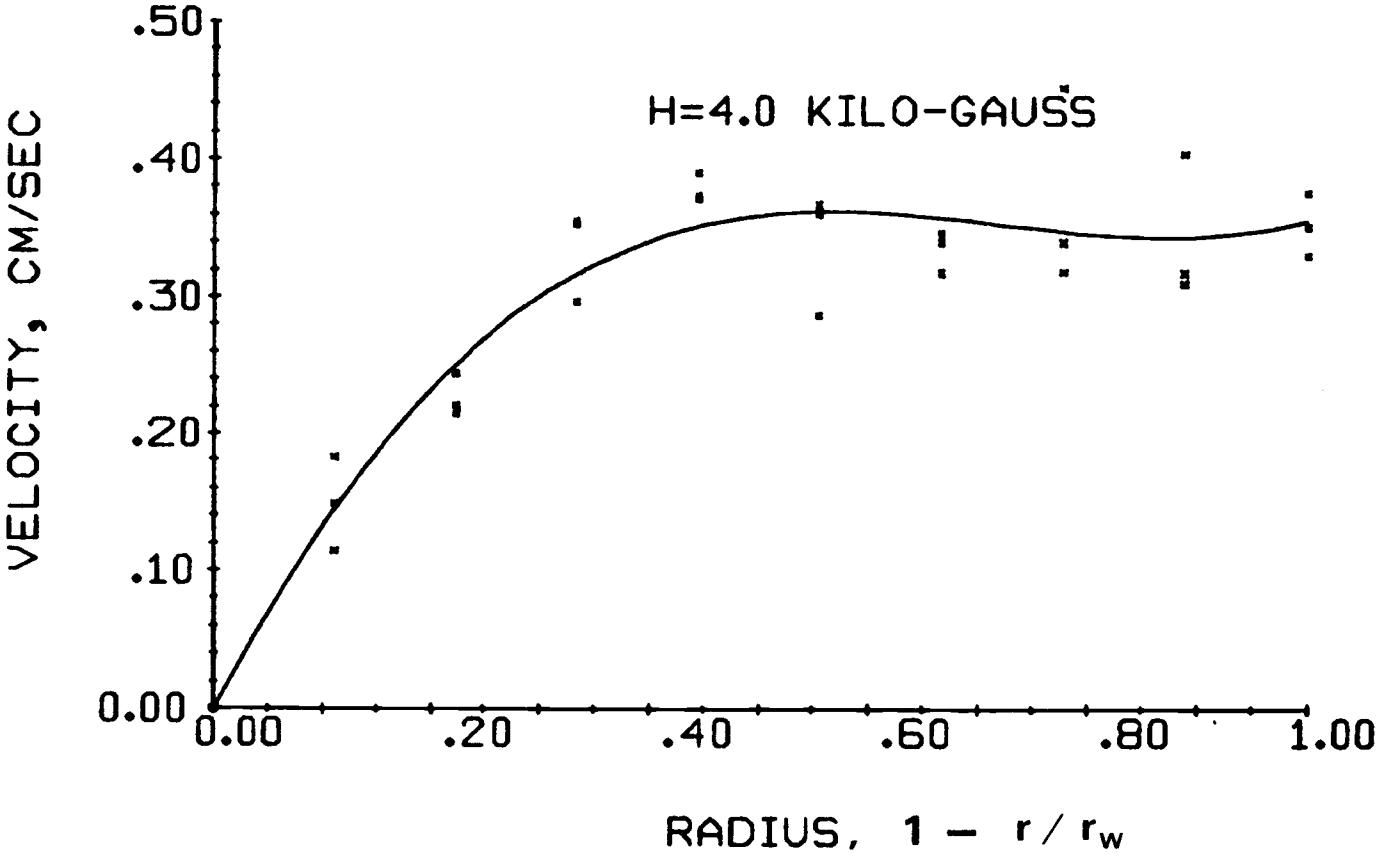

Figure 15. Velocity profile at 0.025 meters downstream from thermal entrance, and with 4.0 kG magnetic field strength.

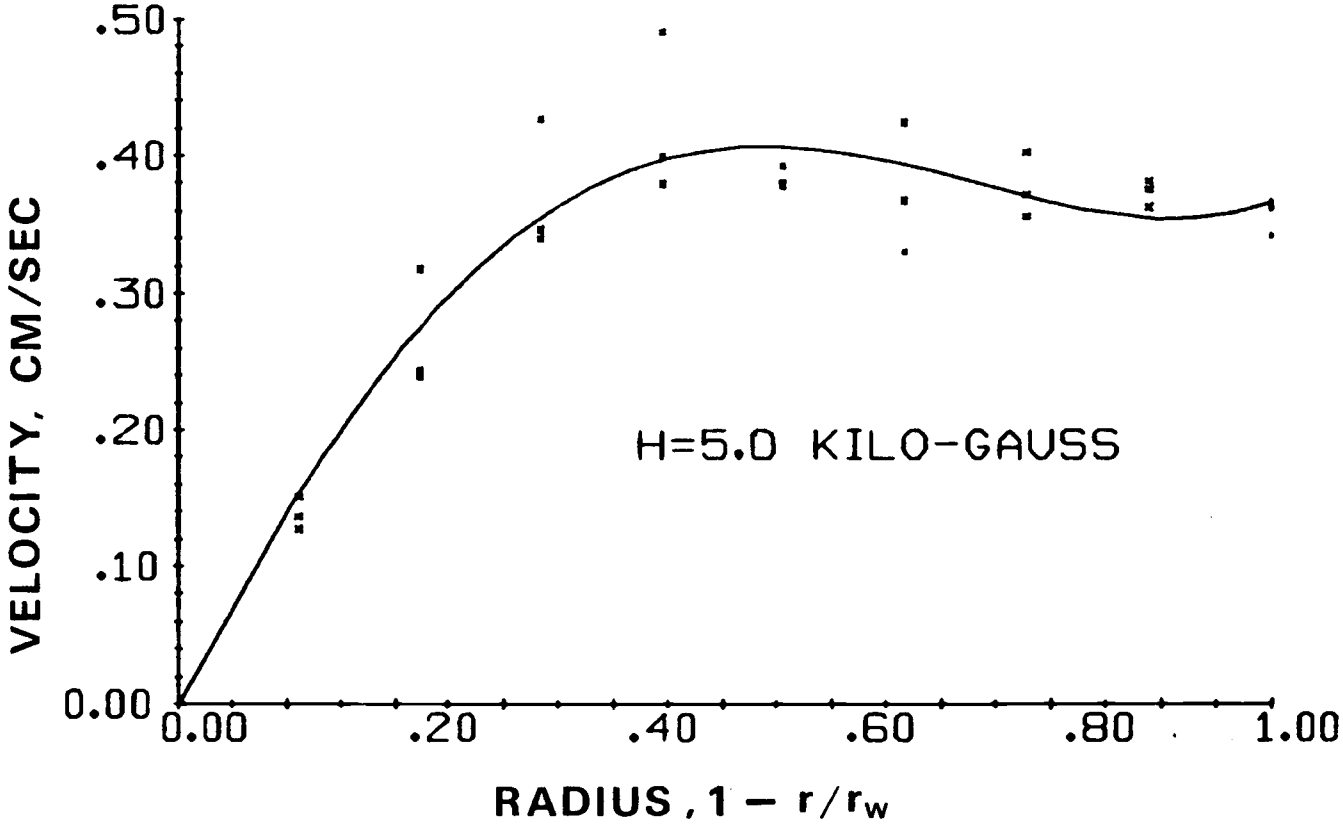

Figure 16. Velocity profile at 0.025 meters downstream from thermal entrance, and with 5.0 kG magnetic field strength.

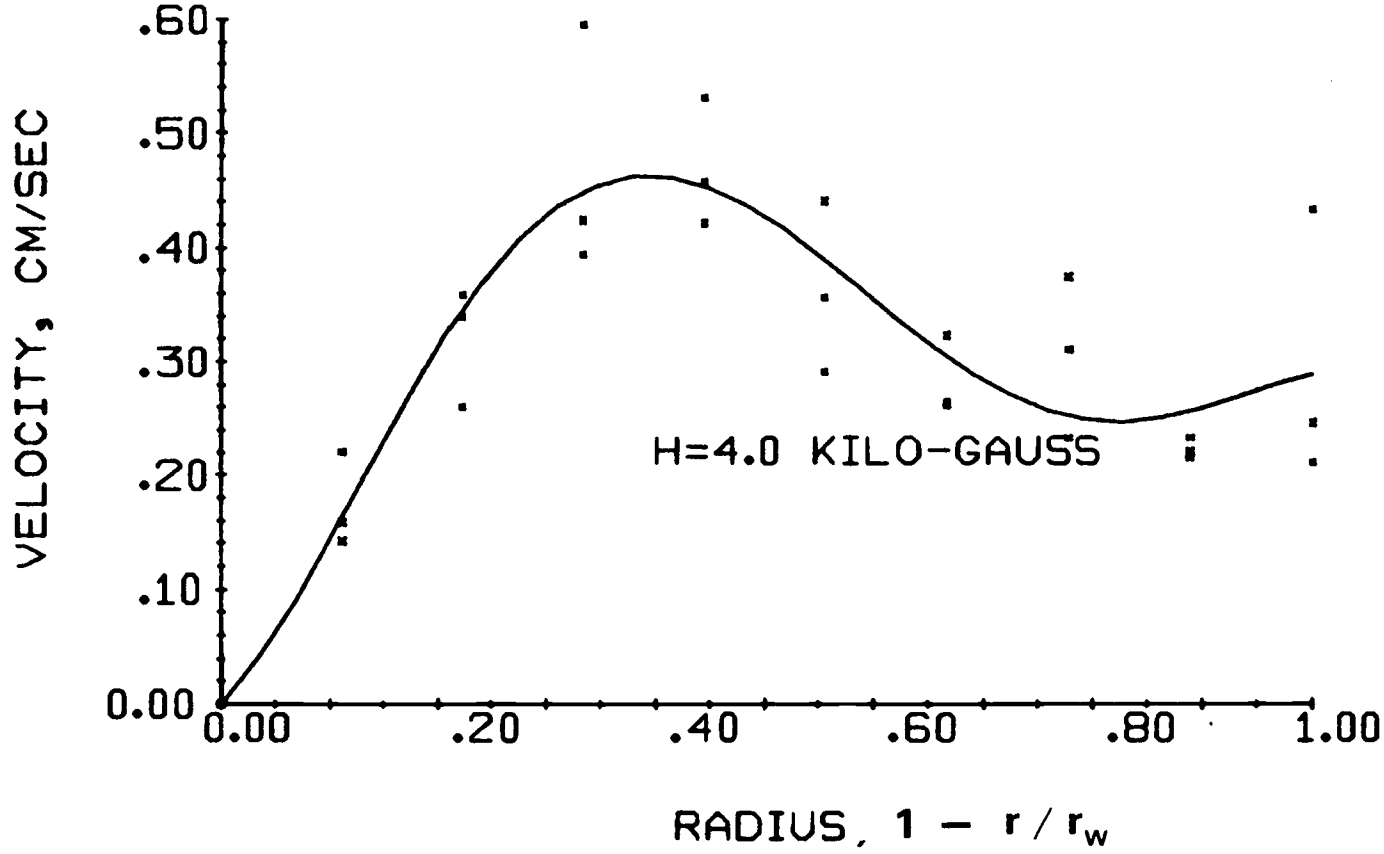

Figure 17. Velocity profile at 0.05 meters downstream from thermal entrance, and with 4.0 kG magnetic field strength.

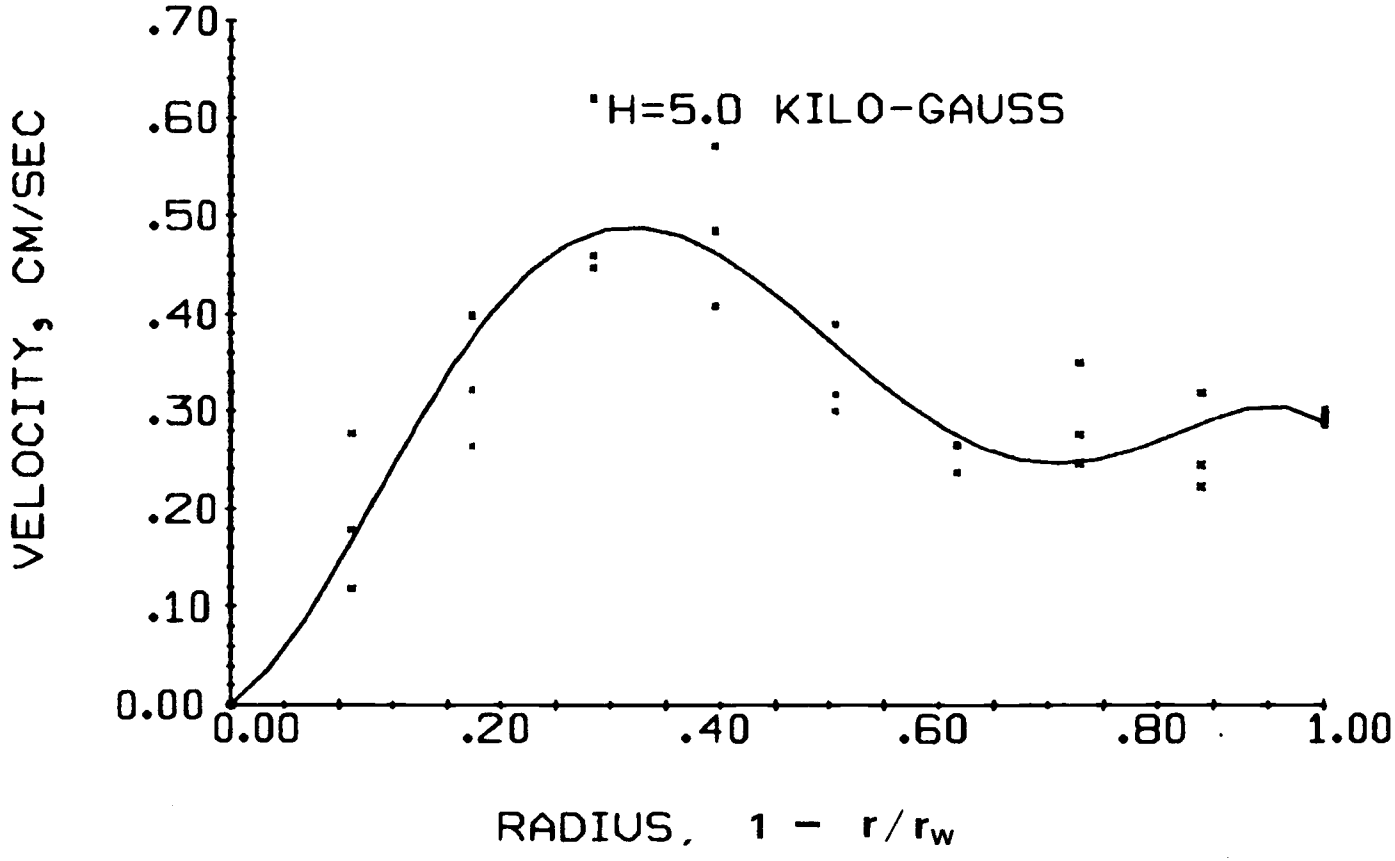

Figure 18. Velocity profile at 0.05 meters downstream from thermal entrance and with 5.0 kG magnetic field strength.

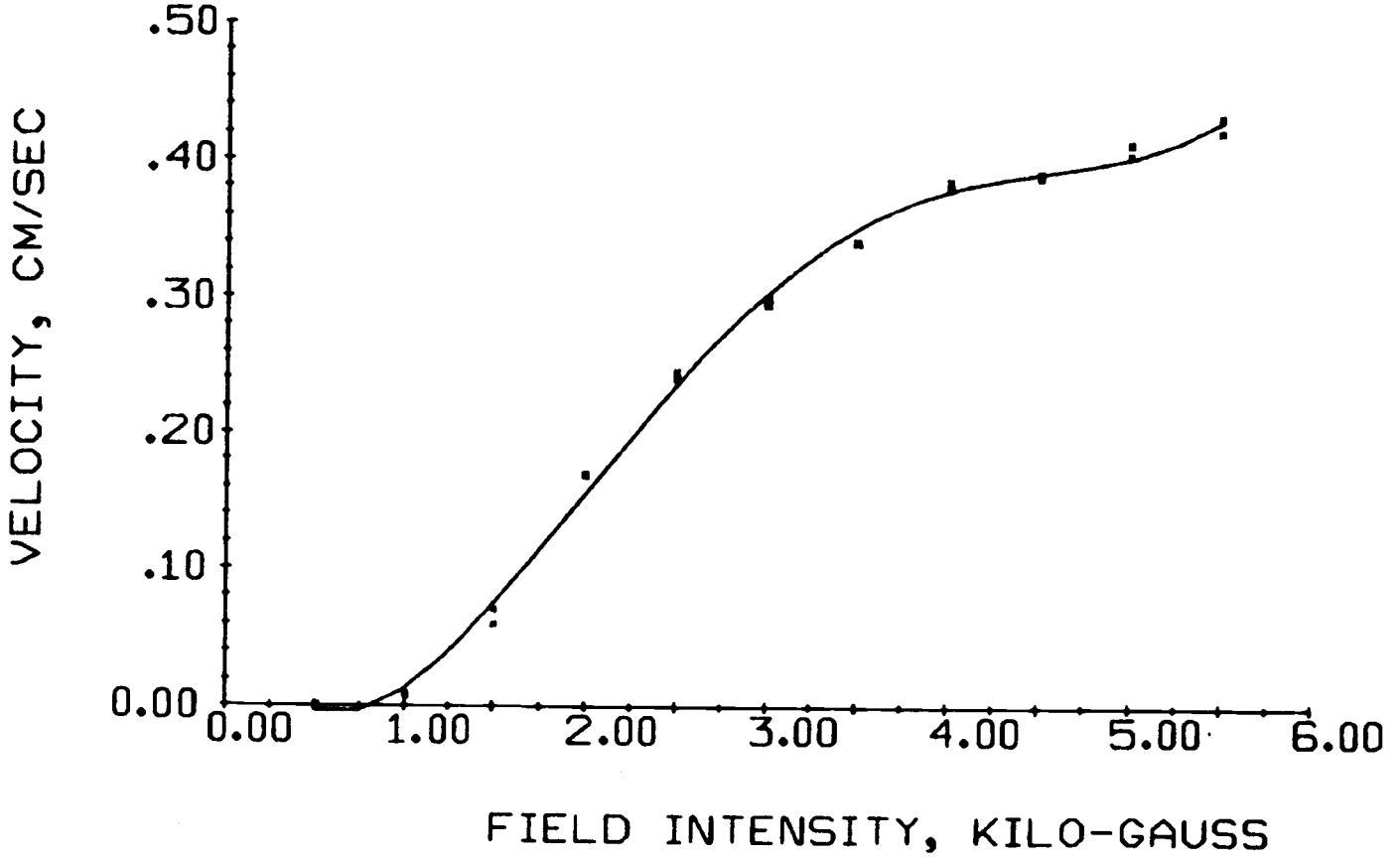

Figure 19. Velocity profile with respect to external magnetic field.

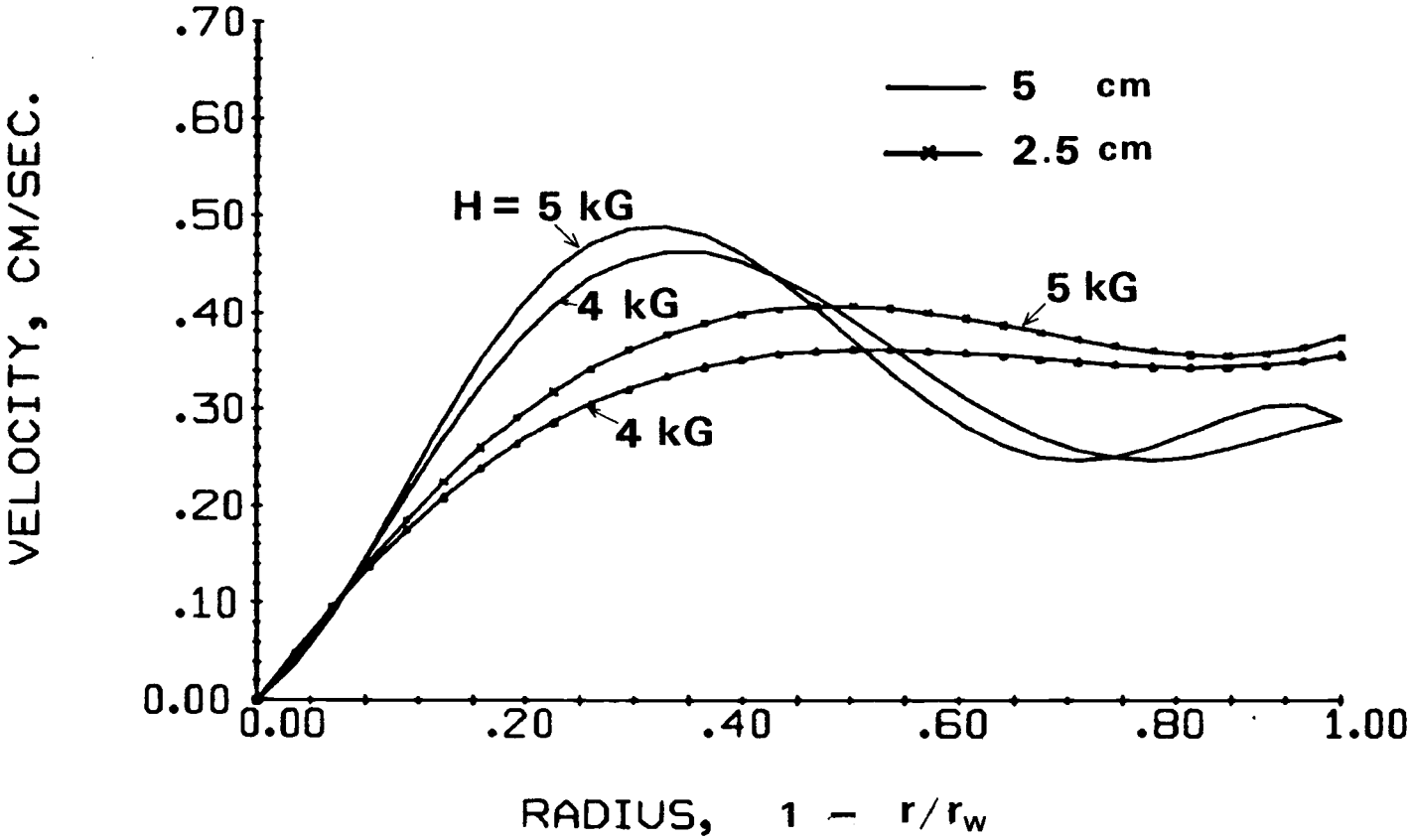

Figure 20. Experimentally measured velocity profiles.

shows the velocity profiles measured at the alternate test sectio n where no magnetic field exists under the loading of 4 kG and 5kG at the main test section. Figures (22) and (23) show the temperature profiles with the magnetic field intensities of 5 kG and 4kG, and the heat flux of 3769 W/m^2. These profiles are nearly the same since the heating rate was the same.

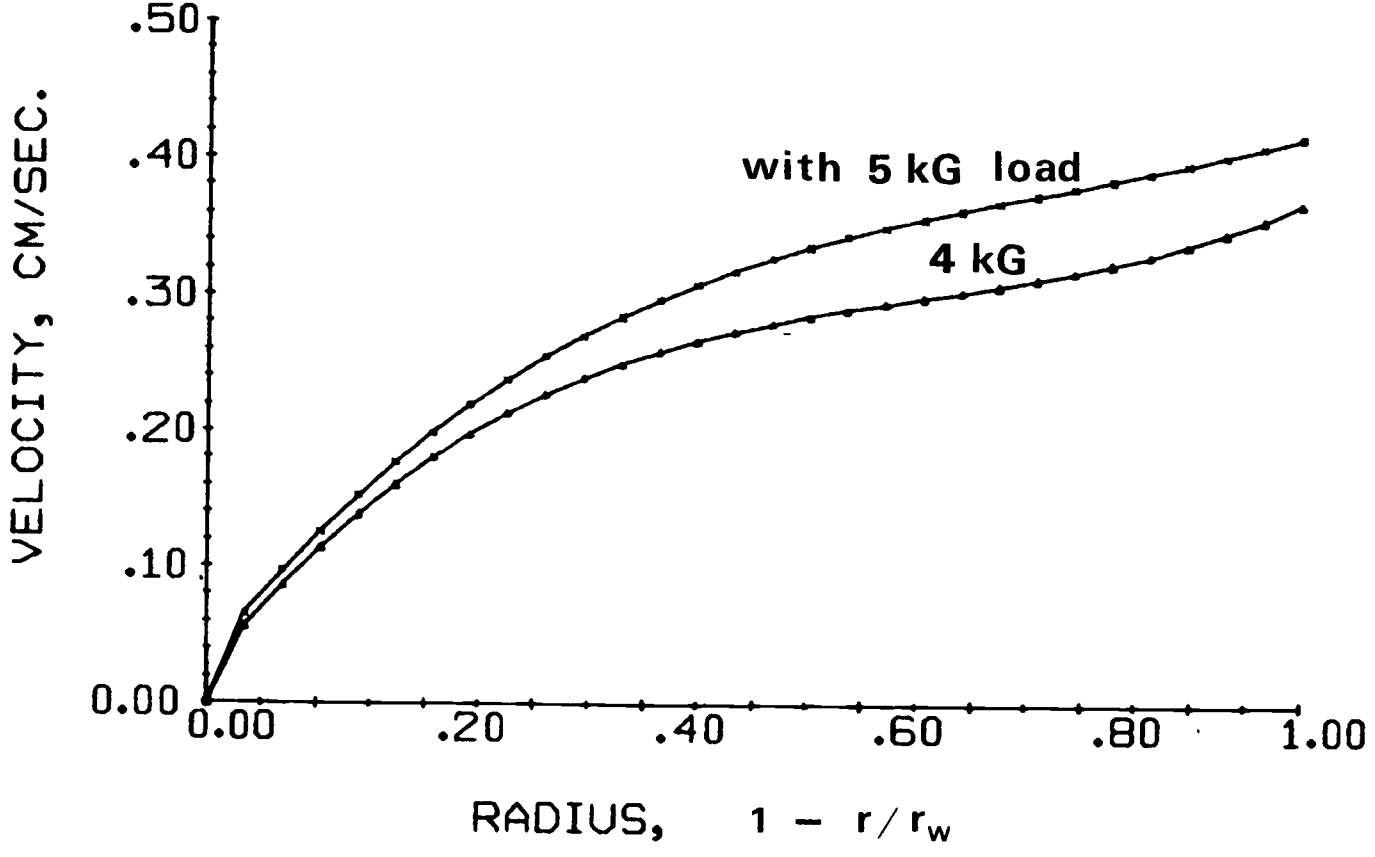

Figure 21. Velocity profiles in the absence of the magnetic field at the alternate test section.

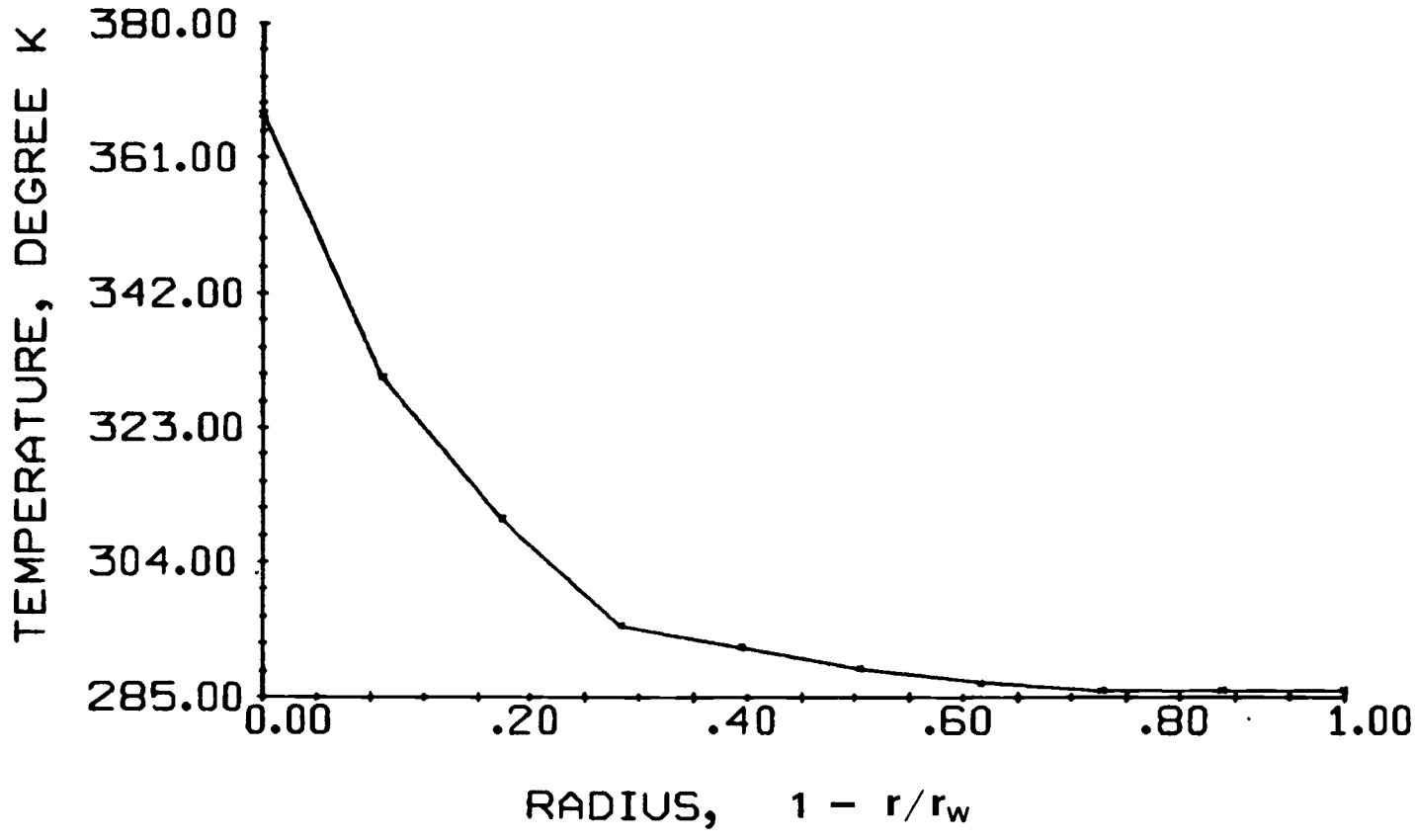

Figure 22. Temperature profile at 0.05 meter from thermal entrance.

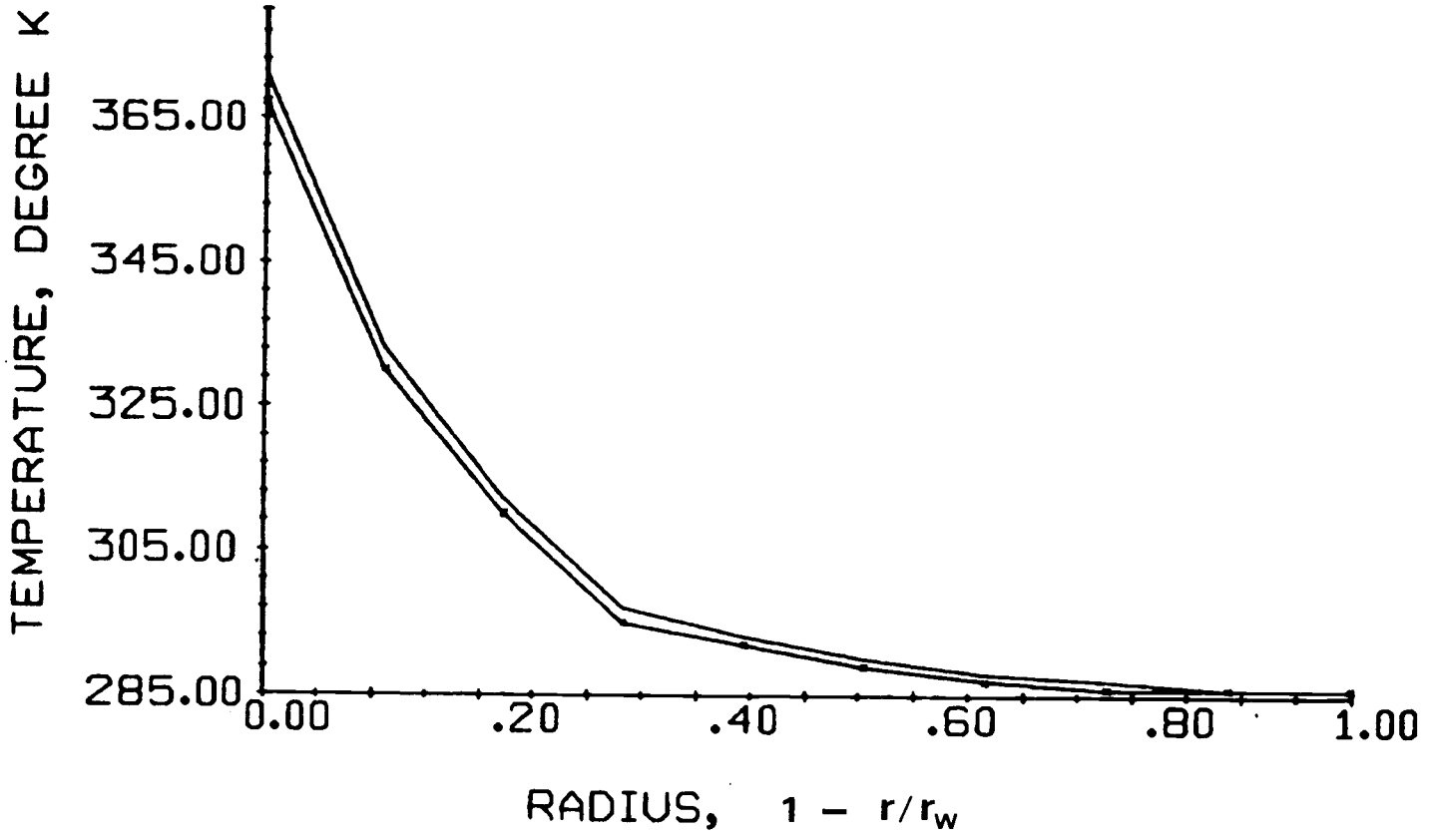

Figure 23. Temperature profiles with respect to applied magnetic fields of 4 kG and 5 kG at 0.05 meter from thermal entrance.

VII. RESULTS AND DISCUSSION

VII-1. Fully Developed Region

For theoretical fully developed flow an analytical solution was calculated by PROGRAM MAGNET given in Appendix B. One sample output page is also attached to the program. Calculated results are plotted in Figures (24), (25), (26), and (27) for selected values of Re and Ra_M. The nature of the problem is similar with the Graetz problem, in which the fully established laminar flow with a constant wall temperature in a round tube is considered [64]. It is also similar to the work which Hallman [65], Hanratty et al. [66], Siegel et al. [67], and Tao [68] did. But considering the problems related to the magnetic properties of the working fluid, the solutions cannot be interpreted as the same. The flow pattern of a magnetic fluid is dependent on the magnetization of a magnetic fluid which is a temperature dependence, and on the magnetocaloric effect. Even though there is no gravity0induced flow for the case of horizontal flow, we can obtain the same type of flow with a magnetic fluid with the internal heat source.

Due to the magnetocalorid effect as a heat source and due to the correlation of magnetization of a magnetic fluid to the fluid temperature, the flow and heat transfer structure become unpredictably unstable at a critical point. This unstable motion at a critical point has been explained by the thermoconvective explosion theory [44]. Equation (26) also explains the magnetocaloric effect

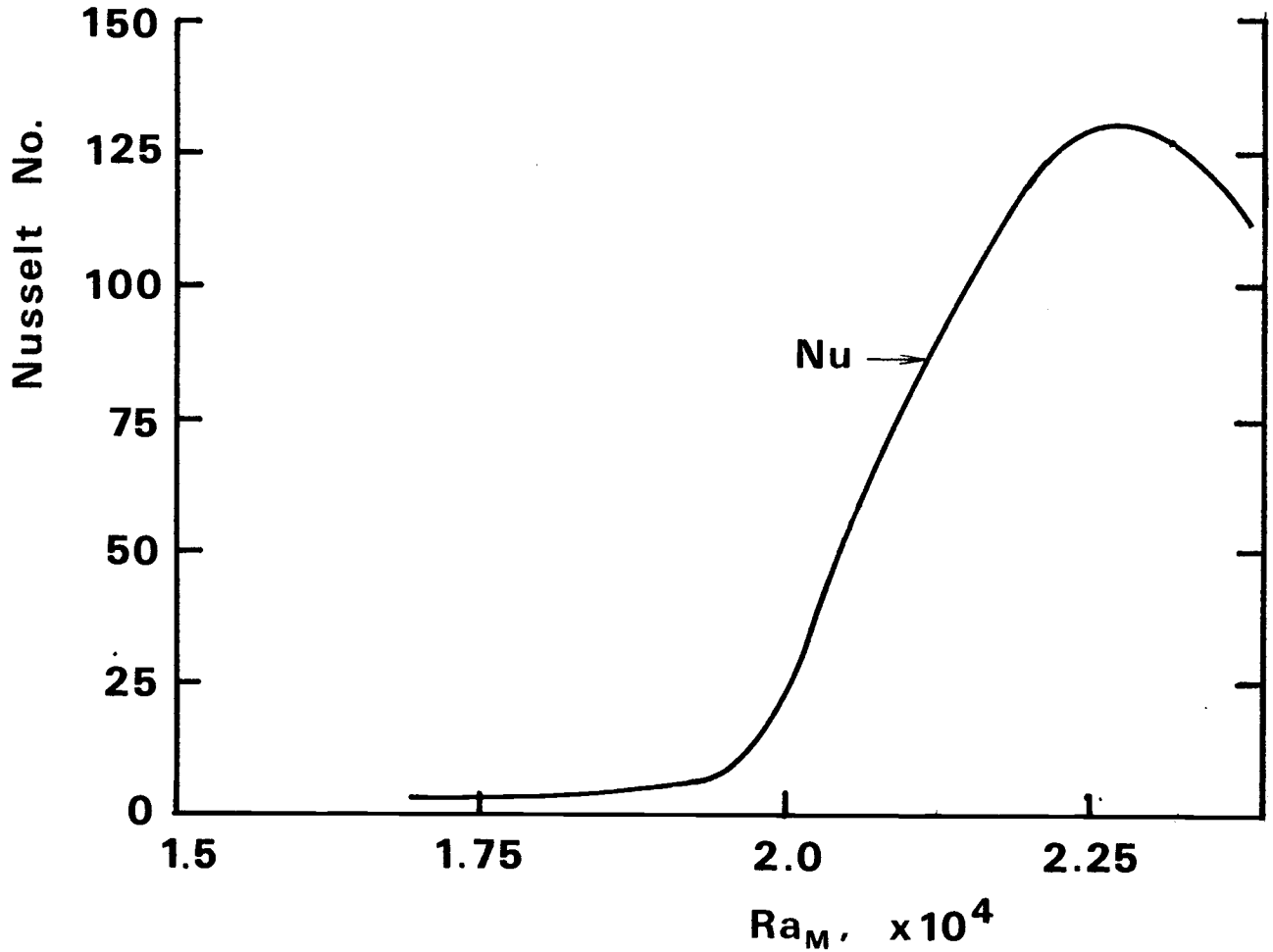

Figure 24. Correlation between Nusselt and magnetic Rayleigh numbers for selected values of Re and Ra_M.

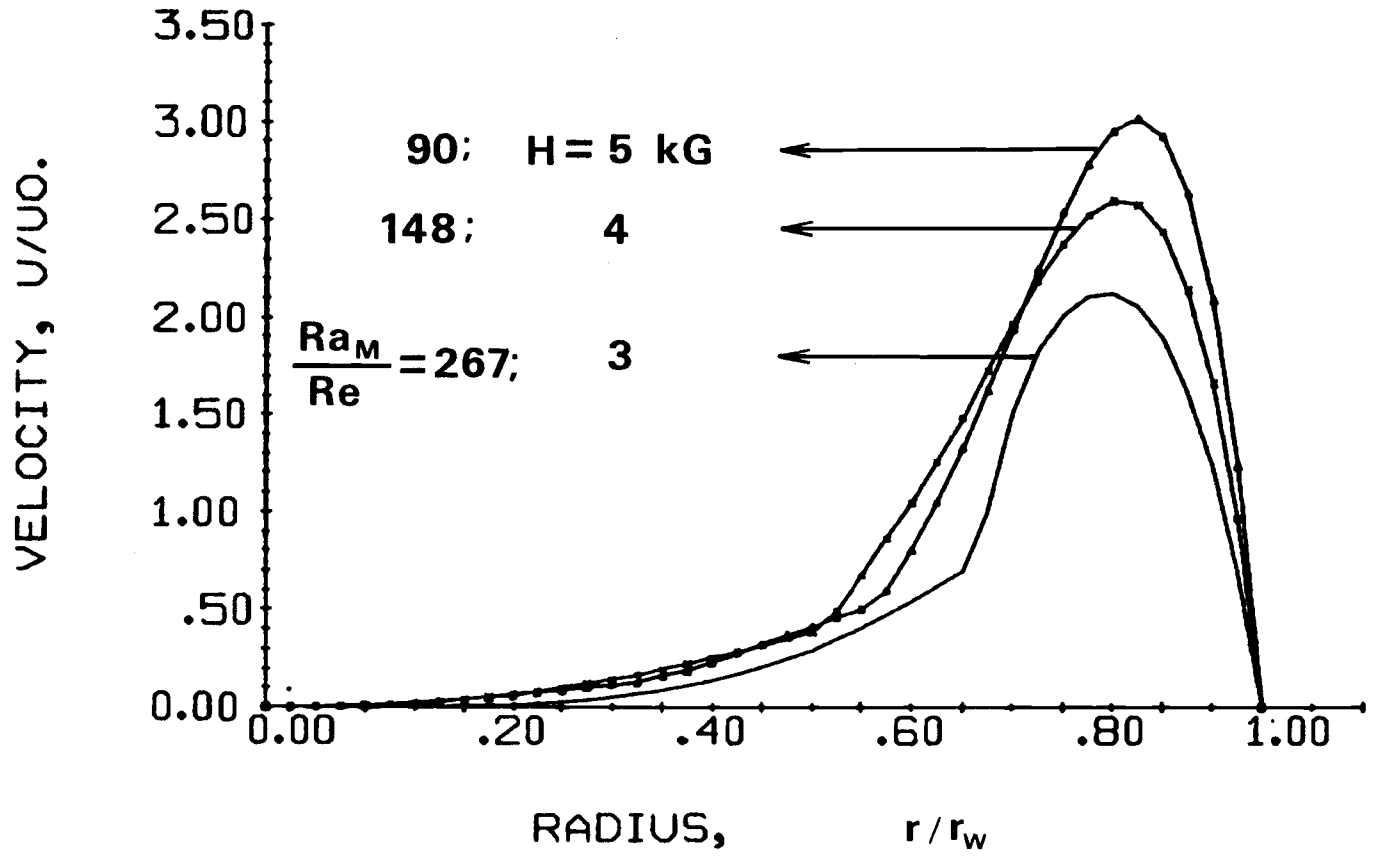

Figure 25. Velocity profiles for various applied magnetic fields against dimensionless radius for selected values of Re and Ra_M.

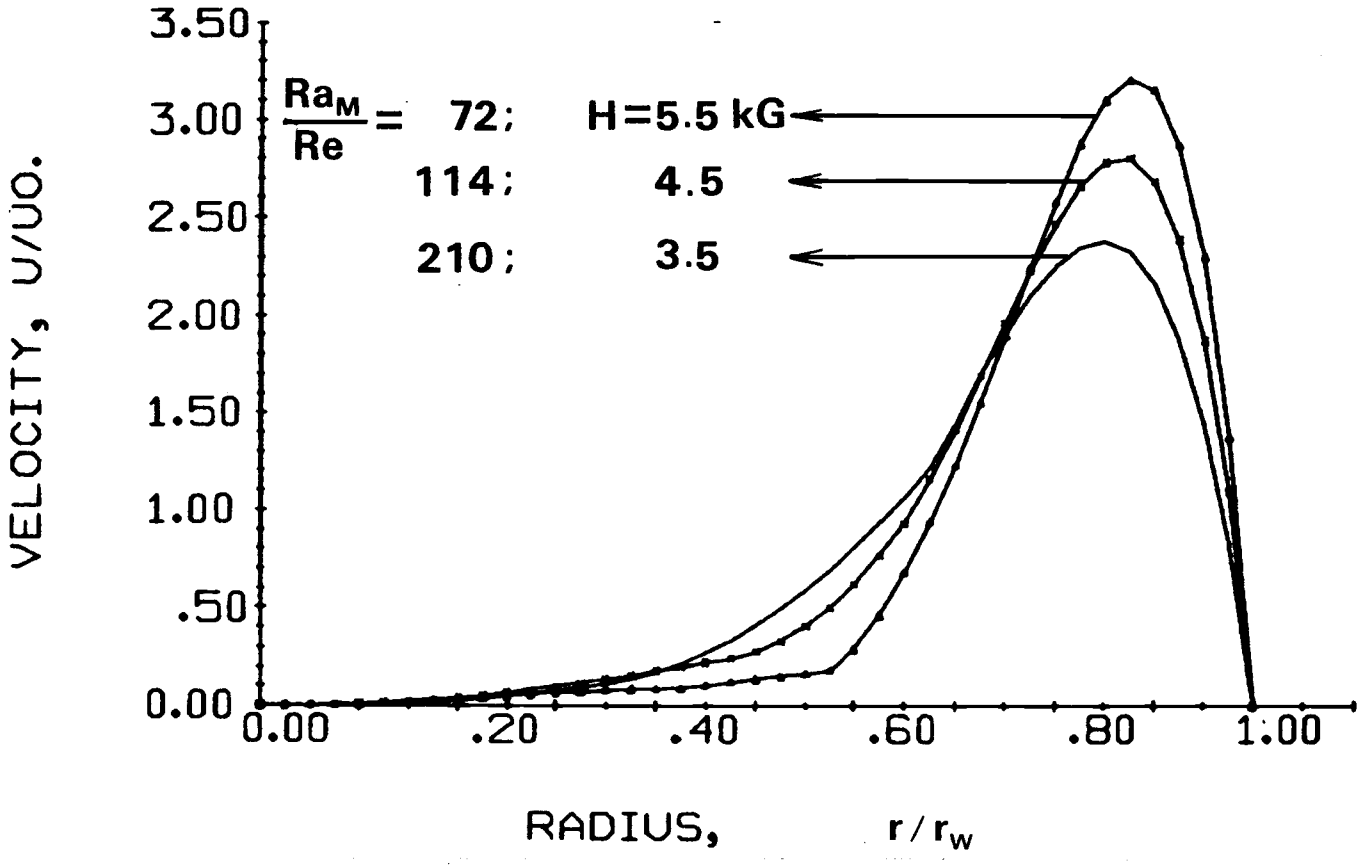

Figure 26. Velocity profiles for various selected magnetic Rayleigh and Reynolds numbers.

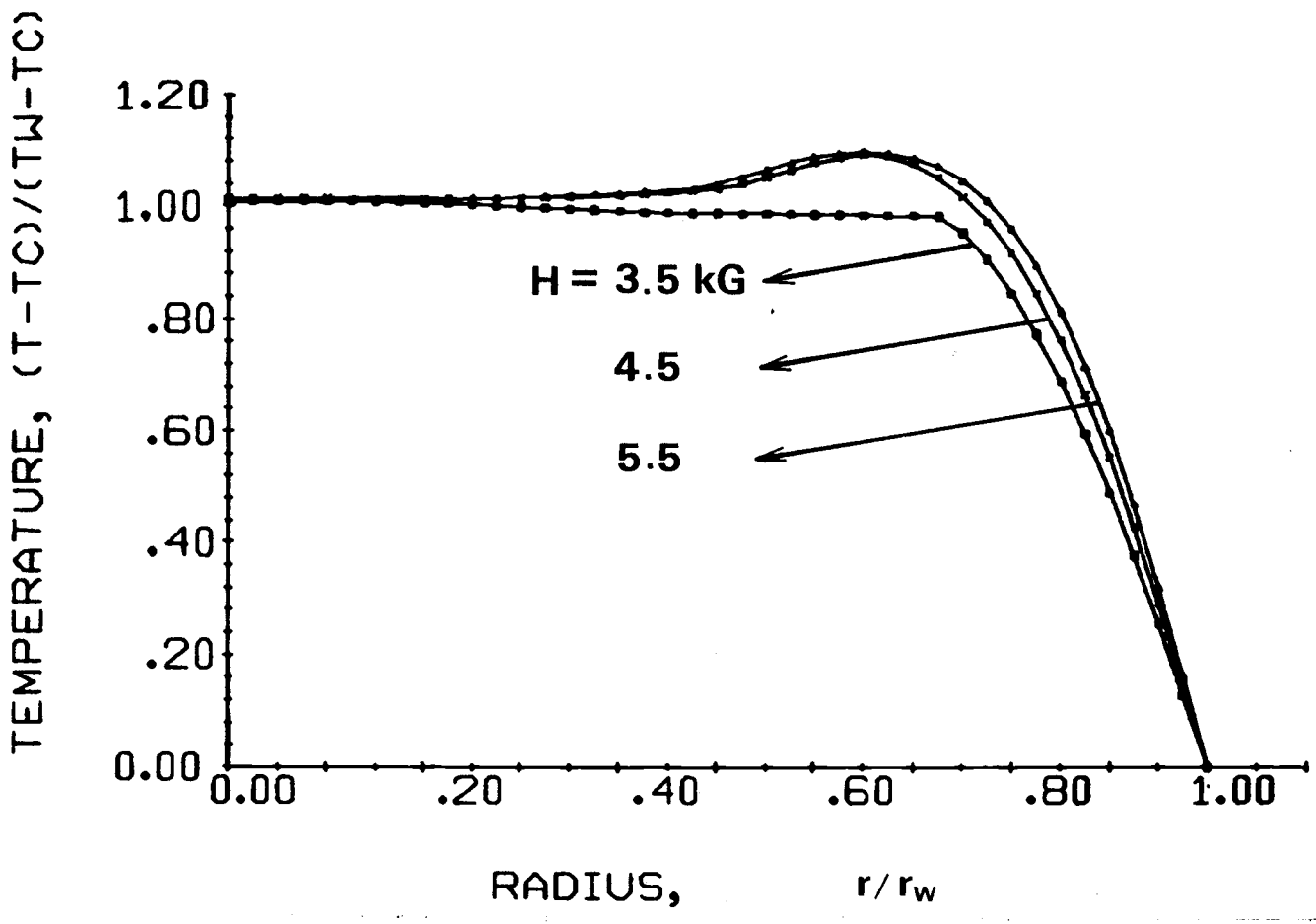

Figure 27. Temperature profiles for various applied magnetic fields against dimensionless radius.

on the flow of a magnetic fluid. The fluid magnetization decreases with heating, so that a magnetic fluid is cooled when it is adiabatically moved to downstream from a position into a region of lower pressure, and is cooled when the magnetic field intensity decreases with distance. Therefore, the velocity and temperature experience the change in their values at a certain point when the magnetic field intensity decreases with distance and the flow is also accelerated. Such a phenomenon was observed in this study. That is, the calculated fluid medium temperature increased up to the temperature ratio $(T-Tw)/(T_c - T_w) = 0.9760$ at H = 4500 Gauss and with the magnetic Rayleigh number [ref. Eq. 30] $Ra_M = 22500$, and then started to decrease gradually. Even though the change is quite small, the effects on the heat transfer are quite visible. Figure (24) shows correlations of Nusselt number for selected values of magnetic Rayleigh and Reynolds numbers. The Nusselt number with respect to the selected magnetic Rayleigh number in Figure (24) has the same trends up to the magnetic Rayleigh number $Ra_M = 22500$, as the results of Hanratty [66] for low Reynolds number gravity induced flow in vertical tubes with constant heat flux, and as a result of Hallman [65] for the combined forced and free laminar heat transfer in vertical tubes with uniform internal heat generation. But over $Ra_M = 22500$, the Nusselt number declines due to the dominant magnetocaloric effect and so-called thermomagnetic explosion phenomenon. As a result an interesting correlation exists between Nusselt and Reynolds numbers

over Ra_M = 22500 resulted from the magnetic properties of a magnetic fluid.

Figures (25) and (26) show the velocity profiles against the dimensionless radius for selected values of Re and Ra_M. And Figure (27) shows the dimensionless temperature profiles against the dimensionless radius of tube. These Figures (25), (26), and (27) have the same tendency as those of the gravity-induced flow.

The discontinuity of the profiles in Figures (25), (26), and (27) between .55 and .65 of dimensionless radius are due to the methods in which the Kelvin function was evaluated. When the argument of Kelvin functions was greater than 6, the asymptotic expansions were used instead of the Kelvin series functions because of a quicker convergence of functions for large arguments.

VII-2. Thermal Entrance Region

In this section, the numerically calculated velocity and temperature, and also the experimentally measured velocity and temperature are given and compared to each other. The numerical

calculation could have covered the entire length of the thermal entry, but the experimental measurements were carried out within 0.05 meter from the thermal entrance because the probe, as explained in Section 3 of Chapter VI, should be put within 0.075 m of the magnet poles (Fig. 14).

Even though there is a small difference in temperature between the probe wire and a neighboring fluid, if the applied magnetic field intensity is strong, the instability of probe or the probe-induced flow over the magnitude of velocity which is going to be measured will be a dominant factor.

For better measurements with a hot-wire anemometry system, it is important that the field intensity remain steady, a small resistance ratio for the probe be placed in a uniform magnetic field, and, if possible, use a magnetic fluid with a low pyromagnetic coefficient. The author feels that measurements in magnetic fluids with hot-wire anemometry systems should be studied further.

Reduced experimental data for velocity and temperature were plotted in Figures (15) through (23). Figures (15), (16), (17), and (18) show the velocity profiles against the dimensionless radius at different distances from thermal entrance in the presence of an applied magnetic field. In the center portion of a flow in the tube, the sinusoidal velocity curve was caused by the high order of polynomial in the regression analysis as one of the reasons, and also possibly by the probe sensitivity due to fluid temperature

change. Another reason could be possibly a slight lack of the above necessary conditions for the probe setting, and a flow fluctuation due to the thermomagnetic explosion phenomenon. These combined problems reflect the scatter of data points in Figures (15), (16), (17), and (18).

The numerical analysis for the thermal entry problem of a magnetic fluid gives some descriptive results for velocity, temperature and dimensionless numbers. Figure 28 shows the velocity profiles at 0, 2.5 cm, and 5 cm from the thermal entrance in the presence of the applied magnetic field of 5.0 kG. From Figure (28) one can see that the velocity development caused by the temperature dependence of magnetization of a magnetic fluid is similar with that of the gravity-induced flow. For a magnetic fluid, as long as there is any axial temperature gradient, the velocity (or momentum) equation coupled with the energy equation generates a specific velocity field with respect to temperature gradient. Such magnetic field-induced flow can also be explained by the magnetic Rayleigh number analysis. First, assume that a magnetic fluid exists at rest. Then when the magnetic field gradient and temperature gradient are formed, the fluid starts flowing. For this convective motion of a magnetic fluid, a correlation between the magnetic field gradient and temperature gradient was developed in Section III-5. It is represented by the magnetic Rayleigh number (Equation 30). Over the critical value of Ra_M the flow motion becomes steady. For a cylindrical geometry flow the critical magnetic

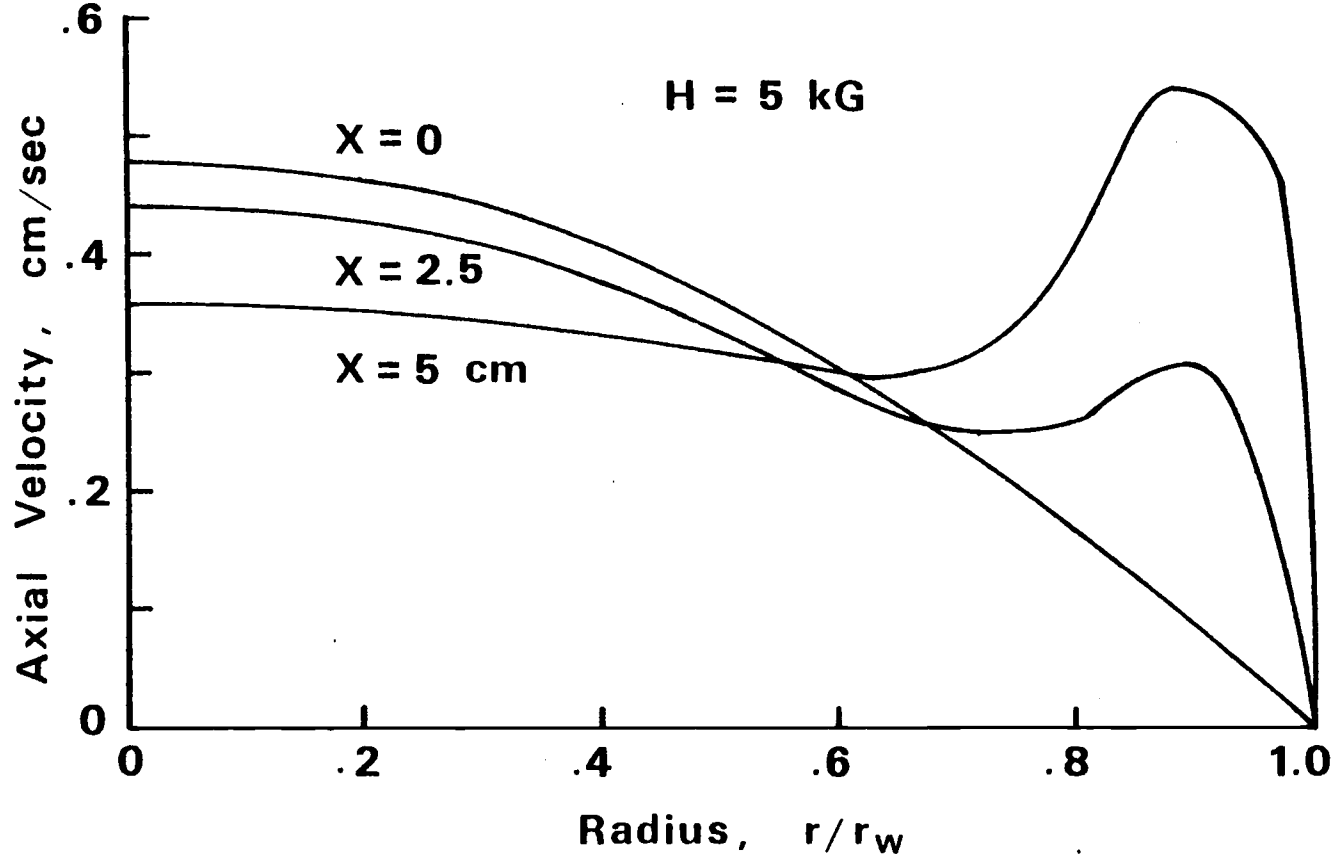

Figure 28. Axial velocity profiles vs. dimensionless radius.

Rayleigh number is 1707 [53].

If a magnetic fluid enters into the region which a magnetic field and circumferential heat flux exist, the fluid will experience the change in velocity pattern caused by the above field and temperature gradients. Figure 28 reflects the influences of the field and temperature gradients.

Figure 29 shows the radial velocity profile at 2.5 cm from the thermal entrance. This radial velocity profile is well matched with the axial velocity in Figure 28.

Figure 30 shows magnetic Rayleigh number along the axial direction. The decline in magnetic Rayleigh number along the axial direction is mainly due to the change in magnitude of the axial temperature gradient and also due to the decrease in magnetic field intensity along the axial direction. The magnetic Rayleigh number has the maximum value at the thermal entrance because of high activity of magnetic fluid particles due to the magnetic moment reorientation and due to the high axial temperature gradient at that point. The magnetic Rayleigh number gradually decreases down to the fully established region. However, the number is still about in the order of 4×10^4 which is far over the critical number. This means that the flow is stable.

There are many factors which dominate the flow field of a magnetic fluid in a duct with a constant heat flux in the presence of an external magnetic field. The major effects on the flow field are due to the steep magnetic field gradient, the pyromagnetic

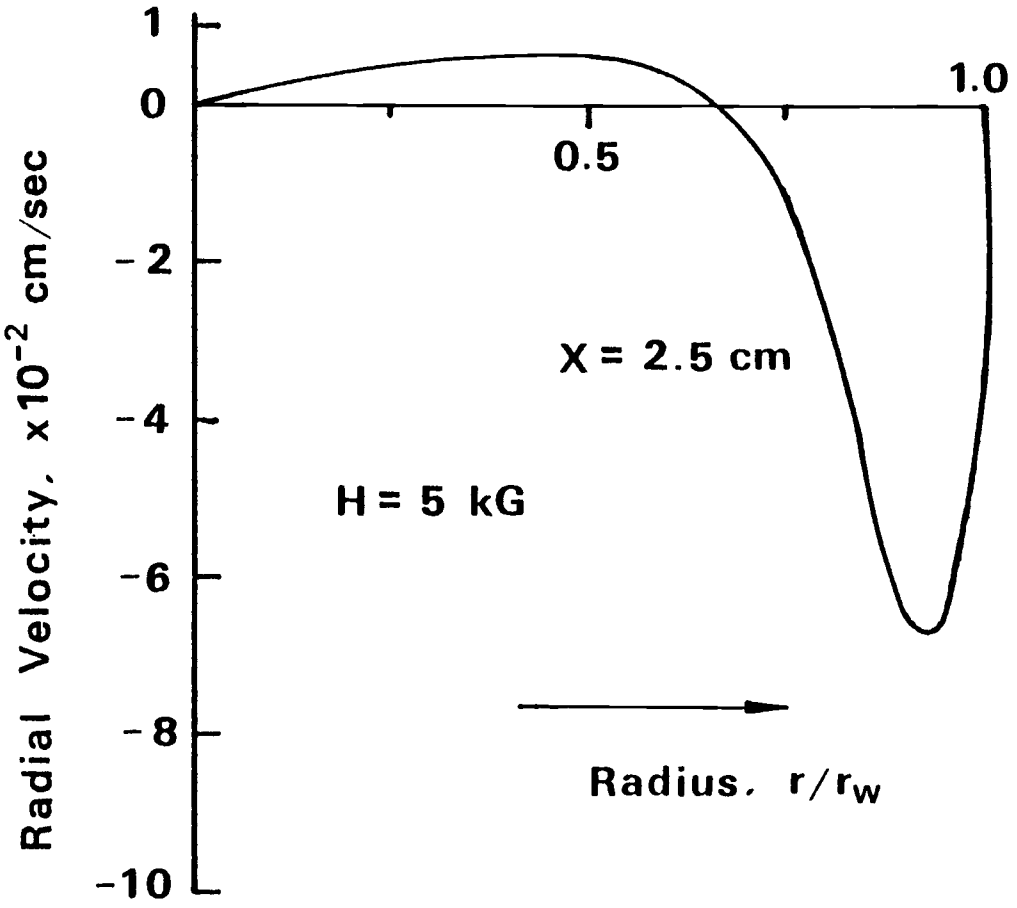

Figure 29. Radial velocity profile vs. dimensionless radius.

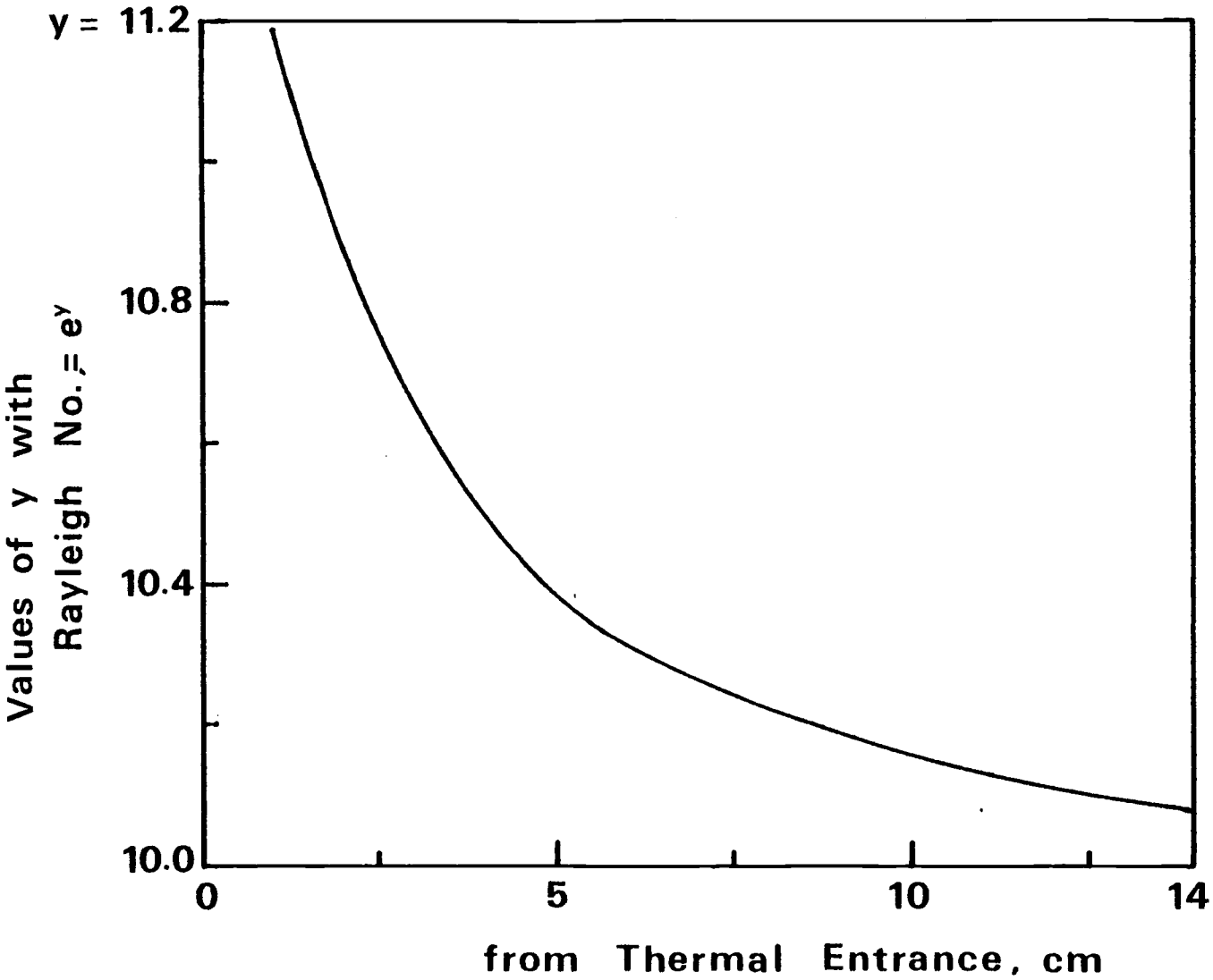

Figure 30. Magnetic Rayleigh number at Re = 136.0 with distance from thermal entrance.

coefficient, and the axial direction temperature gradient. Of course, the thing to be mainly considered is how fast the heat flux is absorbed by the fluid. It depends mostly on the fluid properties. High thermal conductivity and low viscosity of a fluid are desirable. If the fluid has these properties which satisfy the above conditions, then the axial temperature gradient will be formed evidently by rapidly absorbing the heat energy through the wall of a duct, and the temperature dependence of magnetization of a magnetic fluid will speed up the fluid velocity. Such a result suggests that a low Prandtl number fluid like a liquid metal has merit. In fact liquid metals are the promising media for the FHD direct energy conversion system because of not only their low Prandtl number, but also their electrical conductivity.

The two points in Figure (31) show the Nusselt numbers which were obtained from the experimental data under different magnetic field loadings. Compared to the numerically calculated values, the experimental values show good agreement, even though the measurements covered only a limited range of test section.

Figure (32) shows temperature profiles from the experimental measurements and from the numerical calculations. The differences near the wall of the duct are larger than at other locations. One possible reason is that in the numerical calculation, some input data were approximated because they were unavailable. Another reason was an experimental error.

Figures (33) and (34) show the comparison of velocities from

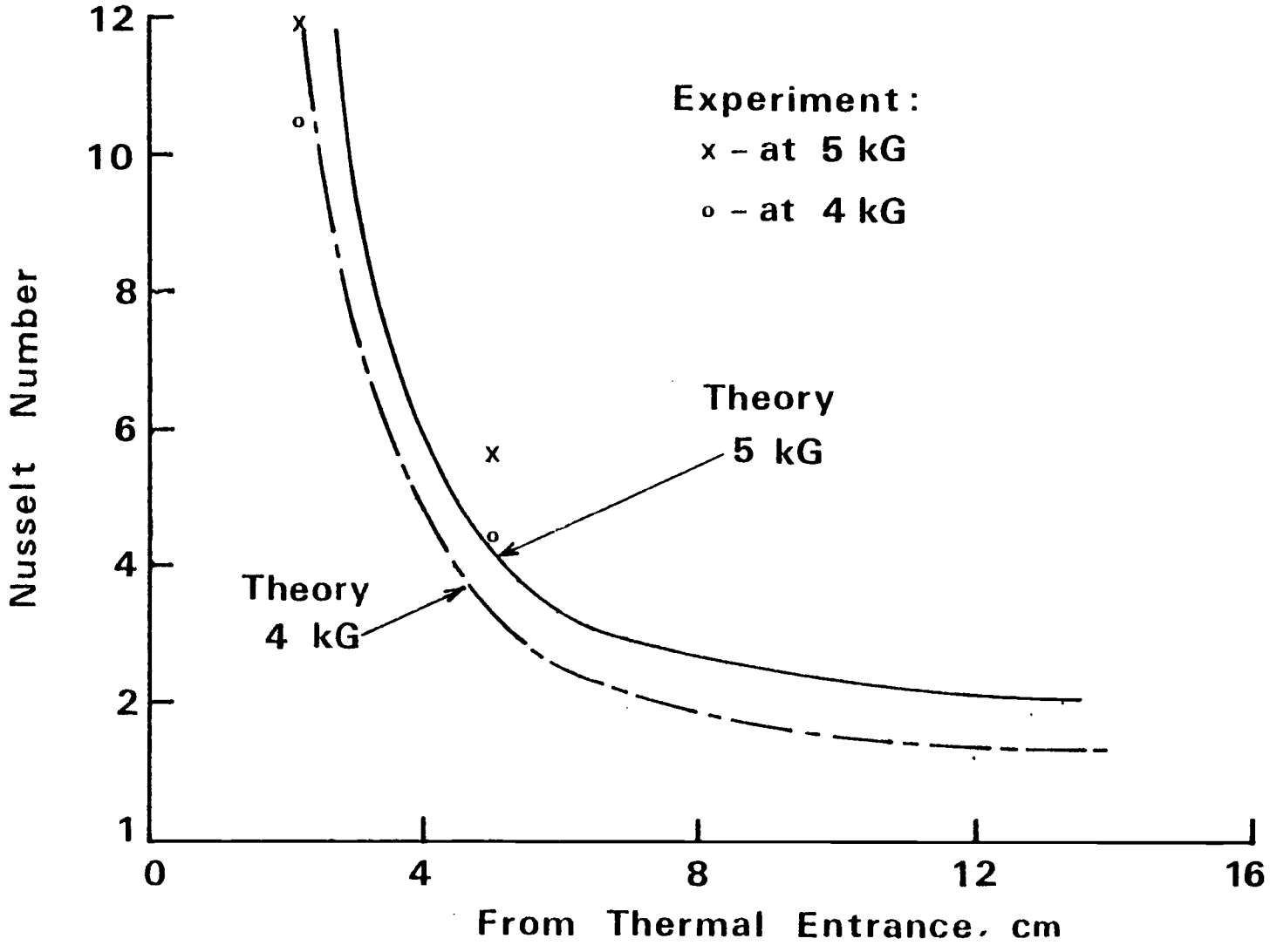

Figure 31. Nusselt numbers with distance from thermal entrance.

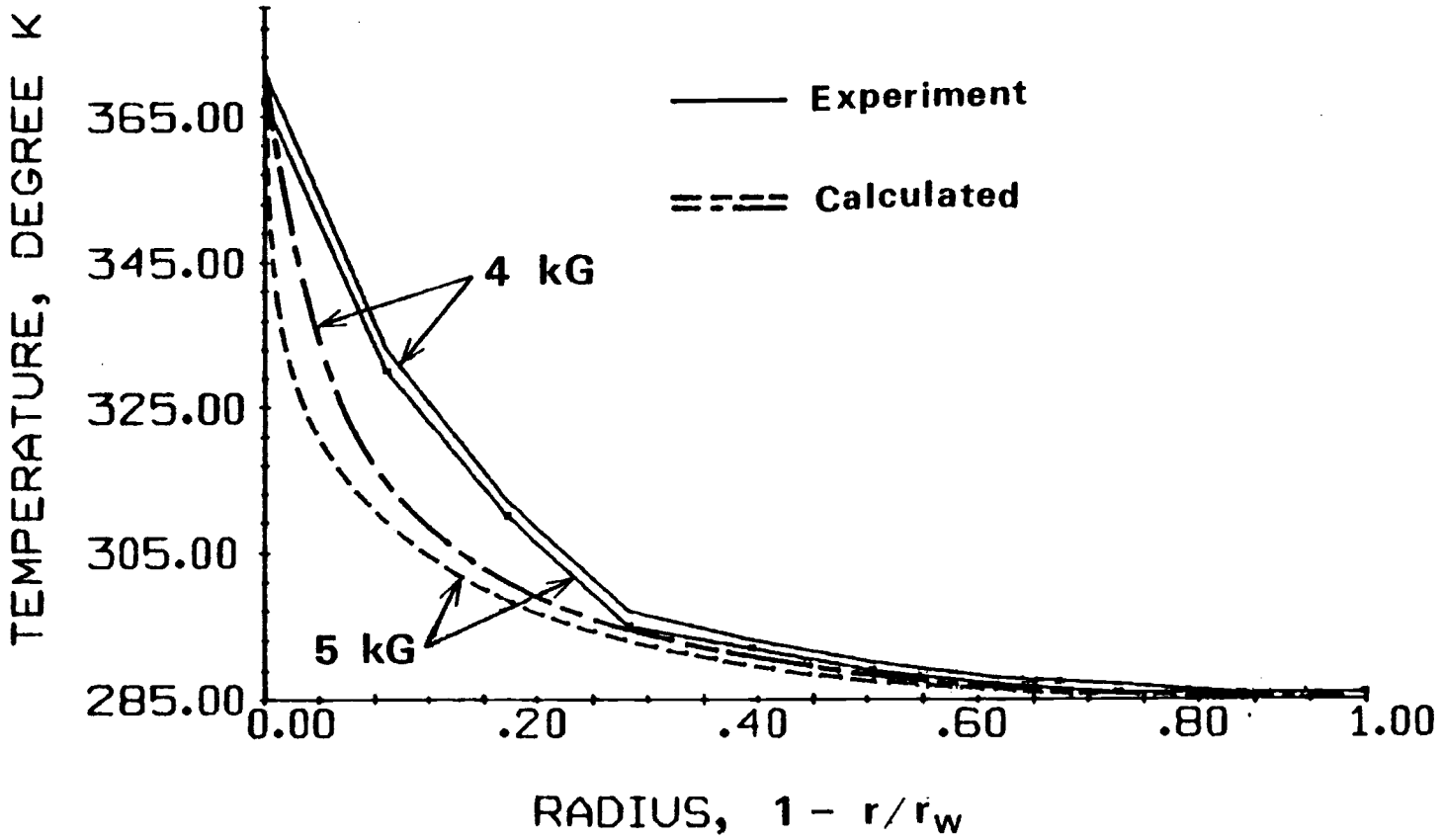

Figure 32. Temperature profile at 0.05 meter downstream from thermal entrance, and with heat flux of 3769 w/m^2.

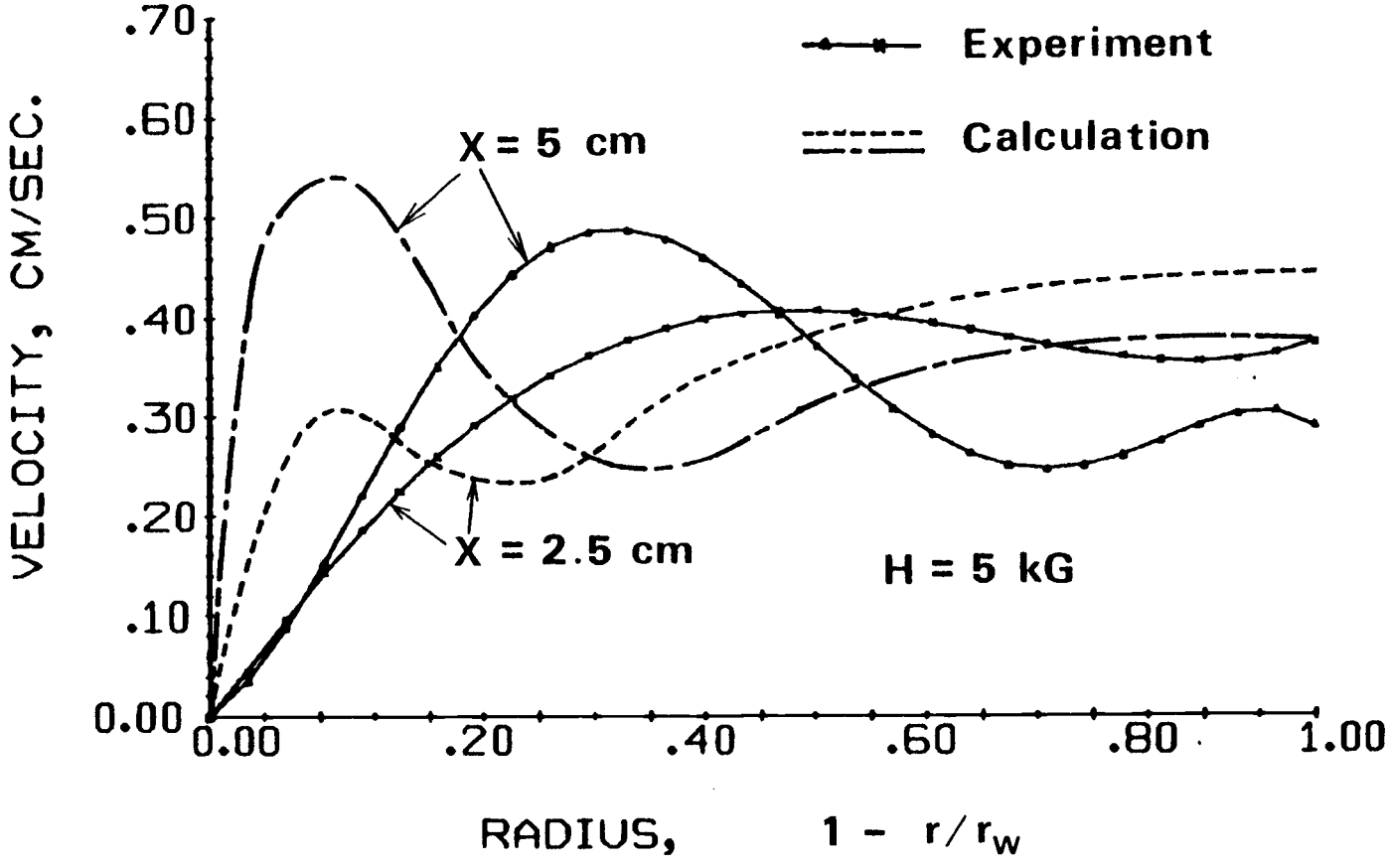

Figure 33. Velocity profiles from experimental measurement and numerical calculations.

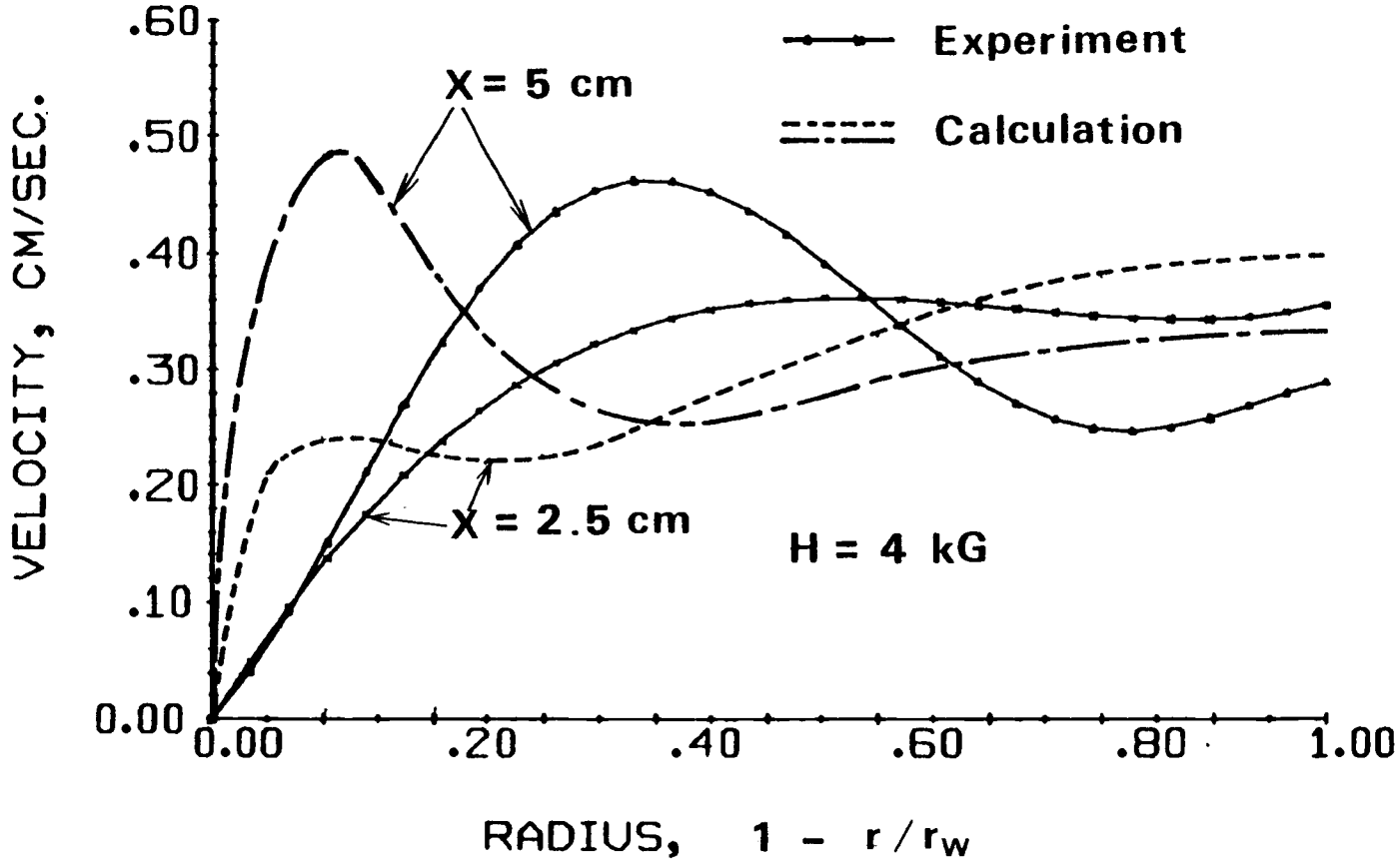

Figure 34. Velocity profiles from experimental measurement and numerical calculations.

experimental measurements and numerical calculations under the applied magnetic field intensities of 4 kG and 5 kG, respectively. The experimental curves are a result of a least squares fit to all experimental data.

The major differences in velocity profiles between measurement and calculation are in the boundary layer near the tube wall.

However, measured and calculated profiles have similar shapes even though the maximum points of the velocity profiles from experimental measurements were shifted inward. The magnitudes of velocities for both cases are almost the same without regard to the shifted velocity distribution.

The velocity differences cannot be explained by a single reason. One possible reason is that the hot-wire calibration curves were obtained in the absence of a magnetic field while experimental measurements were made within a magnetic field. Since the probe generated its own temperature field, local velocities were effected. Another important reason for the differences is due to the approximated thermal and physical properties of the magnetic fluid and in the numerical calculations.

VIII. CONCLUSIONS AND RECOMMENDATIONS

VIII-1. Fully Developed Region

As shown in Figures (25), (26), and (27) the velocity and temperature profiles have the same form as gravity-induced flow because of the similarity in the equations governing the phenomena of flow even though the physical nature of the problems is different.

It is recommended that further study be made for the cooling case and experimental studies in fully developed flow be conducted to verify the results of the analytical calculations.

VIII-2. Thermal Entrance Region

The velocities and temperature were calculated numerically and plotted in Figures (28) - (34). The velocity profiles show that the magnetic field-induced flow existed and the magnetic Rayleigh number showed the flow to be steady. The measured velocity profiles are generally similar to calculated profiles even though shifted inward to the center.

It was found that the Nusselt number has a maximum value near the thermal entrance due to the magnetic moment reorientation and due to the steep axial temperature gradient. Calculated Nusselt numbers generally agreed with the experimental results.

The necessary conditions for the use of a hot-wire Anemometer in a magnetic fluid in the presence of an applied magnetic field were

found. However, further study for using hot-wire anemometry in magnetic fluids is recommended in order to improve the anemometry technique in the presence of an applied magnetic field. The experiment should be repeated for various magnetic fluids. It might give a clue how the pyromagnetic coefficients of magnetic fluids influence the velocity measurement under various applied fields and various probe settings.

More extensive work is needed to prove the relationships between the measurement and the probe setting, and the thermomagnetic fluctuation phenomenon.

As a whole, further studies in every aspect of the problem will be valuable for improving knowledge in thermomagnetic fluctuation of the flow field, the magnetocaloric effects, and the measurement techniques.

BIBLIOGRAPHY

1. Rosensweig, R. E.: "Magnetic Fluid." International Science and Technology, No. 55, 48-56, July 1966.

2. Rosensweig, R. E., R. Kaiser, and G. Miskolczy: "Viscosity of Magnetic Fluid in a Magnetic Field." Journal of Colloid and Interface Science, Vol. 29, No. 4, 680-686, April 1969.

3. Kaiser, R., and G. Miskolczy: "Some Applications of Ferrofluid Magnetic Colloids." IEEE Transactions on Magnetics, Vol. MAG - 6, No. 3, 694-698, September 1970.

4. Chekanov, V. V.: "Pressure Measurement in Ferrofluids." Translated from Magnitnaya Gidrodinamika, No. 4, 16-20, October-December 1977.

5. Kronkalns, G. E.: "Measuring the Thermal Conductivity and the Electrical Conductivity of a Ferrofluids in a Magnetic Field." Translated from Magnitnaya Gidrodinamika, No. 3, 138-140, July-September 1977.

6. McTague, J. P.: "Magnetoviscosity of Magnetic Colloids." The Journal of Chemical Physics, Vol. 5, No. 1, 133-136, July 1969.

7. Hall, W. F., and S. N. Busenberg: "Viscosity of Magnetic Suspensions." The Journal of Chemical Physics, Vol. 51, No. 1, 137-144, July 1969.

8. Kaiser, R., and G. Miskolczy: "Magnetic Properties of Stable Dispersions of Subdomain Magnetite Particles." Journal of Applied Physics, Vol. 41, No. 3, 1064-1972, March 1970.

9. Peterson, E. A., and D. A. Krueger: "Reversible, Field Induced Agglomeration in Magnetic Colloids." Journal of Colloid and Interface Science, Vol. 62, No. 1, 24-34, October 1977.

10. Berkowitz, A. E., J. A. Lahut, I. S. Jacobs., and L. M. Levinson: "Spin Pinning at Ferrite--Organic Interaces." Physical Review Letters, Vol. 34, No. 10, 594-597, March 1975.

11. Popplewell, J., S. W. Charles and R. Chantrell: "The Long-Term Stability of Magnetic Liquids for Energy Conversion Devices." Energy Conversion, Vol. 16, No. 3, 133-138, 1977.

12. Windle, P. L., J. Popplewell and S. W. Charles: "The Long-Term Stability of Mercury Based Ferromagnetic Liquids." IEEE Transactions on Magnetics, Vol. MAG - 11, No. 5, 1367-1369, September 1975.

13. Eringen, A. C.: "Theory of Micropolar Fluids." Journal of Mathematics and Mechanics, Vol. 16, No. 1, 1-18, 1966.

14. Maugin, G. A.: "A Phenomenological Theory of Ferroliquids." International Journal of Engineering Science, Vol. 16, 1029-1044, 1978.

15. Maugin, G. A., and A. C. Eringen: "Deformable Magnetically Saturated Media, I. Field Equations." Journal of Mathematical Physics, Vol. 13, No. 2, 143-154, February 1972.

16. Leal, L. G.: "On the Effect of Particle Couples on the Motion of a Dilute Suspension of Spheroids." Journal of Fluid Mechanics, Vol. 46, Part 2, 395-416, 1971.

17. Bashtovoi, V. G., and B. E. Kashevskii: "Asymmetric Model of a Magnetic Fluid taking into account Finite Anistropy of Ferromagnetic Particles." Translated from Magnitnaya Gidrodinamika, No. 4, 24-32, October-December 1976.

18. Jordan, P. C.: "Association Phenomena in a Ferromagnetic Colloid." Molecular Physics, Vol. 25, No. 4, 961-973, 1973.

19. Bibik, E. E., B. Ya. Matygullin, Yu. L. Raikher, and M. I. Shliomis: "Magnetostatic Properties of Magnetic Colloids." Translated from Magnitnaya Gidrodinamika, No. 1, 68-72, January-March 1973.

20. Blum, E. Ya, R. Ya. Ozols, and A. G. Fedin: "Magnetodiffusion in a Suspension of Ferromagnetic Material." Translated from Magnitnaya Gidrodinamika, No. 3, 3-7, July-September 1976.

21. deGennes, P. G., and P. A. Pincus: "Pair correlation in a Ferromagnetic Colloid." Physica Kondens Materie, Bd. 11, 189-198, 1970.

22. Bogardus, H., D. A. Kruegor, and D. Thompson: "Dynamic Magnetization in Ferrofluids." Journal of Applied Physics, Vol. 49, No. 6, 3422-3428, June 1978.

23. Popova, L. N., and I. E. Tarapov: "Action of a Magnetic Field on the Shape of a Cavitation Bubble in Magnetizable Liquid." Translated from Magnitnaya Gidrodinamika, No. 4, 33-37, October 1976.

24. Kaiser, R., and G. Miskolczy: "Magnetic Properties of Stable Dispersions of Subdomain Magnetite Particles." Journal of Applied Physics, Vol. 41, No. 3, 1064-1972, March 1970.

25. Peterson, E. A., and D. A. Krueger: "Reversible, Field Induced Agglomeration in Magnetic Colloids." Journal of Colloid and Interface Science, Vol. 62, No. 1, 24-34, October 1977.

26. Bailey, R. L., B. A. Hands, and I. M. Vokins: "Magnetic Liquid Vacuum Seals." Vacuum, Vol. 28, No. 10-1, P. 419, 1978.

27. Bailey, R. L., B. A. Hands, and I. M. Vokins: "Magnetic Liquid Seals." Chartered Mechanical Engineering (CME), Vol. 26, No. 2, 46-52, 1979.

28. Ezekiel, F. D.: "Ferrolubricants--New Applications." Mechanical Engineering, ASME, Vol. 97, No. 4, 30-31, 1975.

29. Coulombre, R. E., H. D'Auriol, L. Achnee, R. E. Rosensweig, and R. Kaiser: "Feasibility Study and Model Development for a Ferrofluid Viscous Damper." Rep. NA 55-9431, AVSSD-0222-67 CR, 1967.

30. Shimoiizaka, J., K. Nakatsuka, T. Fujita, and A. Kounosu: "Sink-Float Separators Using Permanent Magnets and Water-Based Magnetic Fluid." IEEE Transactions on Magnetics, Vol. MAG - 16, No. 368-371, March 1980.

31. Sambucetti, C. J.: "Magnetic Ink for Jet Printing." IEEE Transactions on Magnetics, Vol. MAG-16, No. 2, 364-376, March 1980.

32. Barrekette, E. S., and R. A. Myers: "Use of Magnetic Printing for Word Processing and Audio Storage." IBM Technical Disclosure Bulletin, Vol. 20, No. 7, 2909-2911, December 1977.

33. Ezekiel, F. D.: "Use of Magnetic Fluids in Bearings, Lubrication and Damping." ASME Paper No. 75 - DE - 5, in Mechanical Engineering, Vol. 97, No. 7, P. 94, 1975.

34. Rosensweig, R. E.: "Buoyancy and Stable Levitation of a Magnetic Body Immersed in a Magnetizable Fluid." Nature, No. 5036, 613-614, May 1966.

35. Resler, Jr., E. L.,and R. E. Rosensweig: "Regenerative Thermomagnetic Power." Journal of Engineering for Power, ASME, Vol. 89, 399-406, July 1967.

36. Rosensweig, R. E., J. W. Nestor, and R. S. Timmins: "Ferrohydrodynamic Fluids for Direct Conversion of Heat Energy." In Proceedings of A.I.Ch.E-Chem E. Joint Meetings, London, No. 5, 104-118, June 1965.

37. Resler, J., E. L. and R. E. Rosensweig: "Magnetocaloric Power." AIAA Journal, Vol. 2, No. 8, 1418-1422, August 1964.

38. Berkovskii, B. M., and V. G. Bashtovoi: "Convective Heat Transfer Processes in Ferromagnetic Fluids." Heat Transfer-Soviet Research, Vol. 5, No. 5, 137-142, September-October 1973.

39. Zahn, M., and K. E. Shenton: "Magnetic Fluids Bibliography." IEEE Transactions on Magnetics, Vol. MAG-16, No. 2, 387-415, March 1980.

40. Smit, J., and H. P. J. Wijn: Ferrites. John Wiley & Son, Inc., New York, P. 156, 1959.

41. Besancon, R. M. The Encyclopedia of Physics. 2nd Ed. Van Nostrand Reinhold Co., New York, P. 518, 1974.

42. Berkovsky, B. M., ed.: "Thermomechanics of Magnetic Fluids." Proceedings of the International Advanced Course and Workshop on Thermomechanics of Magnetic Fluids, 1977, Washington, D.C.: Hemisphere, 1978.

43. Hsieh, J. S.: Principles of Thermodynamics. McGraw-Hill Book Company, New York, 261-288, 1975.

44. Bashtovoi, V. G., B. M. Berkovskii and A. K. Sinitsyn: "Thermoconvective Explosion in a Ferromagnetic Liquid." Magnitnaya Gidrodinamica, No. 1, 12-18, January-March 1972.

45. Raj, K. Ferrofluidics Corp., Burlington, Mass. Private communication, 16, April 1979.

46. Neil, J. Georgia Pacific Corp., Bellingham, Wa. Private communication, March 1980.

47. Berkovsky, B. M., and R. D. Rosensweig: "Magnetic Fluid Mechanics: A Report on an International Advanced Course and Workshop." Journal of Fluid Mechanics, Vol. 87, Part 3, 521-531, 1978.

48. Neuringer, J. L., and R. E. Rosensweig: "Ferrohydrodynamics." The Physics of Fluids, Vol. 7, No. 12, 1927-1937, December 1964.

49. Eringen, A. C.: "Continuum Foundation of Rheology-New Adventures." Reprinted from Progress in Heat & Mass Transfer, Vol. 5, edited by W. R. Schowalter, Pergamon Press-Oxford, New York, 1-18, 1972.

50. White, F. M.: Viscous Fluid Flow. McGraw-Hill Book Co., New York, P. 116, 1974.

51. Gershuni, G. Z., and E. M. Zhukhovitskii: Convective Instability of an Incompressible Fluid (translated from Russian).

52. Shliomis, M. I.: "Convective instability of a Ferrofluid." Translated from Izvestiya Akademii Nauk SSSR, Mekhanika, Zhidkostii Gaza, No. 6, 130-135, November-December 1974.

53. Berkovskii, B. M., and V. G. Bashtovoi: "Convective Heat Transfer Processes in Ferromagnetic Fluids." Heat transfer-Soviet Research, Vol. 5, No. 5, September-October 1973.

54. Lalas, D. P., and S. Carmi: "Thermoconvective Stability of Ferrofluids." Physics of Fluids, Vol. 14, No. 2, 436-438, 1971.

55. Luikov, A. V., B. M. Berkovsky, and V. G. Bashtovoi: "Convection in Ferromagnetic Fluid Due to Magnetocaloric Effect." Progress in Heat and Mass Transfer, No. 5, 327-331, 1972.

56. Abramowitz, M., and I. A. Stegun: Handbook of Mathematical Functions. Dover Publications, Inc., New York, P. 379, December 1972.

57. Neuringer, J. L., and R. E. Rosensweig: "Ferrohydrodynamics." The Physics of Fluids, Vol. 7, No. 12, 1927-1937, December 1974.

58. Berkovsky, B. M., V. E. Fertman, V. K. Polevikov, and S. V. Isaev: "Heat Transfer Across Vertical Ferrofluid Layers." International Journal of Heat, Mass Transfer, Vol. 19, 891-986, 1976.

59. Berkovsky, B. M., V. E. Fertman, V. K. Polevikov, and S. V. Isaev: "Specific Features of Natural Convection Heat Transfer in Magnetic Fluids." The Proceeding of 6th International Heat Transfer Conference, Toronto, Canada, Vol. 3, M-16, 147-151, August 1978.

60. Buckmaster, J. "Ferrohydrodynamic Boundary Layers." Proceedings of an International Advanced Course on the Thermomechanics of Magnetic Fluid, at the International Centre for Mechanical Sciences (CISM), Udine, Italy, October 1977.

61. Chekanov, V. V.: "Pressure Measurement in Ferrofluids." Translated from Magnitnaya Gidrodinamika, No. 4, 16-20, October-December 1977.

62. Maiorov, M. M., E. Ya. Blum, and A. E. Malmanis: "Experimental Study of the Hydraulics of a Turbulent Ferrohydrodynamic Flow through a Circular Channels." Translated from Magnitnaya Gidrodinamika, No. 4, 143-145, October-December 1975.

63. via Welty, J. R.: "Hot Film Anemometry." Instruction Manual, Liquid Metal Heat Transfer Lab., Department of Mechanical Engineering, Oregon State University, 1974(?).

64. Jakob, M.: Heat Transfer. John Wiley & Sons, Inc., New York, Vol. 1, 1949.

65. Hallman, T. M.: "Combined Forced and Free-Laminar Heat Transfer in Vertical Tubes with Uniform Internal Heat Generation." ASME Transactions, Vol. 78, 1831-1841, November 1956.

66. Hanratty, T. J., E. M. Rosen, and R. L. Kabel: "Effect of Heat Transfer on Flow Field at Low Reynolds Numbers in Vertical Tubes." Industrial and Engineering Chemistry, Vol. 50, No. 5, 815-820, May 1958.

67. Siegel, R., E. M. Sparrow, and T. M. Hallman: "Steady Laminar Heat Transfer in a Circular Tube with Prescribed Wall Heat Flux." Applied Science Research, Section A, Vol. 7, No. 5, 386-392, 1960.

68. Tao, L. N.: "Heat Transfer of Combined Free and Forced Convection in Circular and Sector Tubes." Applied Science Research, Section A, Vol. 9, No. 5, 357-368, 1960.

APPENDICES

APPENDIX A

A-1. The Integrals for Kelvin functions

$$\int_0^1 r\, \mathrm{Ber}(\gamma^{\frac{1}{4}}r)dr = \frac{1}{\gamma^{\frac{1}{4}}}\, \mathrm{Bei}'(\gamma^{\frac{1}{4}})$$

$$\int_0^1 r\, \mathrm{Bei}(\gamma^{\frac{1}{4}}r)dr = -\frac{1}{\gamma^{\frac{1}{4}}}\, \mathrm{Ber}'(\gamma^{\frac{1}{4}})$$

$$\int_0^1 r[\mathrm{Bei}^2(\gamma^{\frac{1}{4}}r) - \mathrm{Ber}^2(\gamma^{\frac{1}{4}}r)]dr$$

$$= -\frac{1}{2}\,[\mathrm{Ber}_0^2(\gamma^{\frac{1}{4}}) + \mathrm{Ber}_1^2(\gamma^{\frac{1}{4}}) - \mathrm{Bei}_0^2(\gamma^{\frac{1}{4}}) - \mathrm{Bei}_1^2(\gamma^{\frac{1}{4}})]$$

$$\int_0^1 r\, \mathrm{Bei}(\gamma^{\frac{1}{4}}r)\, \mathrm{Ber}(\gamma^{\frac{1}{4}}r)dr = \frac{1}{2}\left[\mathrm{Ber}_0(\gamma^{\frac{1}{4}})\, \mathrm{Bei}_0(\gamma^{\frac{1}{4}}) + \mathrm{Ber}_1(\gamma^{\frac{1}{4}})\, \mathrm{Bei}_1(\gamma^{\frac{1}{4}})\right]$$

A-2. The Integrals for Bessel functions

$$\int_0^1 r\, J_0(\gamma^{\frac{1}{4}}r)dr = \frac{1}{\gamma^{\frac{1}{4}}}\, J_1(\gamma^{\frac{1}{4}})$$

$$\int_0^1 r\, I_0(\gamma^{\frac{1}{4}}r)dr = \frac{1}{\gamma^{\frac{1}{4}}}\, I_1(\gamma^{\frac{1}{4}})$$

$$\int_0^1 r\, J_0^2(\gamma^{\frac{1}{4}}r)dr = \frac{1}{2}\,[J_0^2(\gamma^{\frac{1}{4}}) + J_1^2(\gamma^{\frac{1}{4}})] - \frac{1}{2}$$

$$\int_0^1 r\, I_0^2(\gamma^{\frac{1}{4}}r)dr = \frac{1}{2}\,[I_0^2(\gamma^{\frac{1}{4}}) - I_1^2(\gamma^{\frac{1}{4}})] - \frac{1}{2}$$

$$\int_0^1 r\, J_0(\gamma^{\frac{1}{4}}r)\, I_0(\gamma^{\frac{1}{4}}r)dr = \frac{1}{2\gamma^{\frac{1}{4}}}\,[J_0(\gamma^{\frac{1}{4}})\, I_1(\gamma^{\frac{1}{4}}) + J_1(\gamma^{\frac{1}{4}})\, I_0(\gamma^{\frac{1}{4}})]$$

A-3. Asymptotic Expansions of Kelvin functions

$$Ber_\nu(x) = \frac{e^{\frac{x}{\sqrt{2}}}}{\sqrt{2\pi x}}\left\{f_\nu(x)\cos\alpha + g_\nu(x)\sin\alpha\right\} - \frac{1}{\pi}\left\{\sin(2\nu\pi)\,ker_\nu(x) + \cos(2\nu\pi)\,kei_\nu(x)\right\}$$

$$Bei_\nu(x) = \frac{e^{\frac{x}{\sqrt{2}}}}{\sqrt{2\pi x}}\left\{f_\nu(x)\sin\alpha - g_\nu(x)\cos\alpha\right\} + \frac{1}{\pi}\left\{\cos(2\nu\pi)\,ker_\nu(x) - \sin(2\nu\pi)\,kei_\nu(x)\right\}$$

$$Ker_\nu(x) = \sqrt{\frac{\pi}{2x}}\,e^{-\frac{x}{\sqrt{2}}}\left\{f_\nu(-x)\cos\beta - g_\nu(-x)\sin\beta\right\}$$

$$Kei_\nu(x) = \sqrt{\frac{\pi}{2x}}\,e^{-\frac{x}{\sqrt{2}}}\left\{f_\nu(-x)\sin\beta - g_\nu(-x)\cos\beta\right\}$$

$$\alpha = \frac{x}{\sqrt{2}} + \left(\frac{\nu}{2} - \frac{1}{8}\right)\pi \qquad \mu = 4\nu^2$$

$$\beta = \frac{x}{\sqrt{2}} + \left(\frac{\nu}{2} + \frac{1}{8}\right)\pi = \alpha + \frac{1}{4}\pi$$

$$f_\nu(\pm x) \simeq 1 - \sum_{k=1}^{\infty} (\mp 1)^k \frac{(4\nu^2-1)(4\nu^2-3^2)(4\nu^2-5^2)\{(4\nu^2-(2K-1)^2\}\cos\left(\frac{k\pi}{4}\right)}{k!\,(8X)^k}$$

$$g_\nu(\pm x) \simeq \sum_{k=1}^{\infty} (\mp 1)^k \frac{(\mu-1)(\mu-9)\ldots\{\mu-(2k-1)^2\}}{k!\,(8X)^k}\sin\left(\frac{k\pi}{4}\right)$$

$$Bé v_\nu(x) = \left(\frac{\nu}{x}\right) M_\nu \cos\theta_\nu + M_{\nu+1}\cos\left(\theta_{\nu+1} - \frac{\pi}{4}\right)$$

$$Bé i_\nu(x) = \left(\frac{\nu}{x}\right) M_\nu \sin\theta_\nu + M_{\nu+1}\sin\left(\theta_{\nu+1} - \frac{\pi}{4}\right)$$

where

$$M_\nu = \frac{e^{\frac{x}{\sqrt{2}}}}{\sqrt{2\pi x}} \left\{ 1 - \frac{\mu-1}{8\sqrt{2}} \frac{1}{x} + \frac{(\mu-1)^2}{256} \frac{1}{x^2} \right\}$$

$$- \frac{(\mu-1)\,(\mu^2 + 14\mu - 399)}{6144\sqrt{2}} \cdot \frac{1}{x^3}$$

$$\theta_\nu = \frac{x}{\sqrt{2}} + (\frac{1}{2}\nu - \frac{1}{8})\pi + \frac{\mu-1}{8\sqrt{2}} \frac{1}{x} + \frac{\mu-1}{16} \frac{1}{x^2}$$

$$- \frac{(\mu-1)\,(\mu-25)}{384\sqrt{2}} \cdot \frac{1}{x^3}$$

APPENDIX B

Fully Developed Region - PROGRAM MAGNET

```
C
C
C***** THIS PROGRAM HAS THE PURPOSE TO CALCULATE THE VELOCITIES
C***** AND TEMPERATURES IN THE FULLY DEVELOPED FERROHYDRODYNAMIC
C***** (FHD) FLOW.
C
C
      PROGRAM MAGNET(INPUT,OUTPUT)
      COMMON REY, PR, B, FS, DT, AI
      COMMON U(41),T(41)
      DIMENSION UH(41),TH(41),BERG(3),BEIG(3),DBERG(3),DBEIG(3),BER(3),
     1       BEI(3),DBER(3),DBEI(3)
C
C***** INPUT DATA
C
      DATA FRIC,PLEN/0.0356,4.9525/
      DATA TEMPEN/285.0/
C
      DATA RAD,DX,VISCOK,PYRO,DENS,COMAG/0.019050,0.0050,0.000007787,1.0
     $,1220.0,0.00000126/
      DATA COND,HTFLUX,HTCAPA,TEMPEN/6.436,375.9566,5275.4,285.0/
      DATA VISCO,TCURIE,GRAV/0.0095,1043.0,9.8/
      DATA SATMAG/150.0/
      DATA QM,TC,TW/37.59566,288.0,372.0/
      DATA DR/0.025/
      DO 68 NN=1,10
      IF(NN.EQ.1) GO TO 59
      IF(NN.EQ.2) GO TO 61
      IF(NN.EQ.3) GO TO 62
      IF(NN.EQ.4) GO TO 63
      IF(NN.EQ.5) GO TO 81
      IF(NN.EQ.6) GO TO 82
      IF(NN.EQ.7) GO TO 83
      IF(NN.EQ.8) GO TO 84
      IF(NN.EQ.9) GO TO 85
      IF(NN.EQ.10) GO TO 86
  59  FIELD=2000.0
      GO TO 66
  61  FIELD=2500.0
      GO TO 66
  62  FIELD=3000.0
      GO TO 66
  63  FIELD=3500.0
      GO TO 66
  81  FIELD=4000.0
      GO TO 66
```

```
  82  FIELD=4500.0
      GO TO 66
  83  FIELD=5000.0
      GO TO 66
  84  FIELD=5500.0
      GO TO 66
  85  FIELD=6000.0
      GO TO 66
  86  FIELD=6500.0
  66  GRAD=FIELD/0.12
C
      VEL =SQRT(COMAG*PYRO*FIELD*(321.-TEMPEN)/(DENS*GRAV*(2.*FRIC*
     1     PLEN/(2.*RAD)+0.5)))
C
      WRITE 200, RAD, DENS, HTCAPA, TC, TW, VEL, QM, COMAG, PYRO, SATMAG
     $, FIELD, GRAD, VISCO, COND, DR
  200 FORMAT("1",10X,"RADIUS OF A DUCT                          = ",F10.8,/
     $,10X,"DENSITY OF A MAGNETIC FLUID                        = ",F6.1,/,
     $10X,"HEAT CAPACITY OF A MAGNETIC FLUID                   = ",F6.1,/,
     =10X,"TEMPERATURE OF CENTER-LINE                          = ",F5.1,/,
     $10X,"TEMPERATURE OF TUBE-WALL                            = ",F5.1,/,
     $10X,"AVERAGE VELOCITY OF FLUID FLOW                      = ",F5.3,/,
     $10X,"MAGNETOCALORIC HEAT GENERATION                      = ",F8.4,/,
     $10X,"COEFFICIENT OF MAGNETIC PERMEABILITY                = ",E9.3,/,
     $10X,"PYRO-MAGNETIC COEFFICIENT                           = ",F6.1,/,
     $10X,"SATURATED MAGNETIZATION                             = ",F5.1,/,
     $10X,"APPLIED MAGNETIC FIELD INTENSITY                    = ",F6.1,/,
     $10X,"MAGNETIC FIELD GRADIENT IN AXIAL DIRECTION          = ",F9.1,/,
     $10X,"VISCOSITY OF A MAGNETIC FLUID                       = ",F10.7,/,
     $10X,"CONDUCTIVITY OF A MAGNETIC FLUID                    = ",F10.8,/,
     $10X,"STEP-SIZE OF RADIAL DIRECTION                       = ",F10.8)
C
C***** INITIALIZING VARIABLES
C
      N=INT(0.0)
      GAMA=0.0
      AI=HTFLUX/(DENS*HTCAPA*2.0*RAD*VEL)
      FS=RAD*QM/(DENS*HTCAPA*VEL)
C
      REY=DENS*2.0*RAD*VEL/VISCO
      PR=VISCO*HTCAPA/COND
      B=4.0*VEL *(RAD**2.0)*COMAG*PYRO*SATMAG*FIELD*GRAD*PR/(VISCO**2.0)
      DV=TC-TW
      GAMA=B*AI
      WRITE 405, B, AI, GAMA
  405 FORMAT("0",20X,"B= ",F14.3, /,20X,"AI= ",F8.5, /,20X,"GAMA= ",
     1       F14.3)
C
      RAMAG=(COMAG*PYRO*GRAD*(1.0**4.0)/(COND*VISCOK))*(AI-COMAG*PYRO*
     1      GRAD*TEMPEN/(DENS*HTCAPA))
C
```

```
      WRITE 55, RAMAG
   55 FORMAT("0",20X,"MAGNETIC RAYLEIGH NUMBER = ",F10.3)
C
      WRITE 300
  300 FORMAT("0",15X,"COOLING CASE = VEL AND TEMP", 3X,"HEATING CASE =
     1VEL AND TEMP",//,10X,"RADIUS",
     1       3X,"VELOCITY", 3X,"TEMPERATURE",3X,"VELOCITY", 3X,
     2      "TEMPERATURE")
C
      DO 10 J=1,41
C
      R=FLOAT(J-1)*DR
      G=GAMA**0.25
      X=G*R
C
      CALL BESSE(J,X,BJOR,BJ1R,BIOR,BI1R)
      CALL BESSE(J,G,BJO,BJ1,BIO,BI1)
C
      CI=((G*FS/AI)*(-0.5+BI1/(G*BIO))+0.5*G)/(BJ1-BJO*BI1/BIO)
      CT=-1.0*(FS/AI+CI*BJO)/BIO
C
C***** VELOCITY CALCULATION FOR COOLING
C
      U(J)=FS/AI+CI*BJOR+CT*BIOR
C
      DI=AI*REY*PR*CI
      DT=AI*REY*PR*CT
C
C***** TEMPERATURE CALCULATION FOR COOLING
C
      T(J)=(DI*(BJO-BJOR)+DT*(BIOR-BIO))/(DI*(BJO-1.)+DT*(1.-BIO))
      DV=(DI*(BJO-1.0)+DT*(1.0-BIO))/(G**2.0)
C
C
      L=1
      CALL THOMSON(L,G,BERG(1),BEIG(1),DBERG(1),DBEIG(1))
C
C
      IF(X.GT.5.2) GO TO 41
      CALL KELVIN(L,X,BER(1),BEI(1),DBER(1),DBEI(1))
      GO TO 42
   41 CALL THOMSON(L,X,BER(1),BEI(1),DBER(1),DBEI(1))
   42 CCI=G*(-0.5-0.5*FS/AI+FS*DBEIG(1)/(AI*G*BERG(1)))/(DBERG(1)+
     1    BEIG(1)*DBEIG(1)/BERG(1))
C
      CCT=(FS/AI-CCI*BEIG(1))/BERG(1)
C
C***** VELOCITY CALCULATION FOR HEATING
C
      UH(J)=(-FS/AI+CCI*BEI(1)+CCT*BER(1))*G
C
```

```
      DDI=-AI*REY*PR*CCI
      DDT=-AI*REY*PR*CCT
C
C***** TEMPERATURE CALCULATION FOR HEATING
C
      TH(J)=(DDT*(BEI(1)-BEIG(1))+DDI*(BERG(1)-BER(1)))/(DDI*(BERG(1)
     1      -1.0)-DDT*BEIG(1))
C
      WRITE 301, R, U(J),T(J),UH(J),TH(J)
  301 FORMAT(10X,F6.4, 3X,F10.6, 3X,F10.6, 3X,F10.6, 3X,F10.6)
C
   10 CONTINUE
C
      DO=(DDI*(BERG(1)-1.0)-DDT*BEIG(1))/(G**2.0)
      EI=DI/(DI*(BJO-1.)+DT*(1.-BIO))
      ET=DT/(DI*(BJO-1.)+DT*(1.-BIO))
      H=EI*BJO-ET*BIO
C
      A1=FS*H/AI
      A2=CI*H-FS*EI/AI
      A3=CT*H+FS*ET/AI
      A4=CI*ET-CT*EI
      A5=CI*EI
      A6=CT*ET
C
C***** MEDIUM TEMPERATURE CALCULATION FOR COOLING
C
      TM=(A1+A5-A6+FS*TW/(AI*DV))+(2.*A2+2.*TW*CI/DV)*BJ1/G
     1   +(2.*A3+2.*TW*CT/DV)*BI1/G+(BJO*BI1+BJ1*BIO)*A4/G-A5*(BJO**2.
     2   +BJ1**2.)+A6*(BIO**2.-BI1**2.)-TW/DV
C
C***** NUSSELT NUMBER CALCULATION FOR COOLING
C
      HNUSS2=2.*G*(EI*BJ1+ET*BI1)/TM
C
      L=2
      CALL THOMSON(1,G,BERG(1),BEIG(1),DBERG(1),DBEIG(1))
      CALL THOMSON(L,G,BERG(2),BEIG(2),DBERG(2),DBEIG(2))
C
      EHI=DDI/(DDI*(BERG(1)-1.0)-DDT*BEIG(1))
      EHT=DDT/(DDI*(BERG(1)-1.0)-DDT*BEIG(1))
C
      HH=EHI*BERG(1)-EHT*BEIG(1)
C
      B1=-1.0*FS*HH/AI
      B2=CCT*HH+FS*EHI/AI
      B3=CCI*HH-FS*EHT/AI
      B4=CCI*EHT
      B5=CCT*EHI
      B6=CCT*EHT-CCI*EHI
C
```

```
C***** MEDIUM TEMPERATURE CALCULATION FOR HEATING
C
      THM=B1-TW*FS/(DO*AI)+2.0*(B2+TW*CCT/DO)*DBEIG(1)/G-2.0*(B3+
     1    TW*CCI/DO)*DBERG(1)/G-B4*(BERG(1)**2.0+BERG(2)**2.0-BEIG(1)
     2    **2.0-BEIG(2)**2.0)+B6*(BERG(1)*BEIG(1)+BERG(2)*BEIG(2))-TW/DO
C
C***** NUSSELT NUMBER CALCULATION FOR HEATING
C
      HNUSS1=2.0*(+1.0*DDI*DBERG(1)+DDT*DBEIG(1))/(G*DO*THM)
C
C
      WRITE 302, TM, HNUSS2, THM, HNUSS1
  302 FORMAT("0",19X,"MEDIUM TEMP",3X,"NUSSELT NO", 3X,"MEDIUM TEMP",3X,
     1       "NUSSELT NO",//,19X,F10.4, 3X,F10.7, 3X,F10.4, 3X,F10.5)
C
      N=N+1
      CALL SIMPU(N,VELN)
      REY=2.0*RAD*DENS*VELN*VEL/VISCO
      WRITE 58, REY
   58 FORMAT(    19X,"REYNOLDS NUMBER = ",F10.3)
C
      WRITE 303, VEL
  303 FORMAT(    19X,"AVERAGE VELOCITY ="F12.9)
   68 CONTINUE
      STOP
      END
-------------------------------------------------------------------------
      SUBROUTINE BESSEL(I,ARG,FG,FG1)
      COMMON REY, PR, B, FS, DT, AI
      GAMA=ARG**0.25
      CALL BESSE(I,GAMA,BJ0,BJ1,BI0,BI1)
C
      FG=DT*(ARG**0.5)*(BJ1*BI0*BI0-BJ0*BI0*BI1)-AI*REY*PR*((BJ0*BI0*BI1
     1   -BI0*BI1-BJ1*BI0+BJ1*BI0*BI0)*FS/AI+0.5*GAMA*(1.-FS/AI)
     2   *(2.*BJ0*BI0*BI0-BJ0*BI0-BI0*BI0))
C
C
      FG1=0.5*DT*(ARG**(-0.5))*(BJ1*BI0*BI0-BJ0*BI0*BI1)
     1    +0.25*(DT/GAMA)*(BI0*BI0*(BJ0-BJ1/GAMA)+BJ1*BI0*BI1
     2    -BJ0*BI1*BI1-BJ0*BI0*(BI0-BI1/GAMA))-(0.25*FS*REY*PR/(GAMA**
     3    3.0))*(BJ1*BI0*BI1+BJ0*BI1*BI1+BJ0*BI0*(BI0-BI1/GAMA)
     4    -BI1*BI1-BI0*(BI0-BI1/GAMA)-BI0*(BJ0-BJ1/GAMA)-BJ1*BI1+
     5    BI0*BI0*(BJ0-BJ1/GAMA)+2.*BJ1*BI0*BI1)-AI*REY*PR*(0.125*
     6    (ARG**(-0.75))*(1.-FS/AI)*(2.*BJ0*BI0*BI0-BJ0*BI0-BI0*BI0)
     7    +0.5*(ARG**(-0.5))*(1.-FS/AI)*(0.5*BJ1*BI0*BI0+BI0*BJ0*BI1-
     8    0.25*BJ1*BI0-0.25*BJ0*BI1-0.5*BI0*BI1)+0.5*GAMA*FS*B*
     9    (2.*BJ0*BI0*BI0-BJ0*BI0-BI0*BI0)/(ARG**2.))
     1    -(REY*PR/B)*(FS*( BJ0*BI0*BI1-BI0*BI1-BJ1*BI0+BJ1*BI0*BI0)/AI
     2    +0.5*GAMA*(1.-FS/AI)*(2.*BJ0*BI0*BI0-BJ0*BI0-BI0*BI0))
C
      RETURN
      END
```

```
      SUBROUTINE BESSE (I,Y,BJO,BJI,BIO,BII)
      COMMON REY, PR, B, FS, DT, AI
      IF(Y.GT.3.0) GO TO 9
      Z=Y/3.0
      BJO=1-2.2499997*(Z**2.)+1.2656208*(Z**4.)-0.3163866*(Z**6.)+
     $0.0444479*(Z**8.)-0.0039444*(Z**10.)+0.000210*(Z**12.)
      BJI=Y*(0.5-0.56249985*(Z**2.)+0.21093573*(Z**4.)-0.03954289*(Z**6.
     $)+0.00443319*(Z**8.)-0.00031761*(Z**10.)+0.00001109*(Z**12.))
      GO TO 11
    9 S=3.0/Y
      FO=0.79788456-0.00000077*S-0.0055274*(S**2.)-0.00009512*(S**3.)
     1   +0.00137237*(S**4.)-0.00072805*(S**5.)+0.00014476*(S**6.)
      AO=Y-0.78539816-0.04166397*S-0.00003954*(S**2.)+0.00262573*(S**3.)
     1   -0.00054125*(S**4.)-0.00029333*(S**5.)+0.00013558*(S**6.)
      BJO=(Y**(-0.5))*FO*COS(AO)
      FI=0.7988456+0.00000156*S+0.01659667*(S**2.)+0.00017105*(S**3.)
     1   -0.00249511*(S**4.)+0.00113653*(S**5.)-0.00020033*(S**6.)
      AI=Y-2.35619449+0.12499612*S+0.0000565*(S**2.)-0.00637879*(S**3.)
     1   +0.00074348*(S**4.)+0.00079824*(S**5.)-0.00029166*(S**6.)
      BJI=(Y**(-0.5))*FI*COS(AI)
   11 W=Y/3.75
      IF(Y.GT.3.75) GO TO 12
      BIO=1.+3.5156229*(W**2.)+3.0899424*(W**4.)+1.2067492*(W**6.)+
     $0.2659732*(W**8.)+0.0360768*(W**10.)+0.0045813*(W**12.)
      BII=Y*(0.5+0.87890594*(W**2.)+0.51498869*(W**4.)+0.15084934*(W**6.
     $)+0.02658733*(W**8.)+0.00301532*(W**10.)+0.00032411*(W**12.))
C
      GO TO 13
C
   12 BIO=(Y**(-0.5))*(EXP(Y))*(0.39894228+0.01328592/W+0.00225319/(W**
     1    2.)-0.00157565/(W**3.)+0.00916281/(W**4.)-0.02057706/(W**5.)
     2    +0.02635537/(W**6.)-0.01647633/(W**7.)+0.00392377/(W**8.))
C
      BII=(Y**(-0.5))*(EXP(Y))*(0.39894228-0.03988024/W-0.00362018/
     1    (W**2.)+0.00163801/(W**3.)-0.01031555/(W**4.)+0.02282967/(W**
     2    5.)-0.02895312/(W**6.)+0.01787654/(W**7.)-0.00420059/(W**8.))
C
   13 RETURN
      END
```

```
      SUBROUTINE KELVIN(J,X,TER,TEI,DTER,DTEI)
      REAL NU
      DIMENSION BER(3),BEI(3),DBER(3),DBEI(3)
      NU=J
      FAC=FACT=1.0
      L=30
      Y=T=0.0
C
      DO 10 K=1,L
      E=FLOAT(K)
      FAC=E*FAC
      FACT=FACT*FLOAT(K+1)
```

```
      AR=(0.75*(NU-1.0)-0.5*E)*3.141527
      CO=COS(AR)
      SI=SIN(AR)
      YI=CO*((0.25*X*X)**K)/(FAC*FACT)
      TI=SI*((0.25*X*X)**K)/(FAC*FACT)
      Y=Y+YI
      T=T+TI
   10 CONTINUE
      BER(J)=Y
      BEI(J)=T
      P=X/8.0
C
      DBER(J)=X*(-4.0*P*P+14.22222222*(P**6.0)-6.06814810*(P**10.0)
     1         +0.66047849*(P**14.0)-0.02609253*(P**18.0)+0.00045957*
     2         (P**22.0)-0.00000394*(P**26.0))
C
      DBEI(J)=X*(0.5-10.66666666*(P**4.0)+11.37777772*(P**8.0)
     1         -2.31167514*(P**12.0)+0.14677204*(P**16.0)
     2         -0.00379386*(P**20.0)+0.00004609*(P**24.0))
      TER=BER(J)
      TEI=BEI(J)
      DTER=DBER(J)
      DTEI=DBEI(J)
      RETURN
      END
-------------------------------------------------------------------------------
      SUBROUTINE THOMSON(J ,X,SER,SEI,DSER,DSEI)
C
      EXTERNAL COS, SIN, SQRT, EXP
      REAL NU,MOD,KER,KEI,MU,MV
C
      DIMENSION            BERG(3),BEIG(3),DBERG(3),DBEIG(3),BER(3),
     1       BEI(3),DBER(3),DBEI(3)
      DIMENSION                                MOD(3),SETA(3),KER(3),KEI(3)
     1       ,F(3),G(3),Z(50),W(50),ZM(50),WM(50),FN(3),GN(3)
C
C
      NU=J
      MU=4.0*(NU-1.0)**2.0
      MV=4.0*NU**2.0
      ALPA=X/SQRT(2.0)+3.141527*((NU-1.0)/2.0-1.0/8.0)
      BETA=ALPA+3.141527/4.0
      FAC=1.0
      L=30
      ZI=WI=0.0
      ZA=WA=0.0
C
      DO 10 K=1,L
      TOA=1.0
      E=FLOAT(K)
      FAC=E*FAC
      AGG=E*3.141527/4.0
```

```
C
      DO 20 NN=1,K
      TOA=(MU-(2.0*FLOAT(NN)-1.0)**2.0)*TOA
   20 CONTINUE
C
      ZM(K)=TOA*(COS(AGG))/(FAC*(-8.0*X)**K)
      Z(K)=((-1.0)**K)*TOA*(COS(AGG))/(FAC*(8.0*X)**K)
C
      WM(K)=TOA*(SIN(AGG))/(FAC*(-8.0*X)**K)
      W(K)=((-1.0)**K)*TOA*(SIN(AGG))/(FAC*(8.0*X)**K)
      ZI=ZI+Z(K)
      ZA=ZA+ZM(K)
      WI=WI+W(K)
      WA=WA+WM(K)
   10 CONTINUE
C
      FN(J)=1.0+ZA
      F(J)=1.0+ZI
      GN(J)=WA
      G(J)=WI
      ROAT=SQRT(2.0)
C
      KER(J)=(SQRT(3.141527/(2.0*X)))*(EXP(-1.0*X/ROAT))*(FN(J)*
     1       (COS(BETA))-GN(J)*(SIN(BETA)))
C
      KEI(J)=(SQRT(3.141527/(2.0*X)))*(EXP(-1.0*X/ROAT))*(-FN(J)*
     1       (SIN(BETA))-GN(J)*(COS(BETA)))
C
      AIN=2.0*(NU-1.0)*3.141527
C
      BER(J)=(EXP(X/ROAT))*(F(J)*(COS(ALPA))+G(J)*(SIN(ALPA)))/(SQRT(2.0
     1      *3.141527*X))-((SIN(AIN))*KER(J)+(COS(AIN))*KEI(J))/3.141527
      SER=BER(J)
C
      BEI(J)=(EXP(X/ROAT))*(F(J)*(SIN(ALPA))-G(J)*(COS(ALPA)))/(SQRT(2.0
     1    *X*3.141527))+((COS(AIN))*KER(J)-(SIN(AIN))*KEI(J))/3.141527
      SEI=BEI(J)
C
      MOD(J)=(EXP(X/ROAT))*(1.0-(MU-1.0)/(8.0*X*ROAT)+((MU-1.0)**2)
     1       /(256.0*X*X)-(MU-1.0)*(MU*MU+14.0*MU-399.0)/(6144.0*ROAT*
     2       X**3.0))
      MOD(J+1)=(EXP(X/ROAT))*(1.0-(MV-1.0)/(8.0*X*ROAT)+((MV-1.0)**2)
     1       /(256.0*X*X)-(MV-1.0)*(MV*MV+14.0*MV-399.0)/(6144.0*ROAT*
     2       X**3.0))
C
      SETA(J)=X/ROAT+(0.5*(NU-1.0)-1.0/8.0)*3.141527+(MU-1.0)/(8.0*ROAT*
     1        X)+(MU-1.0)/(16.0*X*X)-(MU-1.0)*(MU-25.0)/(384.0*ROAT*
     2        X**3.0)
      SETA(J+1)=X/ROAT+(0.5*NU-1.0/8.0)*3.141527+(MV-1.0)/(8.0*ROAT*
     1        X)+(MV-1.0)/(16.0*X*X)-(MV-1.0)*(MV-25.0)/(384.0*ROAT*
     2        X**3.0)
```

```
C
C
      DBER(J)=((NU-1.0)/X)*MOD(J)*(COS(SETA(J)))+MOD(J+1)*(COS(SETA(J+1)
     1        -3.141527/4.0))
      DSER=DBER(J)
C
      DBEI(J)=((NU-1.0)/X)*MOD(J)*(SIN(SETA(J)))+MOD(J+1)*(SIN(SETA(J+1)
     1        -3.141527/4.0))
      DSEI=DBEI(J)
      RETURN
      END
      SUBROUTINE SIMPU(I,UM)
      COMMON U(41),T(41)
      DATA RAD,NR/0.019050,41/
      DR=RAD/FLOAT(NR-1)
C
      SUM=SUMI=0.0
C
      DO 10 J=1,NR
      DRAD=FLOAT(J-1)*DR
      IF(J.EQ.1) GO TO 5
      IF(J.EQ.NR) GO TO 6
      ITEST=J/2
      TEST=FLOAT(ITEST)
      TESTJ=FLOAT(J)/2.
C
      IF(TEST.EQ.TESTJ) GO TO 4
      SUMI=SUMI+U(  J)*DRAD
      GO TO 10
    4 SUM=SUM+U(  J)*DRAD
      GO TO 10
    5 SUMA=U(  J)*DRAD
      GO TO 10
    6 SUMB=U(  J)*DRAD
   10 CONTINUE
C
      F=SUMA+4.*SUM+2.*SUMI+SUMB
      UM=2.*DR*F/(3.*(RAD**2.))
      RETURN
      END
```

MAGNETIC RAYLEIGH NUMBER = 24893.0

COOLING CASE = VEL AND TEMP HEATING CASE = VEL AND TEMP

RADIUS	VELOCITY	TEMPERATURE	VELOCITY	TEMPERATURE
0.0000	1.582326	1.000000	-.000000	1.007562
.0250	1.558770	.989805	.000522	1.007576
.0500	1.489156	.959676	.002084	1.007617
.0750	1.376584	.910954	.004675	1.007693
.1000	1.226056	.845803	.008273	1.007810
.1250	1.044221	.767098	.012843	1.007980
.1500	.839050	.678290	.018335	1.008219
.1750	.619447	.583229	.024676	1.008543
.2000	.394809	.485979	.031764	1.008972
.2250	.174576	.390623	.039467	1.009530
.2500	-.032230	.301064	.047605	1.010239
.2750	-.217423	.220838	.055953	1.011123
.3000	-.374044	.152953	.064226	1.012208
.3250	-.496665	.099753	.072073	1.013516
.3500	-.581628	.062813	.079073	1.015066
.3750	-.627182	.042883	.084723	1.016873
.4000	-.633521	.039867	.088443	1.018946
.4250	-.602729	.052850	.089569	1.021282
.4500	-.538620	.080166	.087360	1.023866
.4750	-.446499	.119496	.081006	1.026670
.5000	-.332851	.168008	.069646	1.029644
.5250	-.204970	.222512	.052386	1.032717
.5500	-.070555	.279633	.214771	1.059513
.5750	.062701	.335988	.182996	1.072993
.6000	.187526	.388363	.289518	1.082687
.6250	.297439	.433868	.460819	1.088975
.6500	.387085	.470078	.677580	1.091548
.6750	.452498	.495142	.933887	1.089480
.7000	.491287	.507852	1.225737	1.081442
.7250	.502740	.507686	1.547293	1.065838
.7500	.487840	.494796	1.889202	1.040893
.7750	.449197	.469967	2.237473	1.004732
.8000	.390902	.434535	2.572491	.955475
.8250	.318315	.390271	2.868101	.891365
.8500	.237804	.339239	3.090787	.810930
.8750	.156456	.283631	3.199021	.713183
.9000	.081781	.225589	3.142878	.597878
.9250	.021420	.167024	2.864052	.465803
.9500	-.017091	.109431	2.296428	.319134
.9750	-.026513	.053710	1.367380	.161817
1.0000	-.000000	0.000000	-.000000	0.000000
	MEDIUM TEMP	NUSSELT NO	MEDIUM TEMP	NUSSELT NO
	.9214	-4.5931973	.9729	43.30405

APPENDIX C

Thermal Entry Problem - PROGRAM FHD

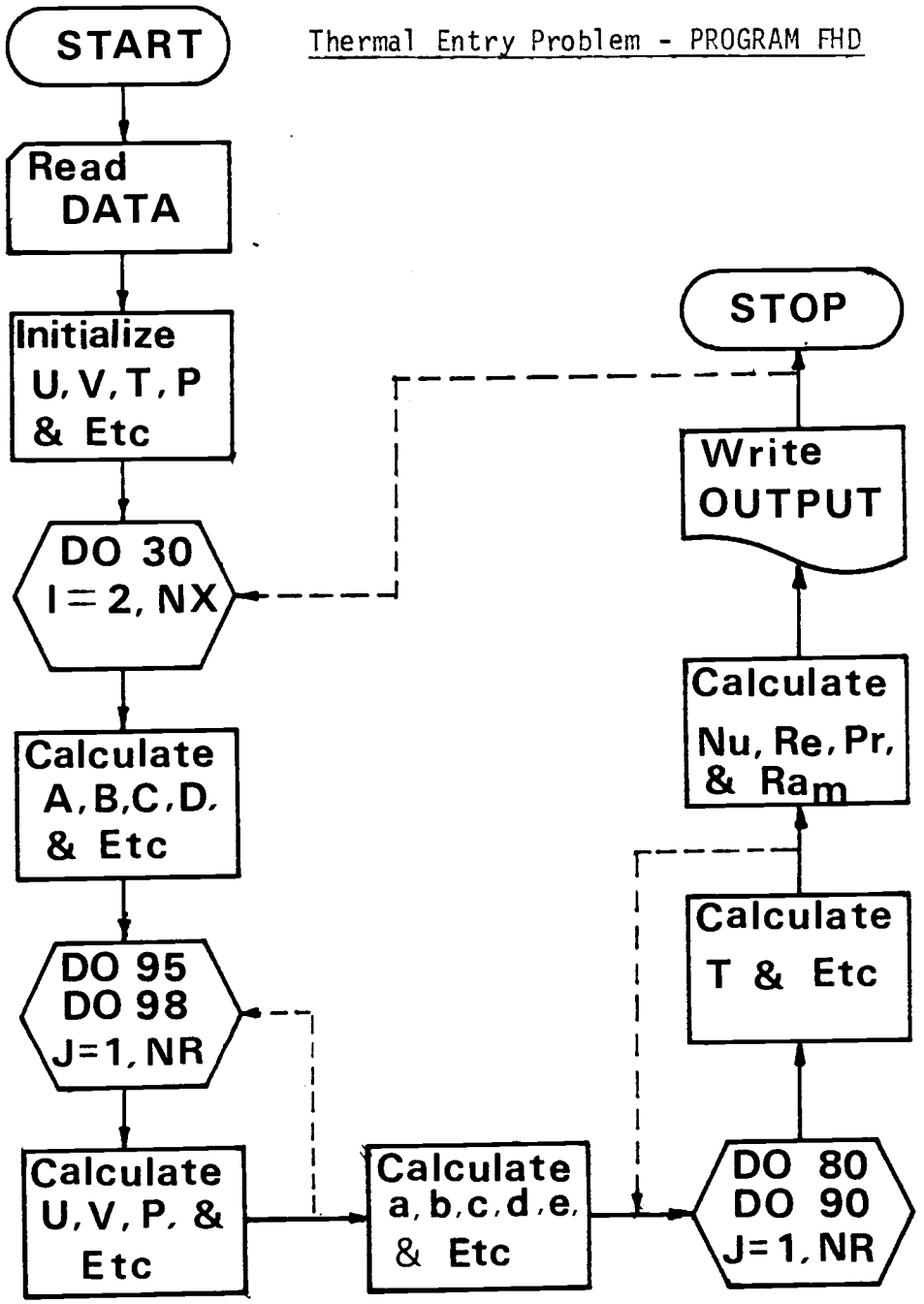

Flow chart for the program FHD to solve Equations (101), (103), and (105).

```
C****** THIS IS A NUMERICAL SOLUTION  FOR THE THERNAL ENTRANCE REGION
C****** OF FERROHYDRODYNAMIC (FHD) FLOW IN A DUCT INTHE PRESENCE OF AN
C****** APPLIED EXTERNAL MAGNETIC FIELD.
C
C
C***** THE FOLLOWINGS ARE INFORMATIONS ABOUT INPUT DATA.
C***** THE INPUT DATA MUST BE ADJUSTED  WITH THEIR UNITS
C***** WHICH ARE GIVEN HERE IN SI UNIT SYSTEM.
C
C      RAD (RADIUS OF TUBE)                    METER
C      DX (STEP-SIZE IN X-DIRECTION)           METER
C      PYRO (PYROMAGNETIC COEFFICIENT)         GAUSS/DEGREE K
C      DENS (DENSITY OF FLUID)                 KILO-GRAM/CUBIC METER
C      COMAG (MAGNETIC PERMEABILITY AT VACUUM)
C                                              NEWTON/SQUARE AMPERE
C      FRIC (FRICTION COEFFICIENT)
C      PLEN (TUBE LENGTH)                      METER
C      COND (THERMAL CONDUCTIVITY OF FLUID)    WATTS/METER DEGREE K
C      HEAT (HEATING RATE)                     WATTS
C      HTCAPA (HEAT CAPACITY)                  WATTS.SEC/KG. DEGREE K
C      TEMPEN (ENTERING FLUID TEMPERATURE)     DEGREE K
C      NX (ITERATION NUMBER OF X-DIRECTION)
C      NR (ITERATION NUMBER OF R-DIRECTION)
C      VISCO (VISCOSITY OF FLUID)              CP
C      TCURIE (CURIE TEMPERATURE)              DEGREE K
C      DL (LENGTH OF HEATING ELEMENT)          METER.
C
C
      PROGRAM FHD(INPUT,OUTPUT)
C
      COMMON U(100,41),V(100,41),PRESX(100,41),T(100,41),DR
      DIMENSION A(41),B(41),C(41),D(41)
      DIMENSION UZ(42),Z(42),DU(41),PLOW(41),RO(41)
      DIMENSION UZI(41),ZI(41),DUI(41),PLOWI(41)
      DIMENSION USCALE(41), TSCALE(41), VSCALE(41), PSCALE(41)
      DIMENSION  ET(41),  ALPA(41),BETA(41),GAMA(41),DELTA(41),EXTA(41)
C
C***** INPUT DATA
C
      DATA RAD,DX,PYRO,DENS,COMAG/0.019050,0.0050,0.1
     $,1220.0,0.00000126/
```

```
C
      DATA FRIC,PLEN/0.0356,4.9525/
      DATA NX,NR/29,21/
      DATA COND,HEAT,HTCAPA,TEMPEN/0.175,100.566,5275.4,285.0/
      DATA VISCO,TCURIE,DL/0.00126,1043.0,0.175/
C
C
C***** INITIALIZE VARIABLES
C
      DO 68 NN=4,4
      IF(NN.EQ.1) GO TO 59
      IF(NN.EQ.2) GO TO 61
      IF(NN.EQ.3) GO TO 62
      IF(NN.EQ.4) GO TO 63
      IF(NN.EQ.5) GO TO 81
      IF(NN.EQ.6) GO TO 82
      IF(NN.EQ.7) GO TO 83
      IF(NN.EQ.8) GO TO 84
      IF(NN.EQ.9) GO TO 85
      IF(NN.EQ.10) GO TO 86
  59  FIELD=3500.0
      GO TO 66
  61  FIELD=4000.0
      GO TO 66
  62  FIELD=4500.0
      GO TO 66
  63  FIELD=5000.0
      GO TO 66
  81  FIELD=5500.0
      GO TO 66
  82  FIELD=6000.0
      GO TO 66
  83  FIELD=6500.0
      GO TO 66
  84  FIELD=7000.0
      GO TO 66
  85  FIELD=7500.0
      GO TO 66
  86  FIELD=8000.0
  66  GRAD=FIELD/0.12
      VISCOK=VISCO/DENS
      HTFLUX=HEAT/(2.0*3.14*RAD*DL)
C
      WRITE 189, FIELD
 189  FORMAT("1",15X,"***FIELD INTENSITY, H = ",F7.1)
      M=INT(0.0)
      DR=RAD/FLOAT(NR-1)
      R=0.0
      V(2,NR)=0.0
      V(1,NR)=0.0
```

```
      II=NR
      VELM=SQRT(COMAG*PYRO*GRAD*(298.-TEMPEN)/(DENS*(2.*FRIC*
     1      PLEN/(2.*RAD)+0.5)))
C
      DO 10 K=1,NR
C
      T(1,K)=TEMPEN
      T(2,K)=TEMPEN
      U(2,K)=2.0*VELM*(1.0-(FLOAT(K-1)*DR/RAD)**2.0)
      U(1,K)=U(2,K)
   10 CONTINUE
      CALL SIMPU(2,UAV)
      DRAD=RAD**2.0
      DO 14 K=1,NR
      PRESX(2,K)=-(8.0*VISCO*VELM/DRAD-8.0*VISCO*VELM/DRAD)
   14 PRESX(1,K)=PRESX(2,K)
C
      JR=NR-1
C
      DO 20 JJ=2,JR
      J=JJ
      V(1,1)=0.0
      V(2,1)=0.0
      I=1
      U(I-1,J)=U(I,J)
      V(I+1,J)=FLOAT(J-1)*V(I+1,J-1)/FLOAT(J)-(0.5*DR/DX)*(U(I+1,J)-
     1         U(I-1,J))
      V(1,JJ)=V(2,JJ)
   20 CONTINUE
C
      X=0.0
C
C***** GENERATE THE TRI-DIAGONAL MATRIX COEFFICIENTS FOR VELOCITY
C***** AND TEMPERATURE CALCULATION.
C
      DO 30 I=2,NX
C
C
C
C **** TEMPERATURE CALCULATION ****
C
C
      IR=I+1
      JR=NR-1
   35 DO 500 J=1,NR
C
      IF(J.GT.1) GO TO 501
      ALPA(J)=0.0
      ALPAP=-4.*COND*DX/(DENS*HTCAPA*(DR**2.))-(2.*V(I,J)-V(I-1,J))
     1      *DX/DR
      BETA(J)=3.*(2.*U(I,J)-U(I-1,J))+8.*COND*DX/(DENS*HTCAPA*(DR**2.)
```

```
     1          )-2.*COND/(DENS*HTCAPA*DX)
      GAMAP=-4.*COND*DX/(DENS*HTCAPA*(DR**2.))+(2.*V(I,J)-V(I-1,J))
     1      *DX/DR
      GAMA(J)=ALPAP+GAMAP
      DELTA(J)=(2.*U(I,J)-U(I-1,J))*(4.*T(I,J)-T(I-1,J))-(2.*T(I,J)-
     1           T(I-1,J))*2.*COND/(DENS*HTCAPA*DX)+VISCO*DX*
     2           ((U(I  ,J+1)-U(I  ,J))**2.)/(4.*DENS*HTCAPA*(DR**2.))
     3           +(2.*U(I,J)-U(I-1,J))*(2.*T(I,J)-T(I-1,J))*2.*DX*COMAG
     4           *PYRO*GRAD/(HTCAPA*DENS)
      EXTA(J)=0.0
C
      GO TO 500
C
  501 IF(J.EQ.NR) GO TO 502
C
      ALPA(J)=-(2.*V(I,J)-V(I-1,J))*DX/DR-2.*COND*DX/(DENS*HTCAPA*
     $        (DR**2.))+COND*DX/(DENS*HTCAPA*DR*FLOAT(J-1)*DR)
      BETA(J)=3.*(2.*U(I,J)-U(I-1,J))+4.*COND*DX/(DENS*HTCAPA*(DR**2.)
     1          )-2.*COND/(DENS*HTCAPA*DX)
      GAMA(J)=(2.*V(I,J)-V(I-1,J))*DX/DR-2.*COND*DX/(DENS*HTCAPA*
     $        (DR**2.))-COND*DX/(DENS*HTCAPA*DR*FLOAT(J-1)*DR)
      DELTA(J)=(2.*U(I,J)-U(I-1,J))*(4.*T(I,J)-T(I-1,J))-(2.*T(I,J)-
     1           T(I-1,J))*2.*COND/(DENS*HTCAPA*DX)+((U(I  ,J+1)-
     2           U(I  ,J-1))**2.)*VISCO*DX/(2.*DENS*HTCAPA*(DR**2.))
     3           +(2.*U(I,J)-U(I-1,J))*(2.*T(I,J)-T(I-1,J))*2.*DX*COMAG
     4           *PYRO*GRAD/(HTCAPA*DENS)
      EXTA(J)=0.0
C
       GO TO 500
C
  502 ALPA(J)=-(2.*V(I,J)-V(I-1,J))*DX/DR-2.*COND*DX/(DENS*HTCAPA*
     $        (DR**2.))+COND*DX/(DENS*HTCAPA*DR*FLOAT(J-1)*DR)
      BETA(J)=3.*(2.*U(I,J)-U(I-1,J))+4.*COND*DX/(DENS*HTCAPA*(DR**2.)
     1          )-2.*COND/(DENS*HTCAPA*DX)
      GAMA(J)=(2.*V(I,J)-V(I-1,J))*DX/DR-2.*COND*DX/(DENS*HTCAPA*
     $        (DR**2.))-COND*DX/(DENS*HTCAPA*DR*FLOAT(J-1)*DR)
      DELTA(J)=(2.*U(I,J)-U(I-1,J))*(4.*T(I,J)-T(I-1,J))-(2.*T(I,J)-
     1           T(I-1,J))*2.*COND/(DENS*HTCAPA*DX)+((U(I  ,J)-
     2           U(I  ,J-1))**2.)*VISCO*DX*2./(DENS*HTCAPA*(DR**2.))
     3           +(2.*U(I,J)-U(I-1,J))*(2.*T(I,J)-T(I-1,J))*2.*DX*COMAG
     4           *PYRO*GRAD/(HTCAPA*DENS)
      ALPA(J)=ALPA(J)+GAMA(J)
      BETA(J)=BETA(J)
      IF(X.GT.0.2) GO TO 37
      DELTA(J)=DELTA(J)-2.*DR*HTFLUX*GAMA(J)/COND
      GAMA(J)=0.0
      EXTA(J)=0.0
      GO TO 500
  37  DELTA(J)=DELTA(J)
      GAMA(J)=0.0
      EXTA(J)=0.0
```

```
C
  500 CONTINUE
C
      Z(1)=DELTA(1)
      DU(1)=BETA(1)
      UZ(1)=GAMA(1)+ALPA(1)
C
      DO 80 J=2,NR
      IF(J.EQ.NR) GO TO 21
      UZ(J)=GAMA(J)
      PLOW(J)=ALPA(J)/DU(J-1)
      DU(J)=BETA(J)-UZ(J-1)*PLOW(J)
      Z(J)=DELTA(J)-Z(J-1)*PLOW(J)
   80 CONTINUE
C
   21 ET(J)=EXTA(J)/DU(J-2)
      PLOW(J)=(ALPA(J)-UZ(J-2)*ET(J))/DU(J-1)
      DU(J)=BETA(J)-UZ(J-1)*PLOW(J)
      Z(J)=DELTA(J)-ET(J)*Z(J-2)-PLOW(J)*Z(J-1)
      T(IR,J)=Z(J)/DU(J)
C
      IZ=NR-1
C
      DO 90 NI=1,IZ
      K=NR-NI
      T(IR,K)=(Z(K)-UZ(K)*T(IR,K+1))/DU(K)
   90 CONTINUE
C
      IQ=I-1
      CALL SIMPU(IQ,UAVI)
      CALL SIMPU(I,UAV)
      L=M+2
      DRADL=RAD**2.0
C
      DO 41 J=1,NR
      PRESX(I+1,J)=-(8.0*VISCO*UAV/DRADL-8.0*VISCO*UAVI/DRADL)
     1         +COMAG*PYRO*FIELD*(T(I+1,J)-T(I,J))/DX
   41 CONTINUE
      DO 40 J=1,NR
      IF(J.GE.2) GO TO 15
C
C
      A(J)=0.0
      AP=-4.*VISCOK*DX/(DR**2.)
      B(J)=3.*(2.*U(I,J)-U(I-1,J))+8.*VISCOK*DX/(DR**2.)
      CP=-4.*VISCOK*DX/(DR**2.)
      C(J)=AP +CP
      D(J)=(2.*U(I,J)-U(I-1,J))*(4.*U(I,J)-U(I-1,J))+2.*(DX/DENS)*
     1     PRESX(I+1,J)+2.*DX*PYRO*COMAG*GRAD*(T(I+1,J)-T(I,J))/DENS
     2     -(2.*V(I,J)-V(I-1,J))*(U(I,J+1)-U(I,J))*2.0*DX/DR
C
```

```
C
      GO TO 40
C
  15  A(J)= -2.*VISCOK*DX/(DR**2.)+VISCOK*DX/(DR*FLOAT(J-1)*DR)
      IF(J.EQ.NR) GO TO 40
      B(J)=3.*(2.*U(I,J)-U(I-1,J))+4.*VISCOK*DX/(DR**2.)
      C(J)=-2.*VISCOK*DX/(DR**2.)-VISCOK*DX/(DR*FLOAT(J-1)*DR)
      D(J)=(2.*U(I,J)-U(I-1,J))*(4.*U(I,J)-U(I-1,J))+2.*(DX/DENS)*
     1     PRESX(I+1,J)+2.*DX*PYRO*COMAG*GRAD*(T(I+1,J)-T(I,J))/DENS
     2     -(2.*V(I,J)-V(I-1,J))*(U(I,J+1)-U(I,J-1))*DX/DR
C
  40  CONTINUE
C
C
C
C **** VELOCITY CALCULATION ****
C
C
C
      U(I+1,NR)=0.0
      V(I+1,NR)=0.0
C
C
      J=1
      ZI(J)=D(J)
      DUI(J)=B(J)
      UZI(J)=C(J)+A(J)
C
C
      DO 95 J=2,JR
      UZI(J)=C(J)
      PLOWI(J)=A(J)/DUI(J-1)
      DUI(J)=B(J)-UZI(J-1)*PLOWI(J)
      ZI(J)=D(J)-ZI(J-1)*PLOWI(J)
  95  CONTINUE
C
      U(I+1,NR-1)=ZI(NR-1)/DUI(NR-1)
      LZ=NR-2
C
      DO 98 LI=1,LZ
      KI=JR -LI
      U(I+1,KI)=(ZI(KI)-UZI(KI)*U(I+1,KI+1))/DUI(KI)
  98  CONTINUE
C
C
C
      DO 60 J=2,JR
      IF(J.EQ.2) V(I+1,J-1)=0.0
      V(I+1,J)=FLOAT(J-1)*V(I+1,J-1)/FLOAT(J)-(0.5*DR/DX)*(U(I+1,J)-
     1         U(I-1,J))
  60  CONTINUE
```

```
C
      M=M+1
C
C***** CALL AVERAGE VELOCITY AND TEMPERATURE.
C
      CALL SIMPU(I,UAV)
      CALL SIMPT(I+1,TAV)
C
      AI=0.2*HTFLUX/(DENS*HTCAPA*2.0*RAD*UAV)
      HTCO=HTFLUX/(T(I+1,NR)-TAV)
      HNUSS=2.0*RAD*HTCO/COND
      RAMAG=(COMAG*PYRO*GRAD*(0.20**4.0)*DENS*HTCAPA/(COND*VISCO))*(AI
     1+COMAG*PYRO*GRAD*TAV/(DENS*HTCAPA))
C
C***** OUTPUT DATA.
C
      REY=2.0*RAD*DENS*UAV/VISCO
      WRITE 100, X, HTCO,HNUSS
  100 FORMAT("0",15X,"**DISTANCE FROM STARTING POINT OF HEATING, X =",
     1F10.8, /,15X,"HEAT TRANSFER COEFFICIENT, H= ",F12.5, /,15X,
     2      "NUSSELT NUMBER, NU= ",F12.5)
      WRITE 58, REY
   58 FORMAT(    15X,"REYNOLDS NUMBER = ",F10.3)
      WRITE 55, RAMAG
   55 FORMAT(    15X,"MAGNETIC RAYLEIGH NUMBER = ",F10.1)
      WRITE 199
  199 FORMAT("0",8X,"RADIUS",3X,"AXIAL VELOCITY",3X,"RADIAL VELOCITY",
     1       3X,"TEMPERATURE",3X,"PRESSURE")
      DO 70 J=1,NR
      RO(J)=FLOAT(J-1)*DR/RAD
      WRITE 406,RO(J),U(I,J),V(I,J),T(I,J),PRESX(I,J)
  406 FORMAT(10X,F4.2,7X,F8.6,7X,F8.6,9X,F6.1,7X,F7.2)
   70 CONTINUE
      X=X+DX
   30 CONTINUE
   68 CONTINUE
      STOP
      END
      SUBROUTINE SIMPU(I,UM)
      COMMON U(100,41),V(100,41),PRESX(100,41),T(100,41),DR
      DATA RAD,NR/0.019050,21/
      SUM=SUMI=0.0
C
      DO 10 J=1,NR
      DRAD=FLOAT(J-1)*DR
      IF(J.EQ.1) GO TO 5
      IF(J.EQ.NR) GO TO 6
      ITEST=J/2
      TEST=FLOAT(ITEST)
      TESTJ=FLOAT(J)/2.
C
```

```
      IF(TEST.EQ.TESTJ) GO TO 4
      SUMI=SUMI+U(I,J)*DRAD
      GO TO 10
    4 SUM=SUM+U(I,J)*DRAD
      GO TO 10
    5 SUMA=U(I,J)*DRAD
      GO TO 10
    6 SUMB=U(I,J)*DRAD
   10 CONTINUE
C
      F=SUMA+4.*SUM+2.*SUMI+SUMB
      UM=2.*DR*F/(3.*(RAD**2.))
      RETURN
      END
      SUBROUTINE SIMPV(I,UM)
      COMMON U(100,41),V(100,41),PRESX(100,41),T(100,41),DR
      DATA RAD,NR/0.019050,21/
      SUM=SUMI=0.0
C
      DO 10 J=1,NR
      DRAD=FLOAT(J-1)*DR
      IF(J.EQ.1) GO TO 5
      IF(J.EQ.NR) GO TO 6
      ITEST=J/2
      TEST=FLOAT(ITEST)
      TESTJ=FLOAT(J)/2.
C
      IF(TEST.EQ.TESTJ) GO TO 4
      SUMI=SUMI+V(I,J)*DRAD
      GO TO 10
    4 SUM=SUM+V(I,J)*DRAD
      GO TO 10
    5 SUMA=V(I,J)*DRAD
      GO TO 10
    6 SUMB=V(I,J)*DRAD
   10 CONTINUE
C
      F=SUMA+4.*SUM+2.*SUMI+SUMB
      UM=2.*DR*F/(3.*(RAD**2.))
      RETURN
      END
      SUBROUTINE SIMPP(I,UM)
      COMMON U(100,41),V(100,41),PRESX(100,41),T(100,41),DR
      DATA RAD,NR/0.019050,21/
      SUM=SUMI=0.0
C
      DO 10 J=1,NR
      DRAD=FLOAT(J-1)*DR
      IF(J.EQ.1) GO TO 5
      IF(J.EQ.NR) GO TO 6
      ITEST=J/2
```

```
      TEST=FLOAT(ITEST)
      TESTJ=FLOAT(J)/2.
C
      IF(TEST.EQ.TESTJ) GO TO 4
      SUMI=SUMI+PRESX(I,J)*DRAD
      GO TO 10
   4  SUM=SUM+PRESX(I,J)*DRAD
      GO TO 10
   5  SUMA=PRESX(I,J)*DRAD
      GO TO 10
   6  SUMB=PRESX(I,J)*DRAD
  10  CONTINUE
C
      F=SUMA+4.*SUM+2.*SUMI+SUMB
      UM=2.*DR*F/(3.*(RAD**2.))
      RETURN
      END
      SUBROUTINE SIMPT(I,TM)
      COMMON U(100,41),V(100,41),PRESX(100,41),T(100,41),DR
      DATA RAD,NR/0.019050,21/
      ADD=ADDI=0.0
C
      DO 20 J=1,NR
      DRAT=FLOAT(J-1)*DR
      IF(J.EQ.1) GO TO 5
      IF(J.EQ.NR) GO TO 6
      JTEST=J/2
      TEST=FLOAT(JTEST)
      TESTA=FLOAT(J)/2.
C
      IF(TEST.EQ.TESTA) GO TO 4
      ADDI=ADDI+U(I,J)*T(I,J)*DRAT
      GO TO 20
   4  ADD=ADD+U(I,J)*T(I,J)*DRAT
      GO TO 20
   5  ADDA=U(I,J)*T(I,J)*DRAT
      GO TO 20
   6  ADDB=U(I,J)*T(I,J)*DRAT
  20  CONTINUE
C
      CALL SIMPU(I,UM)
      FU=ADDA+4.*ADD+2.*ADDI+ADDB
      TM=2.*DR*FU/(3.*UM*(RAD**2.))
      RETURN
      END
```

**DISTANCE FROM STARTING POINT OF HEATING, X = 2.5 CM

HEAT TRANSFER COEFFICIENT, H= 49.33219

NUSSELT NUMBER, NU= 10.74032

REYNOLDS NUMBER = 136.0

MAGNETIC RAYLEIGH NUMBER = 334797.8

RADIUS	AXIAL VELOCITY	RADIAL VELOCITY	TEMPERATURE	PRESSURE
0.00	.004460	0.000000	285.0	-.02
.05	.004449	.000012	285.0	-.02
.10	.004413	.000020	285.0	-.02
.15	.004353	.000027	285.0	-.02
.20	.004269	.000033	285.0	-.02
.25	.004162	.000040	285.0	-.02
.30	.004030	.000045	285.0	-.02
.35	.003876	.000051	285.0	-.02
.40	.003700	.000057	285.0	-.02
.45	.003504	.000061	285.0	-.02
.50	.003292	.000065	285.0	-.02
.55	.003071	.000066	285.0	-.02
.60	.002856	.000062	285.0	-.02
.65	.002667	.000048	285.0	-.02
.70	.002537	.000016	285.0	-.02
.75	.002509	-.000046	285.0	-.02
.80	.002623	-.000158	285.2	-.02
.85	.002888	-.000338	284.1	.16
.90	.003020	-.000583	295.9	.59
.95	.002044	-.000800	296.8	1.73
1.00	0.000000	0.000000	323.7	1.71

**DISTANCE FROM STARTING POINT OF HEATING, X = 5.0 CM

HEAT TRANSFER COEFFICIENT, H= 37.62708

NUSSELT NUMBER, NU= 8.19195

REYNOLDS NUMBER = 136.0

MAGNETIC RAYLEIGH NUMBER = 260431.9

RADIUS	AXIAL VELOCITY	RADIAL VELOCITY	TEMPERATURE	PRESSURE
0.00	.004394	0.000000	285.0	-.00
.05	.004382	.000013	285.0	-.00
.10	.004346	.000022	285.0	-.00
.15	.004287	.000029	285.0	-.00
.20	.004204	.000036	285.0	-.00
.25	.004098	.000043	285.0	-.00
.30	.003968	.000050	285.0	-.00
.35	.003818	.000055	285.0	-.00
.40	.003649	.000060	285.0	-.00
.45	.003465	.000064	285.0	-.00
.50	.003276	.000065	285.0	-.00
.55	.003094	.000060	285.0	-.00
.60	.002942	.000047	285.0	-.00
.65	.002854	.000019	285.0	-.00
.70	.002883	-.000032	285.0	-.00
.75	.003110	-.000117	285.3	.03
.80	.003651	-.000250	287.7	.31
.85	.004570	-.000451	298.5	1.81
.90	.005343	-.000676	333.8	4.78
.95	.004810	-.000892	375.6	9.93
1.00	0.000000	0.000000	403.6	10.06

APPENDIX D

Data Reduction, Regression Analysis - PROGRAM CURFIT

```
      PROGRAM CURFIT(INPUT,OUTPUT,TAPE1,TAPE2,TAPE3=INPUT,TAPE4=OUTPUT)
      DIMENSION WORD(8),NAME(2,7),XIN(400),YIN(400),X(400),Y(400),B(11),
     1  MATRIX(11,11),SUM(20),RHS(11),WARN(3)
      REAL LL,MATRIX
      DATA WORD/"LIN","EXP","LOG","POW","HYP","POL","INV","LIS"/
      DATA NAME/"LINEAR","    ","EXPONENTIA","L   ","LOGARITHMI",
     1 "C  ","POWER     ","    ","HYPERBOLIC","    ","POLYNOMIAL",
     2 "    ","INVERTED P","OLY"/
      DATA WARN/"Y      ","X      ","X AND Y"/
C.....READ THE DATA FROM TAPE1 (FREE-FORMATTED W/INDEP VAR READ FIRST)
      REWIND 1
      READ(1,113)DATA
      WRITE(4,106)DATA
      READ(1,*)N
      READ(1,*)(XIN(I),YIN(I),I=1,N)
      IFLAG3=IFLAG4=0
C.....READ THE TYPE OF FIT
1     WRITE(4,99)
      IF(IFLAG3.EQ.0)WRITE(4,100)
      IFLAG3=1
      READ(3,101)TYPE
      IF(TYPE.EQ.WORD(8)) GO TO 3
      NTYPE=0
      DO 2 I=1,7
    2 IF(TYPE.EQ.WORD(I)) NTYPE=I
      IF(NTYPE.NE.0) GO TO 4
      WRITE(4,102)
      GO TO 1
    3 WRITE(4,103)
      GO TO 1
C.....READ THE LIMITS...IF LL=0. AND UL=0. ALL OF THE DATA WILL BE FIT
    4 IF(NTYPE.LE.5) GO TO 12
      WRITE(4,105)
      READ(3,*)NORDER
12    IF(IFLAG4.EQ.0) GO TO 14
      WRITE(4,115)
      GO TO 15
14    WRITE(4,104)
15    READ(3,*) LL,UL
      IFLAG4=1
      IFLAG=0
      IFLAG2=0
      IF(LL.EQ.0.0.AND.UL.EQ.0.0) IFLAG=1
C.....TRANSFORM THE DATA
      M=0
      DO 25 I=1,N
      IF(IFLAG.EQ.1) GO TO 5
```

```
      IF(XIN(I).GE.LL.AND.XIN(I).LE.UL) GO TO 5
      GO TO 25
    5 M=M+1
      GO TO(6,7,8,11,9,6,9) NTYPE
    6 Y(M)=YIN(I)
      GO TO 10
7     IF(YIN(I).LE.0.0) GO TO 13
      Y(M)=ALOG(YIN(I))
      GO TO 10
8     IF(XIN(I).LE.0.0) GO TO 13
      X(M)=ALOG(XIN(I))
      GO TO 10
    9 Y(M)=1./YIN(I)
   10 X(M)=XIN(I)
      GO TO 25
13    IFLAG2=1
      M=M-1
      GO TO 25
11    IF(YIN(I).LE.0.0.OR.XIN(I).LE.0.0) GO TO 13
      X(M)=ALOG(XIN(I))
      Y(M)=ALOG(YIN(I))
   25 CONTINUE
C.....DO THE REQUIRED SUMATIONS (IF ITS A POLY FIT GO TO 50)
      IF(NTYPE.EQ.6.OR.NTYPE.EQ.7)GO TO 50
      SX=SY=SX2=SY2=SXY=0.0
      DO 30 I=1,M
      SX=SX + X(I)
      SY=SY + Y(I)
      SX2=SX2 + X(I)*X(I)
      SY2=SY2 + Y(I)*Y(I)
      SXY=SXY + X(I)*Y(I)
   30 CONTINUE
C.....CALCULATE THE COEFFICIENTS
      XNUM=SXY-SY*SX/M
      XDEN=SX2-SX*SX/M
      YDEN=SY2-SY*SY/M
      B(2)=XNUM/XDEN
      B(1)=(SY/M)-B(2)*SX/M
      IF(NTYPE.EQ.2.OR.NTYPE.EQ.4) B(1)=EXP(B(1))
      IF(XDEN.EQ.0.0.OR.YDEN.EQ.0.0) GO TO 59
      RSQ=XNUM*XNUM/(XDEN*YDEN)
      NCOEF=2
      GO TO 75
C.....THE  ROUTINE FOR POLYNOMIAL FITTING BEGINS HERE
   50 NCOEF=NORDER + 1
      NP1=NCOEF + 1
      N2=2*NORDER
      DO 55 J=1,N2
      SUM(J)=0.0
      DO 55 I=1,M
   55 SUM(J)=SUM(J) + X(I)**J
```

```
      DO 60 J=1,NCOEF
      RHS(J)=0.0
      DO 60 I=1,M
      IF(X(I)*Y(I).NE.0.0) RHS(J)=RHS(J)+Y(I)*X(I)**(J-1)
60    CONTINUE
C.....SET UP THE NORMAL EQUATION MATRIX
      DO 65 I=1,NCOEF
      MATRIX(I,NP1)=RHS(I)
      DO 65 J=1,NCOEF
      K=I + J
      IF(K.NE.2) MATRIX(I,J)=SUM(K-2)
   65 CONTINUE
      MATRIX(1,1)=M
C.....CALL THE GAUSSIAN ELIMINATION ROUTINE
      CALL GAUSS(MATRIX,B,NCOEF,11)
C.....CALCULATE THE COEF OF DETERMINATION
59    YBAR=0.0
      DO 66 I=1,M
66    YBAR=YBAR+Y(I)
      YBAR=YBAR/M
      SSR=SSTO=0.0
      DO 70 I=1,M
      SSTO=SSTO+(Y(I)-YBAR)**2
      YHAT=0.0
      GO TO (61,62,63,64,67,68,68),NTYPE
61    YHAT=B(1)+B(2)*X(I)
      GO TO 71
62    YHAT=B(1)*EXP(B(2)*X(I))
      GO TO 71
63    YHAT=B(1)+B(2)*ALOG(X(I))
      GO TO 71
64    YHAT=B(1)*X(I)**B(2)
      GO TO 71
67    YHAT=1./(B(1)+B(2)*X(I))
      GO TO 71
68    DO 69 N=1,NCOEF
      IF(B(N)*X(I).NE.0.0) YHAT=YHAT+B(N)*X(I)**(N-1)
69    CONTINUE
      IF(NTYPE.EQ.7) YHAT=1./YHAT
71    CONTINUE
      SSR=SSR+(YHAT-YBAR)**2
70    CONTINUE
      RSQ=SSR/SSTO
C.....FORMAT STATEMENTS
99    FORMAT(/1X,"TYPE OF FIT?")
100   FORMAT(1X,"TYPE LIST FOR A LIST OF AVAILABLE FITTING FUNCTIONS")
  101 FORMAT(A3)
  102 FORMAT(1X,"ILLEGAL FUNCTION, TRY AGAIN")
  103 FORMAT(/1X,"THE FOLLOWING FUNCTIONS ARE AVAILABLE",
     1  /7X,"LINEAR          Y=B(1) + B(2)*X",
     2  /7X,"EXPONENTIAL     Y=B(1)*EXP(B(2)*X)",
```

```
     3  /7X,"LOGARITHMIC     Y=B(1) + B(2)*ALOG(X)",
     *  /7X,"POWER           Y=B(2)*X**B(2)",
     4  /7X,"HYPERBOLIC      Y=1./(B(1) + B(2)*X)",
     5  /7X,"POLYNOMIAL      Y=B(1)+B(2)*X+B(3)*X**2+...+B(N+1)*X**N",
     6  /7X,"INVERTED POLY   Y=1./(B(1)+B(2)*X**1+...+B(N+1)*X**N)")
  104 FORMAT(/1X,"INPUT THE LOWER AND UPPER LIMITS , RESPECTIVELY.",/
     1 3X,"IF BOTH ARE ZERO...ALL THE DATA WILL BE FITTED")
  105 FORMAT(/1X,"INPUT THE ORDER OF THE POLYNOMIAL")
106   FORMAT(//16X,"FITTER",/6X,"LEAST-SQUARES FITTING PROGRAM",/13X,
     1 "VERSION 9/5/79",//8X,"THE DATA FILE IS ",A7)
107   FORMAT(/5X,"TYPE OF FIT- ",A10,A3)
  108 FORMAT(5X,"ORDER- ",I2)
109   FORMAT(7X,"B(",I2,")=",G14.7)
  110 FORMAT(7X,"RSQ=",F7.5)
  111 FORMAT(5X,"LOWER LIMIT",G10.3,/5X,"UPPER LIMIT",G10.3,
     1 /5X,"NO. OF POINTS",I4)
  112 FORMAT(/1X,"WOULD YOU LIKE TO RUN A NEW CASE?")
113   FORMAT(A7)
114   FORMAT(5X,"*** WARNING ***  THIS FIT USES A TRANSFORMATION",
     1 /22X,"WHICH MUST IGNORE NEGATIVE VALUES OF ",A7)
115   FORMAT(1X,"LL&UL?")
116   FORMAT(1X,"WOULD YOU LIKE TO SETUP A DATA FILE FOR PLOTTING?")
117   FORMAT(1X,"HOW MANY POINTS SHOULD BE CALCULATED?")
118   FORMAT(2G11.4)
C.....OUTPUT
75    WRITE(4,107) NAME(1,NTYPE),NAME(2,NTYPE)
      IF(NTYPE.EQ.6.OR.NTYPE.EQ.7) WRITE(4,108) NORDER
      WRITE(4,111) LL,UL,M
      WRITE(4,109)(I,B(I),I=1,NCOEF)
      WRITE(4,110)RSQ
      J=NTYPE-1
      IF(IFLAG2.EQ.1) WRITE(4,114) WARN(J)
      WRITE(4,112)
      READ(3,101) ANS
      IF(ANS.EQ.YES) GO TO 1
C
C*****SET UP A DATA FILE FOR PLOTTING, IF REQUESTED
C
      WRITE(4,116)
      READ(3,101)ANS
      IF(ANS.NE."YES") GO TO 80
      WRITE(2,113) DATA
      WRITE(2,*) M
      WRITE(2,118)(X(I),Y(I),I=1,M)
      WRITE(4,117)
      READ(3,*) NDATA
      XMAX=UL
      XMIN=LL
      IF(UL.NE.0.0.OR.LL.NE.0.0) GO TO 78
      XMIN=XMAX=X(1)
      DO 76 I=2,M
```

```
      IF(XMIN.GT.X(I)) XMIN=X(I)
76    IF(XMAX.LT.X(I)) XMAX=X(I)
78    HX=(XMAX-XMIN)/(NDATA-1)
      WRITE(2,*) NDATA
      DO 74 I=1,NDATA
      YOUT=0.0
      XOUT=HX*(I-1)+XMIN
      GO TO(81,82,83,84,85,86,86),NTYPE
81    YOUT=B(1)+B(2)*XOUT
      GO TO 77
82    YOUT=B(1)*EXP(B(2)*XOUT)
      GO TO 77
83    YOUT=B(1)+B(2)*ALOG(XOUT)
      GO TO 77
84    IF(XOUT.LT.0.0) GO TO 74
      YOUT=B(1)*XOUT**B(2)
      GO TO 77
85    YOUT=1./(B(1)+B(2)*XOUT)
      GO TO 77
86    DO 87 N=1,NCOEF
      IF(B(N)*XOUT.NE.0.0) YOUT=YOUT+B(N)*XOUT**(N-1)
87    CONTINUE
      IF(NTYPE.EQ.7) YOUT=1./YOUT
77    WRITE(2,118) XOUT,YOUT
74    CONTINUE
80    STOP
      END
      SUBROUTINE GAUSS(A,X,N,NDIM)
C.....THE ROUTINE ACCEPTS THE DIMENSIONS OF THE MATRIX AS VARIABLES
      DIMENSION A(NDIM,1),X(NDIM)
      NP1=N+1
      NM1=N - 1
      DO 600 K=1,NM1
      KP1=K + 1
      L=K
      DO 400 I=KP1,N
  400 IF(ABS(A(I,K)).GT.ABS(A(L,K))) L=I
      IF(L.EQ.K) GO TO 500
      DO 410 J=K,NP1
      TEMP=A(K,J)
      A(K,J)=A(L,J)
  410 A(L,J)=TEMP
  500 DO 600 I=KP1,N
      FACTOR=A(I,K)/A(K,K)
      DO 600 J=KP1,NP1
  600 A(I,J)=A(I,J)-FACTOR*A(K,J)
C.....BACK SOLUTION
      X(N)=A(N,NP1)/A(N,N)
      I=NM1
  710 IP1=I + 1
      SUM=0.0
```

```
      DO 700 J=IP1,N
  700 SUM=SUM + A(I,J)*X(J)
      X(I)=(A(I,NP1)-SUM)/A(I,I)
      I=I -1
      IF(I.GE.1) GO TO 710
      RETURN
      END
```

APPENDIX E

Data Plot - PROGRAM FHDPLT

```
      PROGRAM FHDPLT(TAPE2,TAPE5,TAPE6,TAPE7,INPUT,OUTPUT)
      DIMENSION XBAR1(1000),XBAR2(1000),XBAR3(1000),YBAR1(1000),
     1YBAR2(1000),YBAR3(1000)
      DIMENSION X1(400),X2(400),X3(400),Y1(400),Y2(400),Y3(400)
      DIMENSION XMI(10),XMA(10),YMI(10),YMA(10)
      DIMENSION X(400),Y(400),YBAR(1000),XBAR(1000),LABELS(2)
      REWIND 2
      REWIND 5
      REWIND 6
      REWIND 7
      READ(2,50) DATA
   50 FORMAT(A7)
C
      READ(2,*) M
      READ(2,*) (X(I),Y(I),I=1,M)
C
      READ(2,*) NDATA
      READ(2,*) (XBAR(I),YBAR(I),I=1,NDATA)
C
      READ(5,50)DATA1
      READ(5,*)M1
      READ(5,*)(X1(I),Y1(I),I=1,M1)
      READ(5,*)NDATA1
      READ(5,*)(XBAR1(I),YBAR1(I),I=1,NDATA1)
C
      READ(6,50)DATA2
      READ(6,*)M2
      READ(6,*)(X2(I),Y2(I),I=1,M2)
      READ(6,*)NDATA2
      READ(6,*)(XBAR2(I),YBAR2(I),I=1,NDATA2)
C
      READ(7,50)DATA3
      READ(7,*)M3
      READ(7,*)(X3(I),Y3(I),I=1,M3)
      READ(7,*)NDATA3
      READ(7,*)(XBAR3(I),YBAR3(I),I=1,NDATA3)
      PRINT*,"INPUT HBOX, WBOX,HAX,WAX,LABEL"
      READ*,HBOX,WBOX,HAX,WAX,LABEL
C
      IF(EOF(5LINPUT)) 20,30
   20 HBOX=8.5
      WBOX=11.
      HAX=5.
      WAX=7.
      LABEL=1
   30 HOUT=HBOX+1
```

```
      WOUT=WBOX+1
      PRINT*,"ICODE,MODEL"
      READ*,ICODE,MODEL
      CALL BELL
      CALL PLOTYPE(ICODE)
      CALL TKTYPE(MODEL)
      CALL BAUD(2400)
      CALL ERASE
      CALL SIZE(WOUT,HOUT)
      YBIAS=XBIAS=0.0
      IF(HBOX.EQ.0.0.OR.WBOX.EQ.0.0) GO TO 10
      YBIAS=(HOUT-HBOX)/2.
      XBIAS=(WOUT-WBOX)/2.
      CALL SCALE(1.,1.,XBIAS,YBIAS,0.,0.)
      GO TO 10
C
C
C*****DRAW A BOX AROUND THE PLOT******
C
C
      CALL PLOT(0.,0.,0,0)
      CALL PLOT(WBOX,0.,1,0)
      CALL PLOT(WBOX,HBOX,1,0)
      CALL PLOT(0.,HBOX,1,0)
      CALL PLOT(0.,0.,1,0)
C
C*****RESET THE SCALE****
C
  10  YBIAS=YBIAS+((HBOX-HAX)/2.)
      XBIAS=XBIAS+((WBOX-WAX)/2.)
      CALL CHECK(X,M,XMI(1),XMA(1))
      CALL CHECK(Y,M,YMI(1),YMA(1))
C
      CALL CHECK(X1,M1,XMI(2),XMA(2))
      CALL CHECK(Y1,M1,YMI(2),YMA(2))
C
      CALL CHECK(X2,M2,XMI(3),XMA(3))
      CALL CHECK(Y2,M2,YMI(3),YMA(3))
C
      CALL CHECK(X3,M3,XMI(4),XMA(4))
      CALL CHECK(Y3,M3,YMI(4),YMA(4))
C
      CALL CHECK(XMI,2,XMIN,XMAXO)
      CALL CHECK(XMA,2,XMINO,XMAX)
C
      CALL CHECK(YMI,4,YMIN,YMAXO)
      CALL CHECK(YMA,4,YMINO,YMAX)
C
      CALL RANGE(XMIN,XMAX,IFIX(WAX),XMIN1,XMAX1,XTIC)
      CALL RANGE(YMIN,YMAX,IFIX(HAX),YMIN1,YMAX1,YTIC)
      XFACT=WAX/XMAX1
```

```
      YFACT=HAX/YMAX1
      CALL SCALE(XFACT,YFACT,XBIAS,YBIAS,0.,0.)
C
C*****DRAW AND LABEL THE AXIS*****
C
      CALL AXISL(0.,XMAX1,0.,0.,YMAX1,0.,XTIC,YTIC,1,4,2,1,1.,1.,0.2,0)
C
C*****DRAW THE GRID*****
C
C
C*****PLOT THE DATA AS POINTS*****
C
C
C*****PLOT THE FUNCTION AS A LINE*****
C
      CALL VECTORS
      CALL LINE(XBAR,YBAR,1,NDATA)
C
      CALL VECTORS
      CALL LINE(XBAR1,YBAR1,19,NDATA1)
C
      CALL VECTORS
      CALL LINE(XBAR2,YBAR2,0,NDATA2)
C
      CALL VECTORS
      CALL LINE(XBAR3,YBAR3,0,NDATA3)
C
      IF(LABEL.EQ.0) GO TO 11
C
      SCL=7./WAX
      CHT1=0.16/SCL
      CHT2=0.18/SCL
      CHT3=0.220/SCL
C
C*****LABEL THE X AXIS
C
  11  XP1=0.25*XMAX1
      YP1=-0.19*YMAX1
      CALL SYMBOL(XP1,YP1,0.,0.2,18,18HRADIUS, FROM WALL.)
C
C*****LABEL THE Y AXIS*****
C
      XP2=-0.2*XMAX1
      YP2=0.2*YMAX1
      CALL SYMBOL(XP2,YP2,90.,0.2,17,17HVELOCITY, CM/SEC.)
C
C*****LABEL THE FIGURE*****
C
      ICHAR=IGRINPT(XPOS,YPOS)
      CALL SYMBOL(XPOS,YPOS,0.,CHT2,23,23HPROBE CALIBRATION CURVE)
      CALL TEKPAUS
      CALL PLOTEND
      STOP
      END
```